Mobilizing Projects
2nd International Conference of TEMA

Aveiro, 11th and 12th of july 2019

universidade de aveiro
theoria poiesis praxis

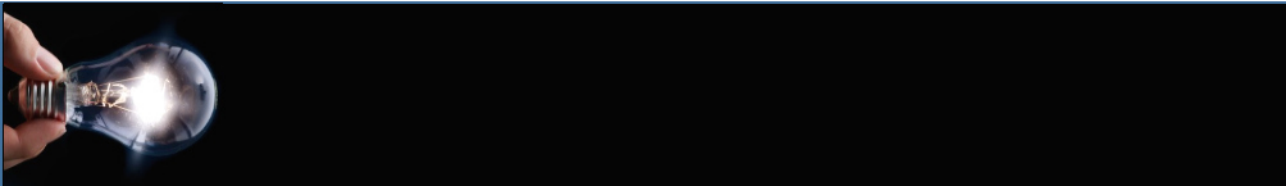

TEMA - Centre for Mechanical Technology and Automation

Pursuing excellence, cutting-edge and impact Research & Innovation since 1996

Based on its Human Capital and Capacities, the Centre for Mechanical Technology and Automation (TEMA) embraces a mission aiming to contribute to a sustainable industry, with specially focus on the surrounding SMEs, and to the wellbeing of society. Sustainable manufacturing aims to contribute to the development of a sustainable industry by developments and innovations on manufacturing engineering and technologies, to increase productivity, improve products quality and reduce waste in production processes. Technologies for the Wellbeing wishes to contribute to the wellbeing of society by the development of supportive engineering systems focusing on people and their needs and intending to improve their quality of life.

TEMA intends to maximize its national and international impact in terms of scientific productivity and its transfer to society by tackling the relevant challenges of our time. TEMA is aware of the major challenges of our days, not only confined to scientific issues but also the societal ones, (a strategic pillar of the Horizon 2020 program), at the same time placing an effort to have its research disseminated, in high impact journals to the international scientific community.

The strategic scientific plan is grounded in six major goals:

- A strong focus on pursuing funding by means of European projects, also in order to enforce the internationalization of the research unit and foster strong international networks;
- Responsible and active participation of TEMA members in pursuing the indicators and objectives defined in the mission and strategy of the research unit, improving dissemination and communication of excellent science;
- Improvement of research through grants and contracts, enhancing the range of income sources;
- Tackle critical societal challenges and issues by means of fundamental and applied research that requires cross inter- and multi-disciplinary cooperation, stimulating entrepreneurial mindsets among researchers;
- Continuous professional development with effective connection to society, at the national and international levels, as part of a strategy aiming to boost growth and competitiveness in expertise areas aligned with the European Research and Innovation agenda;
- To promote outreach activities that effectively integrates the society in TEMA's research and goals.

TEMA aims to: contribute to sustainability in its broad sense through new products, technologies and techniques, being able to respond to new challenges for Portugal and Europe as defined in P2020 and HORIZON 2020 and assisting product market entrance; be an institution of reference not only for young engineers and scientists, but also for senior world-wide recognized professionals; engage in strategic international collaborations around areas in which knowledge and competencies are crucial to the development of TEMA and contribute to the development of competitive as well as responsive research.

Aveiro, July 11th, 2019
The Coordinator,
António Manuel de Bastos Pereira

2nd International Conference on TEMA: Mobilizing Projects
Book of Abstracts

2nd International Conference on
TEMA: Mobilizing Projects
11th and 12th of July 2019

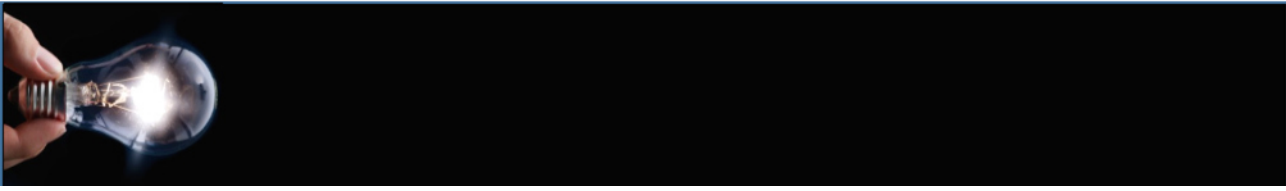

Title:
Book of abstracts of the 2nd International Conference of TEMA: Mobilizing Projects

Editors:
António Pereira, Paula Marques, Margarida Coelho, António Completo, Fernando Neto

Support team:
Ana Quintã, Diana Fidalgo, Kátia Silva, Maria Relvas, Nuno Almeida, Raul Simões

Publisher:
UA Editora
Universidade de Aveiro

1st Edition – July 2019

ISBN: 978-972-789-603-5

This book is supported by the projects:
UID/EMS/00481/2019-FCT - FCT - Fundação para a Ciência e a Tecnologia; and
CENTRO-01-0145-FEDER-022083 - Centro Portugal Regional Operational Programme (Centro2020), under the PORTUGAL 2020 Partnership Agreement, through the European Regional Development Fund

Contents

Sustainable Manufacturing Solutions

Bending response of thin-walled tubular structures filled with cellular metals

Isabel Duarte
Department of Mechanical Engineering, TEMA
University of Aveiro
Aveiro, Portugal
isabel.duarte@ua.pt

Matej Vesenjak, Zoran Ren
Faculty of Mechanical Engineering
University of Maribor
Maribor, Slovenia

Joachim Baumeister
Fraunhofer Institute for Manufacturing Technology and Advanced Materials, IFAM
Bremen, Germany

Hartmut Göhler
Fraunhofer Institute for Manufacturing Technology and Advanced Materials, IFAM
Dresden, Germany

Lovre Krstulović-Opara
Faculty of Electrical Eng., Mechanical Eng. and Naval Architecture
University of Split
Split, Croatia

***Abstract*— Thin-walled tubular structures filled with cellular metals [1-3] have been developed and tested for impact energy absorbers of vehicles to replace the current empty thin-walled metal tubes with various cross sections. The lightweight cellular metals are excellent energy absorber as they can convert impact energy into deformation energy. Herein, a comparative study on the crashworthiness characteristics of thin-walled tubular structures filled with various cellular metals under quasi-static and dynamic three-point bending was performed. Closed-cell metal foams, advanced pore morphology (APM) foam [4], hybrid APM foam [5], and metallic hollow spheres structure (MHSS) [6] were studied as filler of the thin-walled tubular structures. The load–deflection characteristics, deformation and failure modes and energy absorption characteristics of different filled thin-walled tubular structures (Fig. 1) were investigated. Results indicate that the hybrid APM foam and ex-situ foam filled tubes achieved the highest values of the peak load, exhibiting an abrupt failure and a rapid load drop and once the composite structure has reached the peak load. The APM, MHSS and in-situ foam filled tubes show much more ductile crushing deformation, with a predictable failure, showing a lower scatter of bending properties. Results have also demonstrated [2-3] that the structural changes of the outer thin-walled tube induced by the heating treatment ensure higher ductility, avoiding the formation of the cracks. However, the heat treatment of the outer tubes decreases the bending performance in terms of peak load and energy absorption capacity. On the other hand, the strong bonding between the filler and the outer thin-walled tube is a pre-requisite for a good crashworthiness.**

Keywords—cellular metals; filled tubes; advance pore morphology foam; metallic hollow sphere structure; three-point bending; energy absorption.

Figure 1: Specimens (from left to right): empty tube, APM, hybrid APM and MHSS foam filled tubes.

ACKNOWLEDGMENT

This work was supported to the projects UID/EMS/00481/2019-FCT and CENTRO-01–0145-FEDER-022083.

TOPIC

1) b.: Sustainable Manufacturing Solutions – Nanoengineering & Bio-inspired manufacturing.

REFERENCES

[1] I. Duarte, M. Vesenjak and L. Krstulović-Opara, "Dynamic and quasi-static bending behaviour of thin-walled aluminium tubes filled with aluminium foam," Compos. Struct., vol. 109, pp. 48-56, 2014.

[2] I. Duarte, M. Vesenjak, L. Krstulović-Opara, I. Anžel and J.M.F. Ferreira, "Manufacturing and bending behaviour of in situ foam-filled aluminium alloy tubes," Materials & Design, vol. 66, pp. 532-544, 2014.

[3] I. Duarte, M. Vesenjak and L. Krstulović-Opara, "Axial crush behaviour of the aluminium alloy in-situ foam filled tubes with very low wall thickness," Compos. Struct., vol. 192, pp. 184-192, 2018.

[4] K. Stöbener, J. Baumeister, G. Rausch, M. Rausch, "Forming metal foams by simpler methods for cheaper solutions," Met. Powder Rep., vol. 60, pp. 12-16, 2005.

[5] J. Baumeister, M. Monno, M. Goletti, V. Mussi, J. Weise, "Dynamic Behavior of Hybrid APM (Advanced Pore Morphology Foam) and Aluminum Foam Filled Structures," Metals (Basel), vol. 2, 211-218, 2012.

[6] H. Göhler, U. Jehring, J. Meinert, R. Hauser, P. Quadbeck, K. Kuemmel, G. Stephani, B. Kieback, "Functionalized Metallic Hollow Sphere Structures," Adv. Eng. Mater., vol. 16, pp. 335-339, March 2014

Data acquisition and storage platform for injection moulding processes: an IoT approach

Renato Rocha[1], Jorge Ferreira[1,2], Mónica Oliveira[1,2]
[1]*Departament of Mechanical Engineering*
University of Aveiro
[2]*Centre for Mechanical Technology & Automation (TEMA)*
Aveiro, Portugal
renatomrocha@ua.pt, jaff@ua.pt, monica.oliveira@ua.pt

Vítor Santos[1,3]
[3]*Institute of Electronics and Informatics Engineering of Aveiro (IEETA)*
Aveiro, Portugal
vitor@ua.pt

***Abstract*— The continuous rise in plastic injection industry scale and requirements results in increasing demand for the performance of injection tools. High quality standards, as well as high cadence production, associated with the growing complexity of plastic components to inject, results in increasingly aggressive injection cycles for injection molding tools. The systematic overuse applied to injection tools such as high-pressure cycles leads to premature degradation and compromises the quality of the final product [1].**

Data provided by the continuous monitoring of process variables regarding plastic injection molding, can be found extremely useful not only for the gauging of the quality of the product being injected, but also for the prediction of tool failure and maintenance [2]. With the rise of Industry 4.0 and IoT technologies, the centralization of information and data gathered from industrial processes has become a primary approach for companies that want to keep up with the fast-evolving competition. This technological paradigm enables the storage and easy access of data that contains abundant information which can be used for multiple purposes such as prediction or optimization [3].

This paper provides an IoT approach for the monitoring of multiple plastic injection machines. The system presented in this work enables the implementation of multiple acquisition modules that store acquired data on a dedicated server over the Internet. Also, the proposed solution provides an API for data fetch over the web, as well as remote control and monitoring of the installed modules.

Having a centralized storage system with a proper API is mandatory when the monitoring of multiple remote processes is intended. The API provides a way of accessing the data stored in the database server, which allows for the usage of large amounts of data being acquired in real-time and in any part of the globe. Stored data can then be processed with classic or machine learning methods. Data processing will provide the tools for process evaluation, being for predicting injection tool maintenance or to assure final product quality.

This work presents the necessary tools, including hardware, software, firmware as well as architecture concepts, required to monitor multiple injection processes and storing the acquired data in the referred centralized system. This consists in the primary step for data management, storage and conditioning for the application of future processing algorithms.

Keywords—Injection Molding; Acquisition system; Variable Monitoring; IoT; Industry 4.0.

ACKNOWLEDGMENT

This work was funded by the project "In Mould Monitoring 4.0" (University of Aveiro and SF Moldes, SA), It was also supported by the Centre for Mechanical Technology & Automation (UID/EMS/00481/2019-FCT and CENTRO-01-0145-FEDER-022083).

TOPIC

1) a.: Sustainable Manufacturing Solutions – Manufacturing processes & Simulation.

REFERENCES

[1] C. Hopmann, A. Ressmann, M. Reiter, S. Stemmler, D. Abel, A selfoptimising injection moulding process with model-based control system parameterisation, International Journal of Computer Integrated Manufacturing (2015).

[2] Y. Farouq, C. Nicolazo, A. Sarda, R. Deterre, Temperature measurements in the depth and at the surface of injected thermoplastic parts, Measurement: Journal of the International Measurement Confederation (2005).

[3] Radu F. Babiceanu, Remzi Seker, Big Data and virtualization for manufacturing cyber-physical systems: A survey of the current status and future outlook (2006).

Design and sustainability: transforming plastic waste into new long-life products

Catarina Marques[1,2], Teresa Franqueira[2], Victor Neto[1]
[1]Department of Mechanical Engineering, [2]Department of Communication and Art
University of Aveiro
Aveiro, Portugal
cpmarques@ua.pt, teresa.franqueira@ua.pt, vneto@ua.pt

***Abstract*— The plastic industry and the dependence that currently exists on plastic has generated an enormous amount of waste, that consequently, pollutes the environment. It has been estimated that 8300 million metric tons (Mt) of virgin plastics have been produced and if the trend continues, roughly 12000 Mt of plastic waste will be in landfills or in the natural environment by 2050 [1]. This problem has rapidly grown to the point where the current era is characterized as "Age of plastics" [2].**

Overconsumption and discard habit, together with poor lifecycle management contribute to the deposition of these wastes into the environment, especially in the ocean [3]. Therefore, the ocean becomes the final receiver of some plastic materials, that are considered the most abundant and the most problematic for the environment, economy, and health of ocean habitats. That way, it is estimated that each year, 8 million tons of plastic have been ended up in the ocean [4]. The main problem is that it is harmful to marine life which has been imprisonment or has ingested plastic [5], which leads to transference through the food chain, affecting the health and well-being of humans [6].

In this context, the challenge and goal of this work are minimizing this problem by developing products from ocean plastic or likely to get in there one day. In this sense, the work focuses the use of recycled Polyethylene terephthalate (PET), Polypropylene (PP) and High-density polyethylene (HDPE), due to the fact that they are the most used materials and easy to find in the ocean, according to an analysis made during the study. The work consists of doing some experimental procedure with domestic and ocean plastic in two different manufacturing processes, injection molding, and 3D printing. Thus, it's possible to draw conclusions from the behavior and limitations of each material submitted to reprocessing, and consequently satisfy the requirements for each product that will be developed. The results obtained show that the material coming from the ocean presents less tensile strength than the domestic one.

Therefore, will be designed a plant cultivation system for the interior of houses with domestic waste plastic and an item of urban furniture with plastic from the ocean. Also, the products are accompanied by a service with the aim of developing a basis for the process chain, from the collection of the raw material until its new life, based on a sustainable attitude.

In conclusion, the aim of this research is to strategically design to increase the life cycle of the materials by giving them a new life, through the transformation of plastic waste, in order to mitigate the environmental impact resulting from the excessive consumption of disposable products. It should be noted that this current excessive use of products will not be sustainable unless the industry develops more innovative and ecological approaches.

Keywords*— *Plastic recycling; Ocean plastic; Product design; Circular economy.

ACKNOWLEDGMENT

The research here presented was supported by the projects UID/EMS/00481/2019-FCT - FCT - Fundação para a Ciência e a Tecnologia; and CENTRO-01-0145-FEDER-022083 - Centro Portugal Regional Operational Program (Centro2020), under the PORTUGAL 2020 Partnership Agreement, through the European Regional Development Fund. The authors also acknowledge the support of Professors Filomena Cardoso Martins and Ana Paula Gomes, from the Department of Environment and Planning, and of Catarina Lemos, from the UACoopera unit, for the handling of the sea plastic residues.

TOPIC

1) c.: Sustainable Manufacturing Solutions – Manufacturing for Circular Economy.

REFERENCES

[1] Geyer, R., Jambeck, J. R., & Law, K. L., "Production, use, and fate of all plastics ever made" Science Advances. vol. 3, pp. 1-5, July 2017.

[2] Moore, C. J., "How much plastic is in the ocean? You tell me!" Marine Pollution Bulletin. vol. 92, pp. 1-3, 2015.

[3] Martins, J., and Sobral, P., "Plastic marine debris on the Portuguese coastline: A matter of size?" Marine Pollution Bulletin. vol. 62, pp. 2649-2653, 2011.

[4] European Environment Agency, "Marine Litter Watch: Citizens collect plastic and data to protect Europe′s marine environment." Marine Litter Watch. 2014.

[5] Allsopp, M., Walters, A., Santillo, D., & Johnston, P., "Plastic Debris in the World's Oceans." The Netherlands. 2006.

[6] Sobral, P. et al., "Lixo Marinho: um problema sem fronteiras." Parceria Portuguesa para o Lixo Marinho., Lisboa, pp. 1-65, 2015.

Design of an Additive Manufactured Part by Topology Optimisation

B. Barroqueiro
Department of Mechanical Engineering
Centre for Mechanical Technology & Automation
University of Aveiro
3810-193 Aveiro, Portugal
Active Space Technologies, Actividades Aeroespaciais S.A.
Parque Industrial de Taveiro, Lote12, 3045-508 Coimbra, Portugal

A. Andrade-Campos; R.A.F Valente
Department of Mechanical Engineering, Centre for Mechanical Technology & Automation
University of Aveiro
3810-193 Aveiro, Portugal

***Abstract*— Additive Manufacturing (AM) is a process of joining bulk raw materials to make parts from 3D model data, usually layer upon layer, as opposed to subtractive manufacturing and formative methodologies. It is an inherent part of the parts development or production process. It is used to manufacture prototypes and production parts"[1]. Furthermore, AM allows unprecedented design freedom, which can be explored by the Topology Optimization (TO) algorithm. Their interplay allows a new engineering cycle with the potential to design and manufacture disruptive concepts [2]. For instance, in the space industry, there are successful examples, where the interplay of TO and AM allows the reduction of the number of parts, assembling operations, mass and, therefore, cost (e.g. [3, 4]). Thus, a systematic methodology for designing AM parts is presented, being the main goal of this study. The methodology is subdivided into several phases, each phase contains several tasks. Moreover, the data flow between phases is considered and solutions are provided. Finally, the methodology is applied to a space case study and preliminary results of the AM engineering cycle (TO, part design and structural analysis) are analyzed. The obtained solution proved to be efficient in terms of stress distribution and ratio of stiffness/mass.**

Keywords—Topology Optimization; Additive Manufacturing; Case Study; Space Industry.

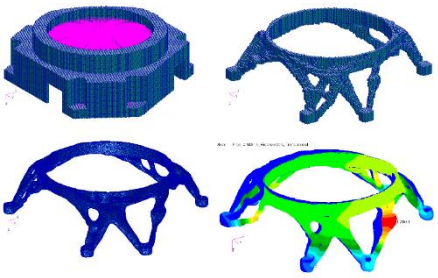

Figure 1: Overview of Design Stages: Design Domain, TO result, Laplacian Smoothing and 1st eigen value and shape of Stiffness Analysis.

ACKNOWLEDGMENT

The authors gratefully acknowledge the financial support of the Portuguese Foundation for Science and Technology (FCT) under the projects CENTRO-01-0145-FEDER-029713 by UE/FEDER through the programs CENTRO 2020 and COMPETE 2020, and UID/EMS/ 00481/2013-FCT under CENTRO-01-0145-FEDER-022083. Financial support of program CENTRO 2020 and UE/FEDER is acknowledged through the project CENTRO-01-0247-FEDER-024039, designated as ADVANSS. B. Barroqueiro also acknowledges the financial support by the FCT through the scholarship SFRH/BD/120779/2016.

TOPIC

1) a.: Sustainable Manufacturing Solutions – Manufacturing processes & Simulation.

REFERENCES

[1] ISO International Standard, ISO 17296: Additive manufacturing General principles Part 3: Main characteristics and corresponding test methods, 2014.

[2] Clausen, Anders. Topology Optimization for Additive Manufacturing. Technical University of Denmark (DTU), 2016. 154 p. (DCAMM Special Report; No. 214).

[3] S. Kébreau, D. P. Cambr´esy, A. Drose, V. Grone, K. Schimanski, F. Syassen, Maturation of additive manufacturing for implementation into Ariane secondary structures: Overview and status of "ALM ISCAR", in: 14th European Conference on Spacecraft Structures, Materials And Environmental Testing, 27-30 September, 2016.

[4] G. Pommatau, F. Montredon, A. Carlino, M. Salvi, E. Kot, F. Clement, S. Abed, Engineering design cycle for an additive layer manufactured secondary structure, from concept to final validation, in: Thales Alenia Space Communication, 27-30 September, 2016.

[5] Aremu A, Ashcroft I, Hague R, Wildman R, Tuck C, Suitability of SIMP and BESO Topology Optimization Algorithms for Additive Manufacture, Wolfson School of Mechanical and Manufacturing Engineering, May, 2016.

[6] ASTM International, West Conshohocken, ASTM WK47031: New Guide for Non-destructive Testing of Additive Manufactured Metal Parts Used in Aerospace Applications, 2014.

Development of a cost-effective multi-axis force sensor for robotics automation

Ricardo Guincho
School of Design, Management and Production Technologies Northern Aveiro
University of Aveiro
Oliveira de Azeméis

Daniel Afonso
TEMA - Centre for Mechanical Technology and Automation
University of Aveiro
Aveiro

***Abstract*— The industry 4.0 revolution centers itself around the automation of industrial processes, with a focus on interconnected manufacturing units and autonomous process control, among others [1]. As industrial robots take the place of human workers in monotonous, repetitive and even dangerous tasks, a need appears for a robotic solution for more intuitive lines of manufacturing, which often depend on human expertise, such as polishing, grinding and assembly [2]. A cost-effective force sensor is developed as a base solution for the automation of such operations. While this sensor is being developed as a part of a mold polishing automation project, it is being designed to be able to be used in any force sensing implementation, within the sensor's own limitations.**

The currently developed system (Figure 1) is capable of detecting (linear) forces in two axes, with the possibility of detection of forces in three orthogonal axes with a slight design modification.

Force calculations are performed within a signal conditioning/controller board (Figure 2) that can communicate directly with the industrial robot system, reducing the computational load on the latter. The use of standard, off-the-shelf, components for the signal conditioning board attempts to ensure the low cost and ease of part repair/replacement, and the controller board allows for one dimensional Analog (DAC) and Digital (PWM) output as a direct communication method with the input cards of an industrial robot controller, as well as Serial TTL, and Serial-USB communication for a more in depth control of the sensor-robot system, allowing for custom robot responses to the measured forces, as well as individual load cell gain adjustment and calibration.

The development of an active response force sensing tool is also underway. It will enable the usage of the tool as a self-correcting closed system that does not require real-time control or direct communication with the robot system, improving ease of implementation in different types of robots.

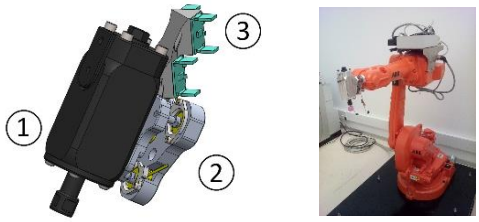

Figure 2: Left: Force Sensor CAD drawing. 1 – Polishing tool module; 2 – Force sensor; 3 – Load cell amplifier structure; Right: Force sensor coupled to a ABB IRB1600 robot.

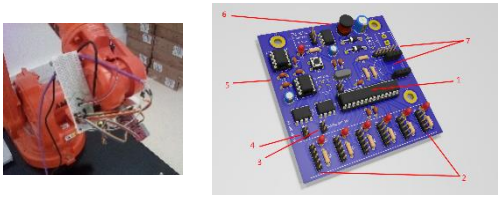

Figure 2: Left: Sensor control board prototype for testing; Right: Sensor control board. 1 – ATMega328 processor unit; 2 – Connection for up to six HX711 load cell amplifiers; 3 – 24V digital output for robot logic; 4 – 0V to 5V Analog output; 5 – 16bit DAC; 6 – Internal regulated power supply; 7 – Serial/USB terminals.

Keywords—force; sensor; automation; robotics; polishing; lowcost.

ACKNOWLEDGMENT

The authors would like to acknowledge the Simoldes S.A. company for supporting the project.

TOPIC

1) a.: Sustainable Manufacturing Solutions – Manufacturing processes & Simulation.

REFERENCES

[1] Pranab K. Muhuri, Amit K. Shukla, Ajith Abraham, "Industry 4.0: A bibliometric analysis and detailed overview", Engineering Applications of Artificial Intelligence, vol. 78, pp. 218-235, 2019.

[2] Abd El Khalick Mohammad, Jie Hong, Danwei Wang, Design of a force-controlled end-effector with low-inertia effect for robotic polishing using macro-mini robot approach, Robotics and Computer-Integrated Manufacturing, vol. 49, pp. 54-65, 2018.

[3] Kalt, Eugene & Monfared, Radmehr & Jackson, Michael, "Towards an automated polishing system - Capturing manual polishing operations", International Journal of Research in Engineering and Technology, vol. 5, pp. 182-192, 2016.

Development of products based on mixtures of polymeric residues

Adriana Costa[1,2], Victor Neto[1], Gonçalo Gomes[2]
[1]Department of Mechanical Engineering, [2]Department of Communication and Art
University of Aveiro
Aveiro, Portugal
aacosta@ua.pt, vneto@ua.pt, goncalo@ua.pt

***Abstract*— With the beginning of mass production only sixty decades ago the growth was so fast, that Jenna Jambeck states that "this kind of increase would break any system that was not prepared to receive it and that is why we have witnessed a leakage of global waste systems to the ocean ". The plastic takes about 400 years to decompose and the ones that do not come to the recycling, are subject 12% to the incineration and 79% are directed to the landfill or dragged to the environment [1].**

The thematic of resources and environmental issues are currently the focus of intense discussion. These issues have led to the argument of improvements by global and business institutions, involving the study and progress of a more sustainable development model, as defined by Per Becker as "development that meets the needs of the present without compromising the ability of future generations to meet their own needs"[2] combining the three assumptions of sustainable development (society, economy and environment).

Also like the biological system, the concept of industrial ecology is based on the principle of organizing the production system, in order to combine the flow of matter and energy dispensed, in order to create a completely closed circuit, using the waste itself or the products already used as raw material, with the objective of reducing the amount of reducing the material consumed [3].

Arises the need to develop products from recycled raw material, namely from industrial polymer waste. However, the conditions under which this type of raw material is obtained, creates a variability of characteristics that hinder its incorporation into new products, especially when produced in mass, where the main goal is to incorporate into new products, not adding any separation processes, creating value and placing them in environments that positively and conscientiously affect the community.

In the present research work it will be studying the transformation process of recycled plastics, through the recognition of case studies and the technologies, techniques and materials used in their transformation. The work will also go through trials of processing of the various materials provided by the recycling company Lifepoly (Oiã, Portugal), which would target the landfill, in order to understand the times, temperatures, volumes and compatibilities of the materials for their reprocessing.

For the creation of new products, the work explores two different manufacturing processes, compression molding and rotomolding. Each process has an associated product (hanger and piggy bank respectively) that will be carried out by prototyping it, which includes the characterization of the reprocessing of the various wastes.

In conclusion, this project aims to consolidate and make feasible the material, designing new products, increasing its life cycle. The main problem involving the reprocess of this type material was the thicknesses, melting points and the time spent. For the improvement of the quality of the waste, it is foreseen the necessity to create metrics like orders of production and careful storage.

The project also will allow this element to incorporate the circular economy enabling the products to be reused, remodeled, remanufactured or recycled, creating a new life to the materials used, contributing to the sustainability of ecosystems.

Keywords*— *Circular Economy; Sustainability; Non-Recyclable Waste; Compression Molding; Rotational Molding.

ACKNOWLEDGMENT

The research here presented was supported by the projects UID/EMS/00481/2019-FCT - FCT - Fundação para a Ciência e a Tecnologia; and CENTRO-01-0145-FEDER-022083 - Centro Portugal Regional Operational Program (Centro2020), under the PORTUGAL 2020 Partnership Agreement, through the European Regional Development Fund.

TOPIC

1) c.: Sustainable Manufacturing Solutions – Manufacturing for Circular Economy.

REFERENCES

[1] Becker, P , “Conceptual Frames for Risk, Resilience and Sustainable Development”, Sustainability Science, pp. 123–148, 2014.

[2] National Geografic, “91%: A Chocante Percentagem de Plástico que Não é Reciclado”, www.natgeo.pt, 2018.

[3] Zanin, M., & Mancini, S. D., “Resíduos plásticos e reciclagem: aspectos gerais e tecnologia”, ed. 2, 2015.

Enabling closed loop additive manufacturing through an on-demand feedstock material customization system

Tiago Gomes, Mylene Cadete, João Dias-de-Oliveira, Victor Neto
Centre for Mechanical Technology and Automation (TEMA), Department of Mechanical Engineering
University of Aveiro
Aveiro, Portugal
tiago.emanuel.gomes@ua.pt, mylene@ua.pt, jalex@ua.pt, vneto@ua.pt

Abstract— Consciousness about the need for circular production models has been growing, derived from alarming issues such as the amount of plastic waste that is ending up in the ocean. Recycling plastics may reintroduce them into the production cycle but there are drawbacks, namely material properties degradation and variability. Those issues often discourage the use of recycled feedstock in traditional mass production technologies. On the other hand, extrusion-based additive manufacturing is promising for integration of those materials, since it requires smaller batches. However, when functionality and consumer-oriented products are considered, the issues stated before may still be a hindrance [1,2].

In this work, the objective is the creation of conditions for reliably printing recycled thermoplastics, with their reparation, accounting for the feedstock properties variability, on demand and in situ. To make it possible, multiple dimensions of the problem will be approached. To begin with, ways of upgrading the feedstock polymer will be explored, studying suitable additives and specific modifiers and stabilizers that may range from polymeric chain extenders [3] to plasticizers [4], among others. Through their use, it is possible to or upgrade material properties. To cope with the feedstock variability, the second phase will explore ways of assessing the material condition in a non-invasive manner, in situ. This has been done to an extent in the literature through spectroscopy techniques like Raman [5]. Handheld spectrometers have also been developed [6]. Complementarily, prediction models that consider factors like number of reprocessing cycles, structure-property, material degradation, 3D printing parameters and final required properties to calculate the amount and type of additive needed to achieve them shall be developed.

Providing a further step on this subject, this work will build on the concept of FGAM (Functionally Graded Additive Manufacturing) [5,6] to achieve high level of control over material composition and distribution, allowing the reliable use of recycled materials. No single system has been reported to integrate material scanning, property prediction and customization capabilities like those targeted for this project. Such a system will facilitate the decision to use recycled material for extrusion-based additive manufacturing, simultaneously extending the freedom of engineers and designers by unlocking intelligent material customization.

Keywords— Additive manufacturing; Predictive models; Additives; Customized feedstock.

ACKNOWLEDGMENT

The research here presented was supported by the projects UID/EMS/00481/2019-FCT - FCT - Fundação para a Ciência e a Tecnologia; and CENTRO-01-0145-FEDER-022083 - Centro Portugal Regional Operational Program (Centro2020), under the PORTUGAL 2020 Partnership Agreement, through the European Regional Development Fund.

TOPIC

1) c.: Sustainable Manufacturing Solutions – Manufacturing for Circular Economy.

REFERENCES

[1] Lee D, Lee Y, Lee K. Development and Evaluation of a Distributed Recycling System for Making Filaments Reused in Three-Dimensional Printers. 2019;141(February):1–8.

[2] Anderson I. Mechanical Properties of Specimens 3D Printed with Virgin and Recycled Polylactic Acid. 3D Print Addit Manuf [Internet]. 2017;4(2):110–5.

Available from: http://online.liebertpub.com/doi/10.1089/3dp.2016.0054

[3] Tuna B, Ozkoc G. Effects of Diisocyanate and Polymeric Epoxidized Chain Extenders on the Properties of Recycled Poly (Lactic Acid). J Polym Environ. 2017;25(4):983–93.

[4] Yang Y, Xiong Z, Zhang L, Tang Z, Zhang R, Zhu J. Isosorbide dioctoate as a " green " plasticizer for poly (lactic acid). JMADE [Internet]. 2016;91:262–8.

Available from: http://dx.doi.org/10.1016/j.matdes.2015.11.065

[5] Ghosh S, Bowmaker GA, Cooney RP, Seakins JM. Infrared and Raman spectroscopic studies of the electrochemical oxidative degradation of polypyrrole. Synth Met. 1998;95:63–7.

[6] Pruett E. Latest developments in Texas Instruments DLP near-infrared spectrometers enable the next generation of embedded compact, portable systems. In: ProcSPIE [Internet]. 2015. Available from: https://doi.org/10.1117/12.2177430.

Enhancing the heterogeneity of a uniaxial test using topology optimization

Filipe Almeida, João Dias-de-Oliveira, A. Gil Andrade-Campos
Centre for Mechanical Technology and Automation (TEMA), Department of Mechanical Engineering
University of Aveiro
Aveiro, Portugal
almeida.filipe@ua.pt; jalex@ua.pt; gilac@ua.pt

***Abstract*— The frequent development and production of new metals in the sheet metal forming industry results in an ever-increasing demand for an accurate prediction of the material's behavior and, consequently, its behavior on sheet forming processes [1,2]. Heterogeneous tests are crucial to swiftly characterize numerically the material and identify the parameters of the constitutive models, as they provide a wider spectrum of stress and strain states per test [1,3].**

In the present work, a different approach is proposed for the development of a heterogeneous specimen. Using topology optimization, the goal is to find the optimal geometry of the specimen which maximizes the incidence of all stress states over the area. A criterion was developed in order to measure the heterogeneity value of a test, which was then used as the objective function for the topology optimization problem. The boundary conditions were defined as a simple uniaxial tensile test, and the goal was to obtain maximum heterogeneity on a single test. The finite difference method is applied to evaluate the local sensitivities and to guide the design optimization method, while using a volume constraint. In addition, some heterogeneous specimens' designs were analyzed, evaluated and ranked under the defined criterion for comparison purposes.

It was concluded that this criterion is accurate when used to rank and compare different specimens in terms of their heterogeneity. Nonetheless, the evaluation of this criterion as an objective function is still under development. The algorithm developed by the author successfully enhances the heterogeneity of a rectangular specimen, covering almost all the required range of heterogeneity for the stress states, while respecting the restrictions of the problem. A final solution for the specimen has not yet been obtained, as the material distribution is still not manufacturable, but current results are promising and will be discussed over this work.

Keywords— Heterogeneous specimen; Topology Optimisation; Characterization of sheet metals

ACKNOWLEDGMENT

The authors acknowledge the financial support of FCT under the projects PTDC/EME-APL/29713/2017 (CENTRO-0 1-0145-FEDER-029713), PTDC/EMS-TEC/6400/2014 (POCI -01-0145-FEDER-016876), PTDC/EME-EME/31243/2017 (P OCI-01-0145-FEDER-031243) and PTDC/EME-EME/30592/ 2017 (POCI-01-0145-FEDER-030592) by UE/FEDER through the programs CENTRO 2020, COMPETE 2020, and UID/EM S/00481/2013-FCT under CENTRO-01-0145-FEDER-022083.

TOPIC

1) a.: Sustainable Manufacturing Solutions – Manufacturing processes & Simulation.

REFERENCES

[1] N. M. Souto, Computational design of a mechanical test for material characterization by inverse analysis. PhD thesis, University of Aveiro, 2015.

[2] P. A. Prates, A. F. Pereira, N. A. Sakharova, M. C. Oliveira, and J. V. Fernandes, "Inverse Strategies for Identifying the Parameters of Constitutive Laws of Metal Sheets" Advances in Materials Science and Engineering, vol. 2016, no. Dic, 2016.

[3] S. Cooreman, D. Lecompte, H. Sol, J. Vantomme, and D. Debruyne, "Identification of mechanical material behavior through inverse modeling and DIC" Experimental Mechanics, vol. 48, no. 4, pp. 421-433, 2008.

Influence of process parameters in asymmetric rolling

M. Pasadidehpoor[1], G. Vincze[1], A.B. Pereira[1], A.B. Lopes[2], M.C. Butuc[1]

[1]*Centre for Mechanical Technology and Automation, Department of Mechanical Engineering, University of Aveiro*
Campus Universitário de Santiago, 3810-193, Portugal

[2]*CICECO, Department of Materials and Ceramic Engineering, University of Aveiro*
Campus Universitário de Santiago, 3810-193, Portugal

***Abstract*— Aluminum alloys are widely used in the automotive industry because they offer high strength to low weight. These characteristics are crucial for car manufacturing. It is well known that the mechanical behavior of aluminum alloys is strongly depended on texture evolution. Thus, controlling the texture of the aluminum sheet it is possible to design specific material properties.**

One useful method to change the texture components is by asymmetric rolling. This type of rolling introduces shear components, which contributes to the improvement of formability in deep drawing due to the fact that during recrystallization do not transform into the cube component.

The aim of this work is to analyses by finite element method the effect of different process parameters such as speed ratio, thickness reduction per pass and rolling route on the shear strain and on the equivalent strain of the material. Part of the theoretical results is compared with the experimental data obtained for AlMgSi alloys.

Keywords—aluminum alloys; anisotropy; hardening behaviour

ACKNOWLEDGMENT

The authors acknowledge the support from the projects POCI-01-0145-FEDER-0323628 (PTDC/EME-ESP/32362/2017), UID/EMS/00481/2013 and CENTRO-01-0145-FEDER-022083.

TOPIC

1) a.: Sustainable Manufacturing Solutions – Manufacturing processes & Simulation.

Influence physical fields on structure and properties of epoxy composites

Yuliia Bardadym
Department of Polymer Modification
Institute of Macromolecular Chemistry of NAS of Ukraine
Kiev, Ukraine
yuliia.bardadym@gmail.com

Edward Sporyagin
Department of Chemical Technology of Macromolecular Compounds
Oles Honchar Dnipro National University
Dnipro, Ukraine

Oleksandr Naumenko
Department of equipment and technology of food production
Ukrainian State University of Chemical Technology
Dnipro, Ukraine

***Abstract*— Thesis is devoted to the study of the effect of external permanent magnetic or electric fields on the structure, thermophysical, dielectric properties of epoxy polymers and their nanocomposites with lead (II) oxide. System studies of structure, thermophysical, thermomechanical and dielectric properties of nanocomposites with metal oxide formed under the influence of external constant physical fields were carried out for the first time. The ideas of constructing mathematical models and mechanisms of the influence of permanent magnetic and electric fields on epoxy polymers and their nanocomposites containing metal oxide have been developed. Based on the results obtained, the method of calculating an electromagnet and a capacitor using the software «Elcut» has been improved.**

Keywords*— *epoxy nanocomposite, elecrtric field, magnetic field, metal oxide, computer, mathematical, simulation.

Polymers are widely used for their relatively low production cost, light weight and ease of processing. Considerable progress has been made over the preceding decade in the development of high-performance polymers. The incorporation of inorganic particles into a polymer matrix takes advantage of both components to create original composite materials with new properties. The most commonly used polymer matrices include amorphous thermoplastics (e.g., polymethylmethacrylate, polycarbonate) and thermosets (e.g., epoxy). Different kinds of inorganic fillers are currently incorporated in those matrices, in particular oxides (e.g., SiO_2, TiO_2, CdO_2, Cr_2O_3, PbO, ZnO), semiconductors (e.g., CdS, PbS, CdTe, CdSe), minerals (e.g., clays, $CaCO_3$), metal and metal alloys (e.g., Au, Ag, Cu, Ge, Fe) [1].

The use of mathematical (computer) simulation plays an important role along with experimental research methods. Modeling using digital computers is one of the most powerful means of research. It enables to calculate and simulate experiments at the design stage. [2].

Therefore, this thesis is devoted to the study of the effect of external permanent magnetic or electric fields on the structure, thermophysical, dielectric properties of epoxy polymers and their nanocomposites containing metal oxide Samples of composites were formed from epoxy resin ED-20 and triethylenetetramine. Stoichiometric ratio was 1 mole of epoxy resin to 0,18 mole triethylenetetramine. Powder PbO was used as fillers. The content of metal oxide was 3 vol. %. The influence of constant magnetic and constant electric fields was $2 \cdot 10^5$ A/m and $1.5 \cdot 10^4$ V/m respectively. All curing processes were done at 293 – 297 K for 24 hours. It was established that the use of external physical fields allows to change the relative deformation of the studied filled epoxy composite materials from 5% to 15%. For samples of EP – CdO, formed under the influence of external constant physical fields, a decrease in the temperature of destruction up to 50 K is observed, the total number of gaseous products registered in the mass spectrum up to 87 units and 18% of the total ion current. However, samples of EP – PbO an increase in the temperature of decomposition maxima of 50 K and up to 13.8% of the total ion current is characteristic. The influence of physical fields on samples of EP – Cr_2O_3 provokes reduction of total ion current by 25%, specific intensity of ion fragments up to 20%. The ideas of constructing mathematical models and mechanisms of the influence of permanent magnetic and electric fields on epoxy polymers and their composites containing metal oxide were developed. Based on the results obtained, the method of calculating an electromagnet and a cylindrical capacitor using the software «Elcut» has been improved.

TOPIC

1) a.: Sustainable Manufacturing Solutions – Manufacturing processes & Simulation.

REFERENCES

[1] J. Loste, J. Lopez-Cuesta, L. Billon, H. Garay, M. Save, "Transparent polymer nanocomposites: An overview on their synthesis and advanced properties," Progress in Polymer Science, vol. 89, pp. 133-158, 2019.

[2] Yu. Bardadym, E. Sporyagin, "The influence of the constant physical fields on structure of polymer composites with cadmium oxide and polyaniline," 7th International Conference Nanomaterials: Application and Properties. – Zatoka, 2017, pp. 03NNSA13-1 – 03NNSA13-4.

Inverse analysis procedures for elastoplastic parameter identification using combined optimisation strategies

B Coelho[1], A Andrade-Campos[2] and J M P Martins[3]
Centre for Mechanical Technology and Automation (TEMA), Department of Mechanical Engineering
University of Aveiro
Aveiro, Portugal
[1] bcoelho@ua.pt, [2]gilac@ua.pt, [3]joao.martins52@ua.pt

***Abstract*— Ensuring accurate and efficient models for the representation of the elastoplastic behavior of sheet metals is one of the main issues in manufacturing simulation processes. Nowadays, there are a few solid numerical methodologies for predicting the material parameters from full-field strain measurements using digital image correlation (DIC) techniques. External methods, such as the Finite Element Model Updating (FEMU), search for the parameter set that minimizes the gap between the experimental and numerical observations. In these methods, a total separation between the experimental and the numerical data occurs. Equilibrium methods, such as the Virtual Fields Method (VFM), search for the parameter set that balances the internal and external work according to the principle of virtual work, where the internal work is calculated using the constitutive model applied to the experimental strain field [1-5]. Both described methods are still expensive and non-robust, which is closely related with the adopted single-stage optimization strategies. Such optimization strategies can undergo problems of initial solution's dependence, non-uniqueness of solution, local and premature convergence, physical constraints violation, etc. Therefore, the choice of an optimization algorithm is not straightforward.**

The aim of this work is to implement and analyze advanced optimization strategies with sequential, parallel and hybrid approaches in a parameter identification problem using both the VFM and the FEMU methods. The performance of a gradient least-squares (GLS) optimization algorithm, a metaheuristic (MH) algorithm and their combination is compared. Moreover, the definition of the objective functions of both VFM and FEMU methods is discussed in the framework of optimization.

Table 1, for instance, provides results of a parallel strategy that combines FEMU and VFM. In this strategy, the objective function is given by the sum of the weighted objective functions of each method (multi-objective approach).

	No noise		Noise	
FEMU weight	**Objective Function**	**Parameters average error**	**Objective Function**	**Parameters average error**
0.0	**5.50E-07**	**0.707%**	**1.78E-03**	**42.994%**
0.2	**5.35E-06**	**0.355%**	**7.05E-03**	**9.936%**
0.5	**6.94E-06**	**0.207%**	**7.35E-03**	**-2.127%**
0.8	**4.06E-06**	**0.080%**	**6.48E-03**	**-6.341%**
1.0	**3.70E-02**	**17.243%**	**4.47E-03**	**-9.409%**

Table 1: Results considering data with and without noise.

The parallel strategy presents significantly lower average errors in the identification of parameters when compared to the single VFM or FEMU approaches (FEMU weight equal to 0 or 1, respectively).

Keywords — calibration of constitutive models; metal plasticity; full-field measurments; finite element model updating; virtual fields method; gradient-based optimisation algorithm; metaheuristic optimisation algorithm.

ACKNOWLEDGMENT

The authors acknowledge the financial support of FCT under the projects PTDC/EME-APL/29713/2017 (CENTRO-0 1-0145-FEDER-029713), PTDC/EMS-TEC/6400/2014 (POCI -01-0145-FEDER-016876), PTDC/EME-EME/31243/2017 (P OCI-01-0145-FEDER-031243) and PTDC/EME-EME/30592/ 2017 (POCI-01-0145-FEDER-030592) by UE/FEDER through the programs CENTRO 2020, COMPETE 2020, and UID/EM S/00481/2013-FCT under CENTRO-01-0145-FEDER-022083.

TOPIC

1) a.: Sustainable Manufacturing Solutions – Manufacturing processes & Simulation

REFERENCES

[1] Cooreman S, Lecompte D, Sol H, Vantomme J, Debruyne D (2008) Identification of Mechanical Material Behavior Through Inverse Modeling and DIC. Experimental Mechanics 48: 421–433.

[2] Haddadi H., Belhabib S. (2012) Improving the characterization of a hardening law using digital image correlation over an enhanced heterogeneous tensile test. Int. J. Mech. Sci. 62(1): 47-56.

[3] Martins JMP, Andrade-Campos A, Thuillier S (2018) Comparison of inverse identification strategies for constitutive mechanical models using full-field measurements. Int. J. Mech. Sci. 145: 330-345.

[4] Kim J-H, Serpantié A, Barlat F, Pierron F, Lee M-G (2013) Characterization of the post-necking strain hardening behavior using the virtual fields method. Int. J. Solids Struct. 50(24): 3829–3842.

[5] Marek A, Davis FM, Rossi M, Pierron F (2019) Extension of the sensitivity-based virtual fields to large deformation anisotropic plasticity. Int. J. Mat. Forming 12(3): 457-476.

[6] Nocedal, J, Wright, S. (2006) Numerical Optimization, Springer-Verlag New York.

Life Cycle Assessment of Heat Recovery System

A Comparative Study Between Aluminium and Polystyrene

Marques, Hugo
Mechanical Engineering Department
University of Aveiro
Aveiro, Portugal
hugo.marques@ua.pt

Oliveira, Mónica & Martins, Nelson
Mechanical Engineering Department
University of Aveiro
Aveiro, Portugal
monica.oliveira@ua.pt & nmartins@ua.pt

***Abstract*— The exploitation of resources associated with the production of electric power reveals a preponderant influence on environmental sustainability. In the OECD countries, electricity consumption in the residential sector corresponds to 31.1% of total electricity consumption, with indoor air heating accounting for 50% of that consumption [1]. In compact envelope buildings, mechanical ventilation is responsible for the loss of 50% of thermal loads [3]. Air-to-air heat recovery systems (HR) are an effective way to reduce ventilation losses as they may pre-heat outdoor air recovering wasted heat from the exhaust air [4]. Currently, most HR systems are made from aluminum alloys. However, the incorporated energy in an aluminum HR system during the production stage is much higher than that required if polymeric materials are used. [5]. The present study focuses on the analysis of sustainable manufacturing solutions for air-to-air HR devices. In this sense, a life cycle assessment (LCA) of an air-to-air HR was done considering two different materials: aluminum and polystyrene. In addition, for the polystyrene LCA two manufacturing technologies were compared: injection molding and extrusion. The LCA evaluates the carbon footprint of a product from the extraction of the raw material to the recycling of the product, in a cradle to grave perspective. The scope of LCA covers the stage of extraction of the raw material, the process of production of materials and product, of the utilization and recycling. The functional unit is defined by the production of a single HR unit.**

The input data expresses the energy consumed at each stage throughout the LCA. The analyzed output data represent greenhouse gas emissions and fossil fuels consumption. These parameters are indicators of environmental impacts, therefore, they deserve a careful analysis during the design phase of the product development cycle.

As for the inventory analysis, only the primary production of aluminum was considered by the Bayer process. The production of polystyrene is based on the polymerization of styrene free radicals. In the manufacture of the air-to-air HR systems, metal forming and laser cutting processes were considered for aluminum, while the injection molding and extrusion were analyzed for the polystyrene. The production of aluminum sheets is considered in the production of aluminum as final product. During product utilization, no energy consumption is taken into consideration. Moreover, both material recycling or its reintegration in the production cycle were disconsidered in both scenarios studied. It should be referred that, except when considering the raw materials stage, transportation distances are within the European scale. Also, the electric consumption is based on the European average values. The method used to assess the environmental impact was IMPACT 2002+ with SimaPro software. The environmental impact analysis is based on the categories of the global warming potential (GWP), namely, non-renewable energy and CO_{2eq} emissions, as summarized in Figure 1.

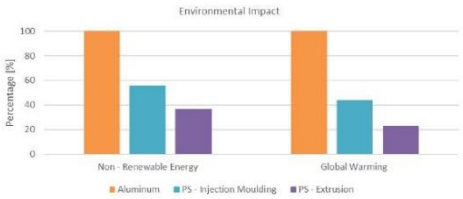

Figure 1: Aluminium GWP and polystyrene.

Keywords—Aluminium; Heat Recovery System; IAQ; Life Cycle Assessment; Polystyrene

ACKNOWLEDGMENT

The authors acknowledge the support of TEMA research unit integrated projects UID/EMS/00481/2019-FCT and CENTRO-01-0145-FEDER-022083.

TOPIC

1) c.: Sustainable Manufacturing Solutions – Manufacturing for Circular Economy.

REFERENCES

[1] International Energy Agency, "Energy Efficiency Indicators: Highlights," 2018.

[2] ASHRAE, Handbook - HVAC Systems and Equipment. Atlanta, GA, 2008.

[3] C. Roulet, F. D. Heidt, F. Foradini, and M. Pibiri, "Real heat recovery with air handling units," *Energy Build.*, vol. 33, pp. 495–502, 2001.

[4] M. Rafati, M. Fauchoux, R. W. Besant, and C. J. Simonson, "A review of frosting in air-to-air energy exchangers," *Renew. Sustain. Energy Rev.*, vol. 30, pp. 538–554, 2014.

[5] C. T. Joen, Y. Park, Q. Wang, A. Sommers, X. Han, and A. Jacobi, "A review on polymer heat exchangers for HVAC&R applications," *Int. J. Refrig.*, vol. 32, pp. 763–779, 2009.

Morphing Shapes by 3D Printing

Mylene S. Cadete, Tiago Gomes, Renato Couto, Luís Alves, João Dias, João Tavares, Mário Oliveira, Victor Neto

Centre for Mechanical Technology and Automation (TEMA), Department of Mechanical Engineering, University of Aveiro, Aveiro, Portugal

mylene@ua.pt; tiago.emanuel.gomes@ua.pt; renatocouto@ua.pt; ldalves@ua.pt; joaoldias@ua.pt; joaoactavares@ua.pt; mdpo@ua.pt; vneto@ua.pt

***Abstract*— Additive manufacturing, often referred to as 3-dimensional (3D) printing technology, has been first developed more than 30 years ago. It has been recognized as a disruptive technology for future advanced manufacturing systems. With a great potential to change everything from our daily lives to the global economy. Significant advances have been made with respect to materials, printers, and processes [1][2]. An example is the Fused Filament Fabrication (FFF) method. Another innovative concept of printing technology known as 4D printing technology has been developed in recent years. 4D printing is the process through which a 3D printed object transforms itself into another structure over the influence of external input. Smart design and smart materials are the main differences of 4D printing compared to 3D printing [2]. Making use of proper design structures and material properties, these objects respond to external stimuli by transforming their shape and/or volume and changing the physical properties, such as Young's modulus, stiffness, and resistance. Specially, smart materials that exhibit the shape memory effect are able to recover their original shape following environmental changes such as changes in humidity, pH, irradiation, and temperature. 4D printing is an interesting research field and has significant potential for expansion [3][4]. In this presentation, preliminary results of morphing shapes will be presented, going from printing strategies design principles to the physical morphing behavior. PLA and PET was used to produce simple samples that where later trigger to change their shape in a hot water bath. [5][6]**

Keywords—3D printing; 4D printing; PLA; PET; morphing.

ACKNOWLEDGMENT

The research here presented was supported by the projects UID/EMS/00481/2019-FCT - FCT - Fundação para a Ciência e a Tecnologia; and CENTRO-01-0145-FEDER-022083 – Centro Portugal Regional Operational Program (Centro2020), under the PORTUGAL 2020 Partnership Agreement, through the European Regional Development Fund.

TOPIC

1) c.: Sustainable Manufacturing Solutions – Manufacturing for Circular Economy.

REFERENCES

[1] W. Gao, Y. Zhang, D. Ramanujan, K. Ramani, Y. Chen, C.B. Williams, P.D. Zavattieri, "The status, challenges, and future of additive manufacturing in engineering" Computer-Aided Design, vol 69, pp. 65–89, 2015.

[2] O. Kwon, W. Jo, J. Choi, H. J. Lee, "4D Printing Technology : A Review" 3D Printing and Additive Manufacturing, vol. 2, pp. 159–167, 2015.

[3] D. Shin, T. Kim, D. Kim, "Review of 4D Printing Materials and their Properties", International Journal of Precision Engineering and Manufacturing-Green Tecnhology, vol. 4, pp. 349–357, 2017

[4] N. Nkomo, "A Review of 4D Printing Technology and Future Trends Nkosilathi", 11th South African Conference on Computational and Applied Mechanics, 2018

[5] B. An, Y. Tao, J. Gu, T. Cheng, X. Chen, X. Zhang, W. Zhao, Y. Do, S. Takahashi, H. Wu, T. Zhang, L. Yao, "Thermorph: democratizing 4D printing of self-folding materials and interfaces" Proceedings of the 2018 CHI Conference on Human Factors in Computing Systems, Paper 260, ACM, 2018

[6] G. Wang, Y. Tao, O. Capunaman, H. Yang, L. Yao, "A-line: 4D printing morphing linear composite structures" Proceedings of the 2019 CHI Conference on Human Factors in Computing Systems, Paper 426, ACM, 2019

Prediction of performance of cutting environments in turning process of Ti-6Al-4V alloy

*C. Veiga[1, 2 *], J. Paulo Davim[2], A.J.R. Loureiro[3]*
[1]*ISEC, Polytechnic Institute of Coimbra*
Rua Pedro Nunes - Quinta da Nora, 3030-199 Coimbra, Portugal
[2] *Department of Mechanical Engineering, University of Aveiro*
Campus Santiago, 3810-193 Aveiro, Portugal
[3, 4]*CEMUC, Department of Mechanical Engineering, University of Coimbra, Pólo II*
Pinhal de Marrocos, P-3030 788 Coimbra, Portugal.
* Corresponding author: E-mail: veiga@isec.pt / celestino@ua.pt

Abstract— Titanium materials, due to their unique mechanical properties, are widely used in industrial applications, being the Ti6Al4V one of the most used alloys [1]. However, machining these materials is challenging due to their low thermal conductivity and elastic modulus, high hardness at elevated temperature, and high chemical reactivity [2]. Finite element simulations (FEM) offer simple cost-effective solutions to offset the cost of experimental trials. The purpose of this work is to evaluate the performance of cutting environments in the turning process of Ti-6Al-4V alloy with cemented carbide insert (ISO-K20), using simulations carried out with the commercial software AdvantEdge FEMTM. Three simulations were modeled and executed, being the modeling based on the cutting speed Vc = 90 m/min, feed rate f = 0.254 mm/rev, depth of cut doc = 1.27 mm, rake angle α = -5°, relief angle β = 10°, insert edge radius r = 0.02 mm, and three different cutting environments, respectively dry, emulsion and liquid nitrogen (LN2). The results obtained show the following: the chips are serrated, and their plastic strain decreased substantially for emulsion and LN2 environments; the magnitude of cutting and trust forces decreased from dry to emulsion and to LN2 environments; the tool tip temperature decreased for emulsion and for LN2 environments; the emulsion and LN2 environments reduced the tool wear and increased the tool life; the distribution or evolution of temperature and plastic strain on the machined surface are similar for all the cutting environments; the maximum temperature (in °C) at the machined surface were 880, 810 and 765, respectively for dry, LN2 and emulsion environments, which may result in martensitic transformation of β phase during rapid cooling, for dry and LN2 environments.

Keywords— Cutting environments; FEM simulation; Titanium alloys; Turning process.

ACKNOWLEDGMENT

The authors acknowledge the Research Unit (UID / EMS / 00481/2013-FCT) and the Research Infrastructure (CENTRO-01-0145-FEDER-022083). The author C. Veiga acknowledge ISEC-IPC for any support granted.

TOPIC

1) a.: Sustainable Manufacturing Solutions – Manufacturing processes & Simulation.

REFERENCES

[1] Adam D. Lampropoulos, Angelos P. Markopoulos and Dimitrios E. Manolakos, Modeling of Ti6Al4V Alloy Orthogonal Cutting with

[2] Smooth Particle Hydrodynamics: A Parametric Analysis on Formulation and Particle Density, Metals 2019, 9, 388; doi:10.3390/met9040388.

[3] Veiga, C., Davim, J.P., & Loureiro, A.J.R., Review on machinability of titanium alloys: the process perspective, Reviews on Advanced Materials Science, IPME, 34, 2, (2013), 148-164.

Spatially-selective femtosecond laser precipitaion of silver clusters and nanoparticles in oxide glass

G. Shakhgildyan, M. Vetchinnikov, A. Lipatiev, S. Lotarev, V. Sigaev
Department of Glass and Glass-Ceramics Technology
Mendeleev University of Chemical Technology of Russia
Moscow, Russia
gshah@muctr.ru

Abstract— **Femtosecond (fs) laser-induced modification of oxide glasses opens new routes for precise space-selective tuning of material properties and development of functional photonic devices including integrated waveguides, optical switches, phase plates, volume optical memory, etc. [1,2]. In this regard, glasses doped with photosensitive agents such as noble metals and semiconductors are of particular interest due to unique optical properties of nanoclusters, nanoparticles or quantum dots that can be precisely precipitated in the confined volume of glass [3,4]. Hence fs modification could become a convenient alternative to conventional nanotechnology methods for the one-step development of 3D nanostructured materials with a wide set of functionalities in sensing, photonics and data storage devices [5]. Here, we report results on the space-selective direct precipitation of Ag nanoclusters and nanoparticles by femtosecond laser pulses inside silicate and phosphate glasses. We synthetized glasses in ZnO-P_2O_5 and K_2O-ZnO-B_2O_3-SiO_2 systems doped with various Ag_2O content using melt quenching technique, laser modifications were made using 1030 nm KGW:Yb Pharos SP femtosecond laser system connected with Aerotech ABL100 positioning system. We demonstrated: (i) one-step micro-modification of optical properties (without the requirement for additional heat treatment) providing formation of micron-sized ring-shaped domains exhibiting both luminescence and plasmonic absorption due to simultaneous aggregation of silver nanoclusters and nanoparticles; (ii) presence of birefringence in the edges of domains with slow axis oriented perpendicularly to the polarization plane of the writing laser beam and retardance growing with the silver content in phosphate glasses. We established that domains formed with laser pulse energy of 50–90 nJ and a number of pulses of 10^5–10^6 exhibit: i) absorption band around 445 nm associated with surface plasmon resonance of silver nanoparticles, ii) luminescence around 450 nm due to the emission of silver clusters, iii) the form birefringence with retardance value up to 33 nm. All observed phenomena were located in the edges of laser written ring-shaped domains. TEM imaging of the domain's edge showed the formation of two groups of spherical silver nanoassemblies: large nanoparticles with sizes 5–30 nm and nanoparticles with 1–4 nm size. Silver nature of precipitated nanoparticles was confirmed both by the analysis of the crystal lattice spacing and by the EDS study. Variation of laser pulse energy allows controlling the modification process and tuning induced optical properties. We propose a possible scenario for the observed phenomena that includes local chemical redistribution of glass network modifiers during the modification process. We showed that by tuning laser parameters it is possible to locally precipitate Ag nanoparticles in glass. In this work by means of TEM and EDS we studied phenomenon of local ions migration during irradiation and proved that fs laser modification of glass leads to migration of glass network modifiers (such silver) to the periphery of written domains, while migrations of network formers direct to the central area of domains. Obtained results give important information about possibilities of local chemical change and open a prospect for application of such technology in multilevel optical data recording and design of nanophotonic devices.**

Keywords—glass, femtosecond laser, silver clusters, silver nanoparticles, luminescence.

ACKNOWLEDGMENT

This study was financially supported by the Russian Foundation for Basic Research (grant 18-33-00595 and 19-32-80032).

TOPIC

1) a.: Sustainable Manufacturing Solutions – Manufacturing processes & Simulation.

REFERENCES

[1] K.C. Phillips, H.H. Gandhi, E. Mazur, "Ultrafast laser processing of materials: a review", Adv. Opt. Photon. 7 (2015) 686–705.

[2] D. Tan, K. Sharafudeen, Y. Yue, J. Qiu, "Femtosecond laser induced phenomena in transparent solid materials: fundamentals and applications", Prog. Mater. Sci. 76 (2016) 154–228.

[3] Shakhgildyan G.Yu, Lipatiev A.S., Vetchinnikov M.P., Popova V.V., Lotarev S.V., Golubev N.V., Ignat`eva E.S., Presniakov M.M., Sigaev V.N., "One-step micro-modification of optical properties in silver-doped zinc phosphate glasses by femtosecond direct laser writing", J. Non-Cryst. Solids 481 631 (2018).

[4] Vetchinnikov M.P., Lipatiev A.S., Shakhgildyan G.Yu, Golubev N.V., Ignat'eva E.S., Fedotov S.S., Lipateva T.O., Lotarev S.V., Vilkovisky G.A., Sigaev V.N. ," Direct femtosecond laser-induced formation of CdS quantum dots inside silicate glass", Opt. Lett. 43 2519 (2018).

[5] Y. Petit, S. Danto, T. Guérineau, A.A. Khalil, A. Camus, E. Fargin, G. Duchateau, JP. Bérubé, R. Vallée, Y. Messaddeq, T. Cardinal, L. Canioni, "On the femtosecond laser-induced photochemistry in silver-containing oxide glasses: mechanisms, related optical and physico-chemical properties, and technological applications", Adv. Opt. Techn., 7(5), pp. 291-309 (2018).

Structural and optical study of evaporated cerium-doped silicon layers

Bekhedda kheira
Centre de Recherche en Technologie des Semi-conducteurs pour l'Energétique (CRTSE)2 Bd Frantz Fanon, B.P.140
Alger-7 Merveilles, Algiers (Algeria),
Tel & Fax: +213 21433511
Bekhedda.kheira@crtse.dz

Brik Afaf
Centre de Recherche en Technologie des Semi-conducteurs pour l'Energétique (CRTSE)2 Bd Frantz Fanon, B.P.140
Alger-7 Merveilles, Algiers (Algeria),
Tel & Fax: +213 21433511
brikafaf@yahoo.com

***Abstract*— The study of semiconductors doped with trivalent rare earth ions (TR3 +) has attracted a lot of interest and appears promising for applications in optoelectronics, notably thanks to the optical properties of rare earth ions. Our choice was cerium because it has several thin emission bands in a spectral range from near UV to infrared.**

The present study focused on evaporation of cerium (Ce) layers on silicon substrates (Si). Next, the applied doping process consists of high temperature annealing to be effective in the incorporation and activation of rare earth ions in silicon. The effect of heat treatment temperature was examined and studied using scanning electron microscopy (SEM) for structural characterizations and UV-Visible optical transmission spectroscopy for optical characterizations.

Keywords*— *Ceruim; evaporation; silicon; UV-Visible.

EXPERIMENTAL RESULTAT

✧*Electronic Microscopy (MEB)*

Scanning electron microscopy was used in this work for the surface observation of cerium samples obtained after various thermal anneals. The first observations were made on a thin film Ce deposited directly on a Si substrate.

These observations demonstrate the presence of a high density of Ce in a Si layer after annealing at 900-1000 ° C for 1 h, Figure 1. (a) and (b). It can be seen in Figures 1(a) and (b) that small particles spread uniformly over the surface are in agglomerates. It will be noted that the higher the temperature or the duration of annealing, the higher the density of the agglomerates. It will be noted that the higher the temperature or the duration of annealing, the higher the density of the agglomerates.

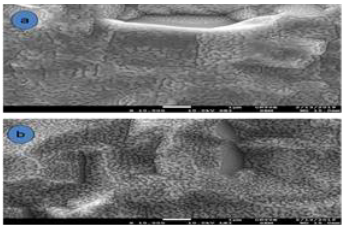

Figure 1: SEM images of a Ce deposit on Si and annealing a T different Temperatures for 1 hour under N2 a) 900 °C, b) 1000°C.

ACKNOWLEDGEMENTS

This work was supported by the Algerian Ministry of Higher Education and Scientific Research.

TOPIC

1) b.: Sustainable Manufacturing Solutions – Nanoengineering & Bio-inspired manufacturing

TAMAZ3D-A New Tool for Technical Ceramics 3D-Printing

Structural properties of zirconia-alumina-based technical ceramics produced by additive manufacturing

J. Baltazar[1], M. Silva[1], P.M.C. Torres[1], S.M. Olhero[1], J.M. Guimarães[2], J. Dias-de-Oliveira[2], J. Pinho-da-Cruz[2], S. Gouveia[3]

[1]Department of Materials Engineering and Ceramics (DEMaC), CICECO (Aveiro Institute of Materials), University of Aveiro
[2]Centre for Mechanical Technology and Automation (TEMA), Department of Mechanical Engineering, University of Aveiro
[3]Institute of Electronics and Informatics Engineering of Aveiro (IEETA), University of Aveiro
Aveiro, Portugal

***Abstract*— Alumina and zirconia are used in the manufacture of the so-called zirconia toughened alumina (ZTA) technical ceramics, used to produce several components, including supports for catalysts and thermal or electrical insulators. Due to the strict quality control in the components, the fabrication of these ceramics requires tight limits in dimensions and properties. From the existing techniques, Additive Manufacturing (AM) and, in particular, Robocasting appears to facilitate the accurate manufacture of such components [1,2]. This technique allows the creation of intricate designs with precise dimensions, and typically uses less material, thus reducing or eliminating wastes [3]. However, the consequences of AM implementation in the industrial system, if not supported by fundamental research, can lead to unnecessary consumption of materials and resources. TAMAZ3D aims to fine-tune the manufacture of technical ceramics, specifically components based on alumina, zirconia or a mixture of both by AM, namely Direct Write Assembling (DWA, also known as robocasting). This project will develop mathematical models and statistical methods to estimate optimal parameters of the components that influence the final material properties and evaluate the technique accuracy, when moving from the CAD model to the result of the ceramic part, after printing and sintering. This work presents an overview of the earliest structural properties for alumina (100Al) and zirconia (100Zr) compositions obtained by robocasting, aiming to correlate processing conditions to the final microstructure. Aqueous based alumina (100Al, Alumina CT3000, Alcoa) and zirconia (100Zr, Zirconia TZ-3YS, TOSOH, Japan) suspensions were prepared with 50-vol% and 45-vol% total solids loading, respectively, using a dispersant agent. The maximum solid loading achieved for each powder and respective amount of dispersant was based on suspension homogeneity and stability evaluated by rheological measurements. From as-stabilized suspensions, inks for DWR were developed by fine-tuning the most appropriate amounts of thickening additives. 3D reticulated samples (parallelepipeds with 45*3*5 mm, following the standard ASTM/C1161-13 [4], Fig. 1), were fabricated by DWR, using a tip nozzle diameter of 0.41 mm. All specimens were then dried and subsequently sintered at 1550ºC. The samples obtained were then structural and mechanically characterized, and their microstructure analyzed by Scanning Electron Microscopy (SEM). Figure 2 presents a cross section of the fracture surface of 100Al (a) and 100Zr samples, being noticeable the porosity inter-filaments for both materials. All specimens were then dried and subsequently sintered at 1550ºC. The samples obtained were then structural and mechanically characterized, and their microstructure analyzed by Scanning Electron Microscopy (SEM). Figure 2 presents a cross section of the fracture surface of 100Al (a) and 100Zr samples, being noticeable the porosity inter-filaments for both materials.**

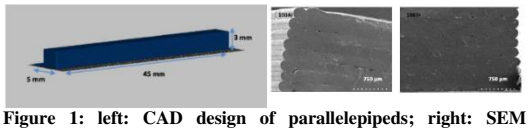

Figure 1: left: CAD design of parallelepipeds; right: SEM microstructure of 100Al and 100Zr samples obtained by robocasting.

Keywords—Alumina; zirconia; technical ceramics; aditive manufacturing.

ACKNOWLEDGMENTS

This work is funded by FEDER funds through the COMPETE 2020 Programme and National Funds through FCT - Portuguese Foundation for Science and Technology under the project number POCI-01-0145-FEDER-030493. This work was also developed within the scope of CICECO-Aveiro Institute of Materials (FCT Ref. UID/CTM/50011/2019), TEMA (FCT Ref. UID/EMS/00481/2019) and IEETA (FCT Ref. UID/CEC/00127/2019) financed by national funds through the FCT/MCTES; and CENTRO-01-0145-FEDER-022083 - Centro Portugal Regional Operational Programme (Centro2020), under the PORTUGAL 2020 Partnership Agreement, through the European Regional Development Fund (ERDF).

TOPIC

1) a.: Sustainable Manufacturing Solutions – Manufacturing processes & Simulation.

REFERENCES

[1] E. Ferraris, J. Vleugels, Y. Guo, D. Bourell, J.P. Kruth, B. Lauwers; Shaping of engineering ceramics by electro, chemical and physical processes; CIRP Annals Manufacturing Technology 65:761784, 2016.

[2] J.N. Stuecker, J.E. Miller, R.E. Ferrizz, J.E. Mudd, J. Cesarano; Advanced support structures for enhanced catalytic activity; Industrial & Engineering Chemistry Research 43(1):51-55, 2004.

[3] Bogna Stawarczyk, Mutlu Özcan, Lubica Hallmann, Andreas Ender, Albert Mehl, Christoph H. F. Hämmerlet, The effect of zirconia sintering temperature on flexural strength, grain size, and contrast ratio, Clin Oral Invest (2013) 17:269-274.

[4] A. International, «Standard Test Method for Flexural Strength of Advanced Ceramics at Ambient», vol. 94, n. Reapproved, 1996.

The use of Plane-Stress Formulation:
Review, features and constraints

Tiago Silva, João Martins, Bernardete Coelho and A. Andrade-Campos
Centre for Mechanical Technology & Automation (TEMA), Department of Mechanical Engineering
University of Aveiro (UA)
Aveiro, Portugal
tiagomsilva@ua.pt

***Abstract*— For many industrial applications and scientific research, the evaluation of engineering parts and the characterization of the materials' behavior with high accuracy is crucial. In addition, this analysis and characterization should consume the minimum time and cost [1]. The use of the plane-stress formulation could decrease the design time by using a 2D analysis instead of the more complex and resources' consumer 3D analysis. The plane-stress formulation is a simplification of the general 3D formulation and, therefore, cannot be used without awareness of its constraints. Furthermore, the plane-stress formulation is often used in sheet metal characterization that uses classical mechanical tests, such as shear, tensile and biaxial tests, in which strain states can reach high levels of triaxial hardening [2, 3].**

The aim of this work is to evaluate quantitatively the limitations of the plane-stress formulation in sheets (thin parts). Focusing on this objective, numerical studies using the plane-stress formulation applied to a simple test sample are presented and analyzed. Moreover, the use of the plane-stress formulation is analyzed and evaluated with the 3D complete formulation, considering testing samples with different thickness. According the testing type – tensile, shear or biaxial – different criteria were selected.

The main conclusions obtained from this work are: (i) the application range of the plane-stress formulation depends on the wall thickness ratio, and (ii) the constraints and the testing type influences the results accuracy.

Keywords*— *Specimen Design, Numerical Analysis, Mechanical Testing, Material Characterisation, Plane-Stress formulation component.

ACKNOWLEDGMENT

The authors gratefully acknowledge the financial support of the Portuguese Foundation for Science and Technology (FCT) under the projects PTDC/EME-APL/29713/2017 (CENTRO-01-0145-FEDER-029713), PTDC/EMS-TEC/6400/2014 (POCI-01-0145-FEDER-016876), PTDC/EME-EME/31243/2017 (POCI-01- 0145-FEDER-031243) and PTDC/EME-EME/30592/2017 (POCI-01-0145-FEDER-030592) by UE/FEDER through the programs CENTRO 2020 and COMPETE 2020, and UID/EMS/00481/2019-FCT under CENTRO-01-0145-FEDER-022083.

TOPIC

1) a.: Sustainable Manufacturing Solutions – Manufacturing processes & Simulation.

REFERENCES

[1] J. M. P. Martins, A. Andrade-Campos, and S. Thuillier, "Comparison of inverse identification strategies for constitutive mechanical models using full-field measurements," Int. J. Mech. Sci., vol. 145, pp. 330–345, Sep. 2018.

[2] E. J. Hearn, "Mechanics of Materials 2 – An Introduction to the Mechanics of Elastic and Plastic Defiormation of Solids and Structural Materials", 3rd Edition, Butterworth-Heinemann, 1997 .

[3] M. Pinheiro and R. G. Wan, "Finite element analysis of diffuse instability using an implicitly integrated pressure-density dependent elastoplastic model," *Finite Elem. Anal. Des.*, vol. 46, no. 6, pp. 487–495, 2010.

Thermo-mechanical analysis of PVC-based Wood Plastic Composite decking boards

Sabiq Sulaiman
Research Fellow, TEMA – Centre for Mechanical Technology and Automation, University of Aveiro
Aveiro, Portugal

Rui Moreira
Assistant Professor, Centre for Mechanical Technology and Automation, Department of Mechanical Engineering, University of Aveiro
Aveiro, Portugal

***Abstract*— Wood-plastic Composite (WPC) decks are innovative building materials used for outdoor flooring in a wide range of applications. When exposed to hot weather conditions, decking floors are facing thermal deformation by bending. This is a very critical situation, where the bending deck can even break the joints affecting the structural integrity of the deck assembly. Persistence of this situation makes the decking floors less safe and are susceptible to accidents. As an initiative to find a solution for this problem, it is necessary to study the thermo-mechanical behavior of the deck materials. In this work, a comprehensive study on different types of deck specimens, non-reinforced and fiber-reinforced, has been carried out in a specially designed test rig to investigate their thermal responses in terms of deformation and induced stress. From the experimental analysis, it has been observed that the thermal effect provided by temperature variations on decking boards may be important in terms of deformation induced by asymmetric thermal loading. The thermal influence was measured in terms of load measured in the free end of a fixed board, as well as the displacement measured in the same location. In case of the reinforced WPCs, the magnitude of response was almost half as compared to the non-reinforced ones. Results shows that the reinforcement has a noteworthy influence on the thermal stability of WPC decking boards.**

Keywords—WPC; deck; PVC-WPC; thermomechanical.

ACKNOWLEDGMENT

This work is done as part of the project SMART COVER POOL AND DECK under (no. 17656) financed by COMPETE 2020. My huge gratitude to my supervisor Prof. Rui Moreira, Assistant Professor, University of Aveiro for his valuable guidance and support throughout this research work.

TOPIC

1) a.: Sustainable Manufacturing Solutions – Manufacturing processes & Simulation.

REFERENCES

[1] "Behavior Of Externally Restrained Noncomposite Concrete Bridge Deck Panels". 2012. ACI Structural Journal 109 (2). doi:10.14359/51683627.

[2] Carroll, Douglas R., Robert B. Stone, Anthony M. Sirignano, Rosanna M. Saindon, Stephen C. Gose, and Marc A. Friedman. 2001. "Structural Properties Of Recycled Plastic/Sawdust Lumber Decking Planks". Resources, Conservation And Recycling 31 (3): 241-251. doi:10.1016/s0921-3449(00)00081-1.

[3] Carroll, Douglas R., Robert B. Stone, Anthony M. Sirignano, Rosanna M. Saindon, Stephen C. Gose, and Marc A. Friedman. 2001. "Structural Properties Of Recycled Plastic/Sawdust Lumber Decking Planks". Resources, Conservation And Recycling 31 (3): 241-251. doi:10.1016/s0921-3449(00)00081-1.

[4] Cheung, Hoi-yan, Mei-po Ho, Kin-tak Lau, Francisco Cardona, and David Hui. 2009. "Natural Fibre-Reinforced Composites For Bioengineering And Environmental Engineering Applications". Composites Part B: Engineering 40 (7): 655-663. doi:10.1016/j.compositesb.2009.04.014.

[5] Defoirdt, Nele, Soetkin Gardin, Jan Van den Bulcke, and Joris Van Acker. 2010. "Moisture Dynamics Of WPC And The Impact On Fungal Testing". International Biodeterioration & Biodegradation 64 (1): 65-72. doi:10.1016/j.ibiod.2009.07.010.

[6] Fell, David R, Jon Thomas, and Eric Hansen. 2006. "Evolving Consumer Preferences For Residential Decking Materials". The Forestry Chronicle 82 (2): 253-258. doi:10.5558/tfc82253-2.

[7] Fell, David R, Jon Thomas, and Eric Hansen. 2006. "Evolving Consumer Preferences For Residential Decking Materials". The Forestry Chronicle 82 (2): 253-258. doi:10.5558/tfc82253-2.

[8] Ganguly, Indroneil, and Ivan L. Eastin. 2009. "Trends In The US Decking Market: A National Survey Of Deck And Home Builders". The Forestry Chronicle 85 (1): 82-90. doi:10.5558/tfc85082-1.

[9] Holbery, James, and Dan Houston. 2006. "Natural-Fiber-Reinforced Polymer Composites In Automotive Applications". JOM 58 (11): 80-86. doi:10.1007/s11837-006-0234-2.

[10] Huang, R., Xiong, W., Xu, X. and Wu, Q. (2012). THERMAL EXPANSION BEHAVIOR OF CO-EXTRUDED WOOD-PLASTIC COMPOSITES WITH GLASS-FIBER REINFORCED SHELLS. BioResources, 7(4).

[11] Jiang, Haihong, and D. Pascal Kamdem. 2004. "Development Of Poly(Vinyl Chloride)/Wood Composites. A Literature Review". Journal Of Vinyl And Additive Technology 10 (2): 59-69. doi:10.1002/vnl.20009.

[12] Jiang, Haihong, and D. Pascal Kamdem. 2004. "Effects Of Copper Amine Treatment On Mechanical Properties Of PVC/Wood-Flour Composites". Journal Of Vinyl And Additive Technology 10 (2): 70-78. doi:10.1002/vnl.20010.

[13] Jiang, Long, Michael P. Wolcott, Jinwen Zhang, and Karl Englund. 2007. "Flexural Properties Of Surface Reinforced Wood/Plastic Deck Board". Polymer Engineering & Science 47 (3): 281-288. doi:10.1002/pen.20705.

[14] Jiang, Long, Michael P. Wolcott, Jinwen Zhang, and Karl Englund. 2007. "Flexural Properties Of Surface Reinforced Wood/Plastic Deck Board". Polymer Engineering & Science 47 (3): 281-288. doi:10.1002/pen.20705.

[15] Lopez, J. L., M. Sain, and P. Cooper. 2005. "Performance Of Natural-Fiber-Plastic Composites Under Stress For Outdoor Applications: Effect Of Moisture, Temperature, And Ultraviolet Light Exposure". Journal Of Applied Polymer Science 99 (5): 2570-2577. doi:10.1002/app.22884.

[16] Machado, José S., Sara Santos, Fernando F.S. Pinho, Fábio Luís, Ana Alves, Rita Simões, and José Carlos Rodrigues. 2016. "Impact Of High Moisture Conditions On The Serviceability Performance Of Wood Plastic Composite Decks". Materials & Design 103: 122-131. doi:10.1016/j.matdes.2016.04.030.

[17] Machado, José S., Sara Santos, Fernando F.S. Pinho, Fábio Luís, Ana Alves, Rita Simões, and José Carlos Rodrigues. 2016. "Impact Of High Moisture Conditions On The Serviceability Performance Of Wood Plastic Composite Decks". Materials & Design 103: 122-131. doi:10.1016/j.matdes.2016.04.030.

[18] Oksman, K., M. Skrifvars, and J.-F. Selin. 2003. "Natural Fibres As Reinforcement In Polylactic Acid (PLA) Composites". Composites Science And Technology 63 (9): 1317-1324. doi:10.1016/s0266-3538(03)00103-9.

[19] Pickering, K.L., M.G. Aruan Efendy, and T.M. Le. 2016. "A Review Of Recent Developments In Natural Fibre Composites And Their Mechanical Performance". Composites Part A: Applied Science And Manufacturing 83: 98-112. doi:10.1016/j.compositesa.2015.08.038.

[20] Tamrakar, Sandeep, Roberto A. Lopez-Anido, Alper Kiziltas, and Douglas J. Gardner. 2011. "Time And Temperature Dependent Response Of A Wood–Polypropylene Composite". Composites Part A: Applied Science And Manufacturing 42 (7): 834-842. doi:10.1016/j.compositesa.2011.03.011.

[21] Zhou, Aixi, and Thomas Keller. 2005. "Joining Techniques For Fiber Reinforced Polymer Composite Bridge Deck Systems". Composite Structures 69 (3): 336-345. doi:10.1016/j.compstruct.2004.07.016.

Weldability of an advanced high strength steel

Bruno S. Carvalho[1], Rafael O. Santos[1,2], António B. Pereira [1]
[1]TEMA–Centre for Mechanical Technology and Automation, Department of Mechanical Engineering, University of Aveiro Campus de Santiago, 3810-193, Aveiro, Portugal
[2]CEFET/RJ - Campus Angra dos Reis
Rua do Areal, 522, 23953-030, Angra dos Reis, Brasil

***Abstract*— This work aimed to study the laser weldability of the recently developed third generation steel Gen3 980T. Currently, the automotive industry is looking for solutions that promote environmental sustainability and road safety [1]. The advanced high-strength steels are one of the proposed solutions, so it becomes pertinent to study joining processes of these materials, as for example the one selected in this work, the laser welding [2]. For the present study, small samples were welded in butt joint type with and without filler metal. For the welding process, it was used the pulsed Nd:YAG equipment SISMA SWA300. After the welds, tensile tests, microstructures, hardness tests, and XRD analysis were performed. The purpose of all this experimental work was to obtain reliable conclusions regarding the mechanical and microstructural properties of this new material, as well as its weldability with and without filler metal. The base metal, unaffected by the heat, presented a microstructure consisting of ferrite, martensite and a low percentage of retained austenite. An essentially martensitic microstructure was observed in the central zone of the weld bead where high values of hardness were measured. For the base metal the tensile strength was 1055 MPa with a maximum elongation of 23%. With respect to welded samples without filler metal, the weld bead showed higher tensile strength than the base metal, the same was observed for welded samples with filler metal equal to the base metal. The welds with filler metal different than the base metal broke through the bead.**

Keywords—laser welding; third generation steel; Gen3 980T steel; tensile tests; microstructure; hardness tests

ACKNOWLEDGMENT

This work is supported by the projects

UID/EMS/00481/2019-FCT - FCT - Fundação para a Ciência e a Tecnologia;

Projeto nº 32466, POCI-01-0145-FEDER-032466, Aviso 02/SAICT/2017 – SAICT;

Projeto nº 33912. AAC nº 03/SI/2017 - I&DT Empresarial (Copromoção);

CENTRO-01-0145-FEDER-022083 - Centro Portugal Regional Operational Programme (Centro2020), under the PORTUGAL 2020 Partnership Agreement, through the European Regional Development Fund

TOPIC

1) a.: Sustainable Manufacturing Solutions – Manufacturing processes & Simulation.

REFERENCES

[1] M.Y. Demeri, Advanced High Strength Steels – Science, Technology, and Applications. ASM International, 2013.

[2] S. Mahadev and T. Muralidhar, Welding and Joining of Advanced High Strength Steels. Woodhead Publishing, 2015.

[3] M. Young, The Technical Writer's Handbook. Mill Valley, CA: University Science, 1989.

Technologies for the Well-Being

Acoustic emission due to road traffic

Antonio Pascale, Paulo Fernandes, Margarida C. Coelho
Department of Mechanical Engineering / Centre for Mechanical Technology and Automation (TEMA)
University of Aveiro
Aveiro, Portugal
a.pascale26@studenti.unisa.it, paulo.fernandes@ua.pt, margarida.coelho@ua.pt

Claudio Guarnaccia
Department of Civil Engineering
University of Salerno
Fisciano, Italy
cguarnaccia@unisa.it

***Abstract*— The noise pollution created by the road traffic can lead to physical, social and psychological damages on the human well-being. In order to protect the environment and the human health, the UE enacted the directive 2002/49/CE [1]. This directive imposed the creation of noise maps, the information of the people on the effects of noise pollution, imposed to the nations the obligation to reduce the noise in the critical areas and suggested several actions for increasing the awareness and assessment of noise.**

In road traffic noise modeling, a single vehicle can be considered like a point-like noise source. Its noise emission is mainly due to three causes: the engine, the rolling (contact between the tires and the road surface) and the aerodynamics. The aerodynamics' contribution can be neglected if the vehicle's speed is lower than 130 km/h or can be included in the rolling part.

The main objective of this work is to include noise related variables in the assessment of the road network performance. This research is being developed under the work package "6 - Impacts assessment for a smart, green and integrated mobility" of the "MobiWise: from mobile sensing to mobility advising" R&D project.

With the CNOSSOS model [2] it is possible to calculate the sound power level of four categories of vehicles (light motor vehicles, medium heavy vehicles, heavy vehicle and powered two-wheelers). The source sound power level is calculated for each band of octave (from 125 Hz to 4 kHz) based on the vehicle speeds. This model uses different formulas for sound power level due to the propulsion and to the rolling for each category of vehicles. The sound power level depends on the noise source and for a single vehicle's transit it is possible to calculate the equivalent continuous sound level (Leq) using the relationship between the two physical quantities given by the model.

In order to study the noise pollution produced by road traffic, predictive models can be applied. These models can be based on statistic approach [3] or, when the mean speed is taken into account, on a semi dynamic structure [4, 5]. More advanced models can include a microscopic description of the noise produced by the single vehicle or can be based on innovative computing techniques, such as cellular automata, neural network, etc. [6]. For the purpose of assessing road traffic noise in a relatively small environment, simple models can still lead to robust results, when validating with field measurements. For this reason, in traffic management and emissions studies, a good compromise between the easiness of implementation and the efficacy of the model must be pursued, keeping in mind that these procedures could be transferred to municipalities and/or road networks practitioners who may not be experts in advanced mathematical modeling.

Keywords—noise pollution, road traffic, CNOSSOS-EU, noise predictive models.

ACKNOWLEDGMENT

The authors acknowledge the financial support of the following projects: TEMA – CENTRO 01-0145-FEDER-022083; Strategical Project UID/EMS/00481/2019-FCT (FCT-Portuguese Science and Technology Foundation); and MobiWise (P2020 SAICTPAC/0011/2015), co-funded by COMPETE2020, Portugal2020 - Operational Program for Competitiveness and Internationalization (POCI), European Union's ERDF (European Regional Development Fund), and FCT.

TOPIC

2) b.: Technologies for the Wellbeing – Innovative technologies for Smart Cities.

REFERENCES

[1] https://eur-lex.europa.eu/LexUriServ/LexUriServ.do?uri=OJ:L:2002:189:0012:0025:IT:PDF.

[2] S. Kephalopoulos, M. Paviotti and F. Anfosso-Lédéee, "Common Noise Assessment Methods in Europe. Publications Office of the European Union, Luxembourg, pp. 180, August 2012.

[3] J. Quartieri, N.E. Mastorakis, G. Iannone, C. Guarnaccia, S. D'Ambrosio, A. Troisi, T.L.L. Lenza, "A Review of Traffic Noise Predictive Models". Proceedings of the WSEAS International Conference on "Applied and Theoretical Mechanics" (MECHANICS'09), Puerto de la Cruz, Tenerife (Spain), 14-16 December 2009. ISBN: 978-960-474-140-3 / ISSN: 1790-2769, pp. 72-80.

[4] J. Quartieri, G. Iannone, C. Guarnaccia, "On the Improvement of Statistical Traffic Noise Prediction Tools". Proceedings of the 11th WSEAS Int. Conf. on "Acoustics & Music: Theory & Applications" (AMTA '10), Iasi, Romania, 13-15 June 2010. ISBN: 978-960-474-192-2/ ISSN: 1790-5095, pp. 201-207.

[5] C. Guarnaccia, J. Bandeira, M. C. Coelho, P. Fernandes, J. Teixeira, G. Ioannidis, J. Quartieri, "Statistical and Semi-Dynamical Road Traffic Noise Models Comparison with Field Measurements". Proceedings of the 2nd Int. Conf. on Mathematical Methods & Computational Techniques in Science & Engineering (MMCTSE), Murray Edwards College, University of Cambridge, UK, February 16-18, 2018.

[6] C. Guarnaccia, "Advanced Tools for Traffic Noise Modelling and Prediction". WSEAS Transactions on Systems, Issue 2, Vol.12, pp. 121-130 (2013), Print ISSN: 1109-2777, e-ISSN: 2224-2678.

Adsorption heat pumps for space and water heating: from component to complete system

J. M. S. Dias

Department of Mechanical Engineering
University of Aveiro
Aveiro, Portugal
joaomdias@ua.pt

V. A. F. Costa

Department of Mechanical Engineering
University of Aveiro
Aveiro, Portugal
v.costa@ua.pt

***Abstract* — By 2016, the residential sector accounted for 25.4% of Europe's final energy consumption, from which 79.2% was used for space and water heating [1]. Most of this energy comes from non-renewable and environmentally harmful energy sources. Heat pumps can draw heat from free low temperature energy sources (e.g. ambient air, the ground or water bodies) and use it to provide water and space heating for residential buildings [2]. Contrary to conventional vapor compression heat pumps (VCHPs) that work with global warming potential (GWP) refrigerants (mainly CFCs and HCFCs), adsorption heat pumps (AHPs) cause low environmental impact as they use zero or almost zero GWP refrigerants. Water, ammonia, ethanol and methanol are common environmentally friendly refrigerants used on AHPs, contributing to decrease the greenhouse gases' emissions. VCHPs rely on a compressor that requires electrical energy to work whereas AHPs can be driven by natural gas, waste heat or solar or geothermal energies.**

In order to improve the coefficient of performance (COP) and specific heating power (SHP) of AHPs, physical models that are capable of describing an AHP system must be developed [3]. First, it is necessary to build a model for the adsorber, which is the main component of an AHP. Then, the remaining components must be added to the model. Despite the many different adsorber types found in literature, it has been acknowledged by many researchers that the externally coated tube adsorber provides the best COP and SHP for most applications. Thus, physical models for this type of adsorber were developed and analyzed. A dimensional analysis of a coated tube adsorber is presented in [4]. That study concluded that a 2D distributed parameter model is suitable to accurately describe an externally coated tube adsorber. The partial differential equations (PDE) system composing the physical model is solved by using the method of lines to discretize along the radial and axial coordinates through the finite difference method. First, the axial coordinate is discretized and then, every element is discretized along the radial direction. The forward finite difference and the centered finite difference schemes were used for the first and second order derivatives, respectively, and the PDE system reduced to a system of ordinary differential equations (ODE) which can be solved using Matlab.

The adsorber's physical model has to be integrated with the physical models for the remaining system's components, namely the evaporator, the condenser, the water tank and the regeneration heater. Only then, a complete AHP system can be simulated and its performance evaluated. The physical model of a complete AHP system has been developed, representing a significant advance on the scientific knowledge of AHPs. Preliminary results show that the optimal conditions for the adsorber considered alone are not always optimal for the complete system. Furthermore, the operation limits of the complete system are more strict then those of the standalone adsorber. The complete AHP system must be further investigated and experimental data must be obtained to allow validation through comparisons with the simulations' results.

Keywords—Adsorption heat pump; adsorber; physical model; coeficient of performance; specific heating power; system's performance.

ACKNOWLEDGMENT

The present study was developed in the scope of the Smart Green Homes Project [POCI-01-0247-FEDER-007678], a copromotion between Bosch Termotecnologia S.A. and the University of Aveiro. It is financed by Portugal 2020 under the Competitiveness and Internationalization Operational Program, and by the European Regional Development Fund.

The authors acknowledge the Portuguese Foundation for Science and Technology for the financial support provided through project UID/EMS/00481/2013-FCT, and CENTRO-01-0145-FEDER-022083.

Cofinanciado por: COMPETE 2020 PORTUGAL 2020 UNIÃO EUROPEIA Fundo Europeu de Desenvolvimento Regional

TOPIC

2) a.: Technologies for the Wellbeing – Multiscale technologies and devices for medicine, environment and energy.

REFERENCES

Eurostat, "Energy consumption in households," Eurostat: statistics explained, 2018. [Online]. Available: https://ec.europa.eu/eurostat/statistics-explained/index.php?title=Energy_consumption_in_households.

J. L. Sawin, K. Seyboth, and F. Sverrisson, "Renewables 2017: Global status report," 2017.

J. M. S. Dias and V. A. F. Costa, "Adsorption heat pumps for heating applications: A review of current state, literature gaps and development challenges," Renew. Sustain. Energy Rev., vol. 98, pp. 317–327, Dec. 2018.

J. M. S. Dias and V. A. F. Costa, "Which dimensional model for the analysis of a coated tube adsorber for adsorption heat pumps?," Energy, vol. 174, pp. 1110–1120, May 2019.

Application of Intelligent Supervised Predictive Control in Smart Green Buildings

Yahya Sheikhnejad[1], Nelson Martins[1], Jorge Ferreira[1]
1TEMA, Department of Mechanical Engineering, University of Aveiro
Aveiro, Portugal

***Abstract* — Nowadays two main problems of rapid continuous growth of world population and depletion of fossil fuel resources simultaneously cause a serious energy provision problem. To solve this issue, the global consensus is on stepping into the roadmap of agenda 2030 to mitigate human footprint on an environment with the emphasis on the management of energy consumption. By focusing on residential/commercial buildings, this study presented a new generation of adaptable intelligent control systems in which energy consumption tends to be minimized without sacrificing occupants' thermal comfort. With this methodology, artificial intelligence (AI), as well as multi-objective optimization, is responsible for model modification toward the optimum HVAC setpoints by which two opposing objectives be met. In fact, the considered energy management, as a non-destructive retrofitting procedure, can be applied to both new and existing buildings and with any level of HVAC technology.**

The supervisory predictive control includes advanced simulation and optimization algorithms which interact with conventional machine-level controllers of HVAC systems, in order to define optimized set points considering current and forecasted operation conditions. Toward materializing this idea, there are some publications have already addressed this concern by adaptive surrogate modelling [1] or Ventilation control strategy using ANN [2]. A novel deep learning method also have been used to improving prediction performance for indoor temperature in public buildings [3] while Bolchini et al. [4] proposes a methodology for monitoring and data analysis in buildings, leading the user in the design and implementation of smart environments able to collect information on spaces and the comfort.

The purpose of this study is to develop an intelligent supervised predictive control model and algorithms for tuning building HVAC setpoints in order to manage energy consumption while providing thermal comfort measured by PPD and PMV.

Neural network (NN) as a powerful branch of AI can be employed to eliminate time-consuming building energy simulation process and predict the building reaction corresponding to its condition. In addition, among learning paradigms, supervised machine learning with a fast and accurate performance is adopted while Feed-forward multi-layer perceptron is used as a robust architecture for the NN. Moreover, the gradient descent method of optimization for back propagation algorithm is employed to reduce NN error during iterative procedure. Also, particle swarm optimization (PSO) algorithm, as a stochastic global optimization method, is suitable for high dimensional, non-convex, non-continuous problems. The thermal comfort for the occupants measures by the Fanger's approach illustrated in [5]. A python code is being developed to handle the tasks corresponding to ANN, PSO and running EnergyPlus to extract output results. A platform should be established for communication between building thermal simulator (EnergyPlus commercial software) and Python optimizer code. This platform can be made by BCVTB software.

Keywords— Machine learning, Supervised predictive control, Smart green building.

ACKNOWLEDGEMENT

The present study was developed in the scope of **the Smart Green Homes** Project [POCI-01-0247-FEDER-007678], a co-promotion between **Bosch Termotecnologia S.A.** and the **University of Aveiro**. It is financed by Portugal 2020 under the Competitiveness and Internationalization Operational Program and by the European Regional Development Fund.

TOPIC

2) a.: Technologies for the Wellbeing – Multiscale technologies and devices for medicine, environment and energy.

REFERENCES

[1] D.A. Goncalves,PhD thesis, , University of Aveiro, 2016.

[2] S. Cao, C. Ren, Ventilation control strategy using low-dimensional linear ventilation models and artificial neural network, Build. Environ. 144 (2018) 316–333. doi:10.1016/j.buildenv.2018.08.032.

[3] C. Xu, H. Chen, J. Wang, Y. Guo, Y. Yuan, Improving prediction performance for indoor temperature in public buildings based on a novel deep learning method, Build. Environ. 148 (2019) 128–135. doi:10.1016/j.buildenv.2018.10.062.

[4] C. Bolchini, A. Geronazzo, E. Quintarelli, Smart buildings : A monitoring and data analysis methodological framework, Build. Environ. 121 (2017) 93–105. doi:10.1016/j.buildenv.2017.05.014.

[5] L. Peeters, R. de Dear, J. Hensen, W. D'haeseleer, Thermal comfort in residential buildings: Comfort values and scales for building energy simulation, Appl. Energy. 86 (2009) 772–780. doi:10.1016/j.apenergy.2008.07.011.

Assessing the emission impacts of autonomous vehicles in metropolitan freeways

Ricardo F.Tomás, Paulo Fernandes, Eloísa Macedo, Jorge M. Bandeira, Margarida C. Coelho
Department of Mechanical Engineering / Centre for Mechanical Technology and Automation (TEMA)
University of Aveiro, Portugal
ricardotomas@ua.pt; paulo.fernandes@ua.pt; macedo@ua.pt; jorgebandeira@ua.pt; margarida.coelho@ua.pt

***Abstract*— Road transport was in 2016 responsible for 74% of the 33% energy consumed by the transport sector [1]. Passenger cars accounted for 41% of the transport greenhouse gases (GHG) in the European Union countries, in 2016 [2].**

Intelligent Transport Systems (ITS) have been supporting the autonomous vehicles (AVs) technology, that offer numerous benefits such as to allow for more productive use of time spent in vehicles, reduce energy use and land use [3].

AVs have shown promising results at both social and economic levels but there is no consensus about their environmental benefits in a context of traffic context. Thus, this research assessed the environmental and traffic performance impacts of the AVs in an urban freeway corridor in a metropolitan area. The proposed methodology resorted to VISSIM tool to code and assess traffic operations [5]. Vehicular emissions were estimated using the Vehicle Specific Power (VSP) and EMEP/EEA methodologies [6;7].

The case study is based in the city of Porto (Portugal), which according to data from 2016 from TomTom, was the second city in the National ranking where drivers spent more time in traffic (~31 minutes) [8]. The candidate freeway is a stretch (~9km in length) of the Via de Cintura Interna (VCI), 8 interchanges, 3-4 lanes by travelling direction, 80 km/h speed limit and an average daily traffic ranged from 113 680 to 149 520 [9].

Three different AV penetration rates based on long-term market prediction (10%,20% and 30%) for through traffic along VCI were implemented [10]. These scenarios were compared in terms of emissions (carbon dioxide, carbon monoxide, nitrogen oxides and hydrocarbons) and traffic performance (travel time and stop-and-go situations) against current situation – conventional vehicles (CVs) only. Emissions and traffic performance scenarios were assessed on three levels: 1) overall study domain; 2) corridor; and 3) impact of AVs on CVs.

Results confirmed that impacts of AVs were not statistically significant for penetration rates below 30% in the overall study domain (reductions up to 2% for pollutants emissions and average travel time). Corridor-level analysis showed that a decrease of 5% on emissions can be expected with AVs technology, but travel time is penalized up to 13% for both AVs and CVs, comparing to the actual situation. Furthermore, results showed that the increase of AV rates may result in higher travel times for CV, although stop-and-go situations decreased.

In summary, this research sought to contribute for better understanding of future AV penetration rates scenarios for both traffic performance and carbon dioxide, carbon monoxide, nitrogen oxides and hydrocarbon emissions on congested freeways. Also, it provides solid knowledge of the differences in traffic-related impacts between AV and CV, and of the incorporation of eco-routing algorithms to govern AV operations.

Keywords—Autonomous Vehicles; Mixed Traffic; Freeway Corridors; Emissions.

TOPIC

2) b.: Technologies for the Wellbeing – Innovative technologies for Smart Cities.

ACKNOWLEDGMENT

The authors acknowledge IT-Porto,for providing the traffic data,and the financial support of the following projects:TEMA–CENTRO 01-0145-FEDER-022083;Strategic Project UID/EMS/00481/2019-FCT (FCT-Portuguese Science and Technology Foundation);@CRUiSE project(PTDC/EMS-TRA/0383/2014),funded within Project 9471–Reforçar a Investigação,o Desenvolvimento Tecnológico e a Inovação and supported by European Community Fund FEDER;MobiWise(P2020 SAICTPAC/0011/2015),co-funded by COMPETE2020,Portugal2020-Operational Program for Competitiveness and Internationalization (POCI),European Union's ERDF (European Regional Development Fund),and FCT;CISMOB (PGI01611, funded by Interreg Europe Programme); DICA-VE (POCI-01-0145-FEDER-029463),Driving2Driverless(POCI-01-0145-FEDER-031923)and inFLOWence (POCI-01-0145-FEDER-029679)projects funded by FEDER through COMPETE2020-Programa Operacional Competitividade e Internacionalização (POCI),and by national funds(OE),through FCT/MCTES.

REFERENCES

[1] EEA, "Final energy consumption by sector and fuel," Environmental European Agency, January 2019. [Online]. Available: https://www.eea.europa.eu/data-andmaps/indicators/finalenergyconsumption-by-sector-9/assessment-4.[Accessed 9 June 2019].

[2] Transport & Environment, "CO2 emissions from Cars: the facts," European Federation for Transport and Environment AISBL, Brussels, Belgium, 2018.

[3] V. A. C. v. d. Berg and E. T. Verhoef, "Autonomous cars and dynamic bottleneck congestion: the effects on capacity, value of time and preference heterogeneity," Transportation Research Part B, vol. 94, pp. 43-60, 2016.

[4] PTV AG., "PTV VISSIM 9 User Manual: Planung Transport Verkehr AG," Karlsruhe, Germany, 2016.

[5] US EPA, "Methodology for developing emission rates for EPA's multi-scale motor vehicle & equipment emission system," Prepared by North Carolina State University for US Environmental Protection Agency, Ann Arbor, Michigan, 2002.

[6] EEA, "EMEP/EEA air pollutant emission inventory guidebook. Exhaust emissions from road transport.," European Environmental Agency, 2013.

[7] TomTom, "Traffic congestions statistics for Porto based on TomTom's historical database for 2016," 2018. [Online]. Available: https://www.tomtom.com/en_gb/trafficindex/city/porto.

[8] IMT, "Relatório de Tráfego na Rede Nacional de Auto-Estradas [In Portuguese]," Portuguese Institute for Mobility and Transport, 2018.[Online].Available:http://www.imtip.pt/sites/IMTT/Portugues/InfraestruturasRodoviarias/RedeRodoviaria/Relatrios/Relat%C3%B3rio%20de%20Tr%C3%A1fego%20%204%C2%BA%20Trimestre%20de%202018.pdf.

[9] J. Nieuwenhuijsen, G. H. d. A. Correia, D. Milakis, B. v. Arem and E. v. Daalen, "Towards a quantitive method to analyse the long term innovation diffusin of automated vehicles technology using system dynamics," Transportation Research Part C: Emerging Technologies, vol. 86, pp. 300-327, 2017.

Chondrocyte incorporation onto electrospun scaffolds for cartilage tissue engineering

Ângela Semitela, Gonçalo Ramalho, Paula A.A.P. Marques and António Completo
TEMA, Department of Mechanical Engineering, University of Aveiro, Portugal

Cátia Sousa and Alexandrina Mendes
CNC, Centre for Neuroscience and Cell Biology, University of Coimbra, Portugal

***Abstract*— Cell incorporation onto three-dimensional (3D) biocompatible scaffolds is a crucial step to obtain functional tissue-engineered cartilage. The efficacy of the use of scaffolds depends on their ability to interact with cells, which begins with the incorporation process [1]. Several seeding techniques have been successfully on uniformly incorporating cells through the scaffolds [2], however those cannot be applied for electrospun scaffolds. The characteristic small pore size of these structures prevents cell infiltration, relegating tissue formation to the surface. Several methodologies have been reported to increase pore size of the electrospun scaffolds using sacrificial materials, but these manipulations generally led to degradation of the scaffold final mechanical properties [3]. Cellular integration during the scaffolds construction by electrospinning can be a suitable approach to develop functional tissue constructs, using electrospraying technology. Cell electrospraying, a concept first introduced in 2005 by Jayasinghe, enables the deposition of living cells onto specific targets by exposing the cell suspension to an external high intensity electric field [4]. Several cell types have been electrosprayed and survived with no significant influence on a genetic, genomic and physiological level [5]. Here, the preliminary combination of polymer electrospinning with cell electrospraying was performed, in an attempt to overcome the challenges of cell infiltration into electrospun scaffolds for cartilage tissue engineering. First, several chondrocyte electrospraying experiments were performed to access the optimal electrospraying conditions. Then, using the selected parameters, the preliminary association of chondrocyte electrospraying with polymer electrospinning was performed alternating the two technologies. The polymer selected here was the polycaprolactone (PCL) and gelatin, already reported as beneficial for cartilage repair purposes [6]. The prepared scaffolds were then cultured for 7 days and the respective cell viability assessed. The percentage of viability was calculated as a ratio of the metabolic activity of the electrosprayed chondrocytes and the metabolic activity of chondrocytes that did not underwent any process. The chondrocyte distribution was also evaluated. Post-electrosprayed chondrocytes viabilities were considerably high (> 80%), particularly at low needle to collector distances, confirming that the electrospraying process did not significantly influenced chondrocyte function. At higher working distances, cell loss may occur within the electrospraying chamber, resulting in decreased cell viability. The combination of both technologies was accomplished, by alternating between PCL and gelatin electrospinning and chondrocyte electrospraying. It was possible to incorporate the chondrocytes within the electrospun PCL and gelatin layers, with an apparently uniform cell distribution through the scaffolds. The presence of gelatin on the scaffolds allowed for a rapid cell attachment, due to the presence of cell recognition domains (RGD) [6]. A partial dissolution of gelatin might also have occurred, resulting in an enhanced pore size for cell migration [6]. The successful cellular integration onto the electrospun scaffolds confirmed that this technique can a promising alternative for cell incorporation into the 3D scaffolds during its electrospinning.**

Keywords – Cartilage tissue enginnering; Electrospun scaffolds; Biopolymeric biomaterials.

ACKNOWLEDGMENT

This work was supported by the Portuguese funding of Program COMPETE-FEDER, Programa Operacional Competitividade e Internacionalização through the projects POCI-01-0145-FEDER-028424, and CENTRO-01-0145-FEDER-022083. Also, by Fundação para a Ciência e Tecnologia I.P. (FCT, IP) through the projects PTDC/EME-SIS/28424/2017 and UID/EMS/00481/2019. The authors thank to FCT for the PhD grant SFRH/BD/133129/2017.

TOPIC

2) a.: Technologies for the Wellbeing – Multiscale technologies and devices for medicine, environment and energy.

REFERENCES

[1] Braghirolli, D. I.; Zamboni, F.; Acasigua, G. A. X.; Pranke, P. Association of Electrospinning with Electrospraying: A Strategy to Produce 3D Scaffolds with Incorporated Stem Cells for Use in Tissue Engineering. Int. J. Nanomedicine 2015, 10, 5159–5170.

[2] Villalona, G. A.; Udelsman, B.; Duncan, D. R.; McGillicuddy, E.; Sawh-Martinez, R. F.; Hibino, N.; Painter, C.; Mirensky, T.; Erickson, B.; Shinoka, T.; et al. Cell-Seeding Techniques in Vascular Tissue Engineering. Tissue Eng. Part B Rev. 2010, 16 (3), 341–350.

[3] Baker, B. M.; Gee, A. O.; Metter, R. B.; Nathan, A. S.; Marklein, R. A.; Burdick, J. A.; Mauck, R. L. The Potential to Improve Cell Infiltration in Composite Fiber-Aligned Electrospun Scaffolds by the Selective Removal of Sacrificial Fibers. Biomaterials 2008, 29 (15), 2348–2358.

[4] Jayasinghe, S. N.; Townsend-Nicholson, A. Stable Electric-Field Driven Cone-Jetting of Concentrated Biosuspensions. Lab Chip 2006, 6 (8), 1086–1090.

[5] Jayasinghe, S. N. Cell Electrospinning: A Novel Tool for Functionalising Fibres, Scaffolds and Membranes with Living Cells and Other Advanced Materials for Regenerative Biology and Medicine. Analyst 2013, 138 (8), 2215.

[6] Zhang, Y.; Ouyang, H.; Chwee, T. L.; Ramakrishna, S.; Huang, Z. M. Electrospinning of Gelatin Fibers and Gelatin/PCL Composite Fibrous Scaffolds. J. Biomed. Mater. Res. - Part B Appl. Biomater. 2005, 72 (1) 156–165.

Could CAVs be future eco-driving agents to influence the environmental performance of road traffic?

Mónica Rodrigues, Eloisa Macedo, Paulo Fernandes, Margarida Coelho, Mario Andrade Jorge M. Bandeira
Department of Mechanical Engineering, Centre for Mechanical Technology and Automation
University of Aveiro, Portugal
monica.joana@ua.pt; jorgebandeira@ua.pt; macedo@ua.pt; mariosandrade@ua.pt; paulo.fernendes@ua.pt; margarida.coelho@ua.pt

***Abstract*—Connected Autonomous vehicle (CAVs) could be an environmental boon or disaster, depending on public policy [1]. At operational level, CAV technologies are expected to improve fuel economy and reduce emissions per unit of distance thanks to more gradual acceleration and deceleration patterns [2] and fewer stop-and-go movements [3]. Under a likely transitional stage of co-existence of connected and automated vehicles (CAVs) and conventional vehicles (CVs), this study explores the potential effects of CAVs to reduce greenhouse gases (GHG) and pollutant emissions in different road types based on improved operational parameters. For that purpose, CAVs were assumed to behave as eco-driving agents to influence the environmental performance of overall traffic. A microscopic traffic and emission model platform was applied to simulate a European medium-sized city during the morning peak period. Three roadway sections, including motorway, rural and urban, were selected to evaluate in detail the impact of CAVs in different roads types and over multiple CAVs penetration rates (MPR) to address the following questions:**

What is the potential reduction of carbon dioxide (CO_2) and nitrogen oxides (NO_X) emissions resulting from CAVs operating in different road typologies?

How can network-wide emissions and fuel consumption vary according to different MPR of CAVs?

May CAVs significantly influence the energetic and environmental performance of CVs on different road types?

Results allow assessing the main research questions defined, concretely:

CAVs impacts were particularly beneficial for the environment in the road segment "national road", with emission reductions up to 12%. In the urban corridor, the impacts were shown to be detrimental due to an inefficient configuration of the car following adjustment parameters (CFAP) in the local context and a slight increase in the capacity of the upstream intersections. At the motorway level operating at low volume-to-capacity (V/C) ratio, impacts are negligible. Nevertheless, an optimization of the speed to 90 km/h allows reductions up to 18% of CO2 and 32% of NOx.

In sections outside the urban context, the environmental impacts resulting from the presence of CAVs are positive, following a strong linear relationship and in line with higher MPR.

CAVs showed to significantly influence the energetic and environmental performance of CVs ranging from 3 to 13%. These results suggest that even CAVs will be predominantly fully electric in the near future, the impact on network-wide emissions should be taken into account and adjusted to different driving scenarios.

ACKNOWLEDGMENT

The authors acknowledge the support of the projects: UID/EMS/00481/2019-FCT - Fundação para a Ciência e a Tecnologia (FCT); CENTRO-01-0145-FEDER-022083 - Centro2020 Regional Operational Programme, under the PORTUGAL 2020 Partnership Agreement, through the European Regional Development Fund; @CRUiSE (PTDC/EMS-TRA/0383/2014); Mobiwise (P2020 SAICTPAC/0011/2015); DICA-VE (POCI-01-0145-FEDER-029463); and InFLOWence (POCI-01-0145-FEDER-029679).

TOPIC

2) b.: Technologies for the Wellbeing – Innovative technologies for Smart Cities.

REFERENCES

[1] Greenwald JM, Kornhauser A. It's up to us: Policies to improve climate outcomes from automated vehicles. Energy Policy [Internet]. 2019;127(September 2018):445–51. Available from: https://doi.org/10.1016/j.enpol.2018.12.017.

[2] Kockelman K, Nichols A. Anticipating the Emissions Impacts of Autonomous Vehicles Using the MOVES model. In: 96th Annual Meeting of the Transportation Research Board [Internet]. Washington D.C.; 2017.

[3] Anderson, J., Kalra, N., Stanley, K., Sorensen, P., Samaras, C., & Oluwatola, O. (2016). *Autonomous Vehicle Technology: A Guide for Policymakers*. RAND Corporation. https://doi.org/10.7249/RR443-2

Development of a virtual bench for simulation and monitoring of water heating devices

Jonathan Oliveira[1], André Quintã[1,2], Jorge A. F. Ferreira[1,2], Vítor A. F. Costa[1,2]
[1]Mechanical Engineering Department, University of Aveiro
[2]TEMA, Centre for Mechanical Technology and Automation
Aveiro, Portugal

Abstract— In recent years, there has been a noticeable growth on the development and use of thermal systems where fluid flow, heat transfer and transport of energy play the dominant role. These systems encompass many engineering fields related to manufacturing, energy technology, power generation, air conditioning, and aerospace and automobile engineering, just to mention a few. Energy transfer among different parts of the systems usually involves some thermal components. Understanding of thermal energy conversion and transfer is critical for maintenance and proposal of measures to increase the efficiency of all the energy supply chain. This includes energy conversion, transmission and storage, searching for better control of available energy resources [1]. Water heating is a relevant part of the household's energy consumption, mainly using tankless gas water heaters (TGWH) for that purpose. There are design and engineering challenges to develop more efficient devices, with lower energy consumption and lower emissions of pollutant gases, simultaneously with increased comfort from the user point of view [2].

A simulated environment is the less expensive and fastest way to evaluate the relative merits of different control schemes for a given thermal system. A technique to accelerate the controllers' development is proposed and implemented. Hardware-in-the-loop simulation (HILS) proved to be useful to test hardware controllers in real time simulated virtual environments [3].

Under the scope of the Smart Green Homes project it was proposed a virtual test bench with a TGWH to support the multiple phases of controller's development, whether it is to control a real or a virtual system.

A methodology has been proposed to design the experimental platform in order to perform different experiments, such as:
Data acquisition (open-loop experiences);
Real time virtual simulation;
Microcontroller controlled virtual model;
Virtual controller controlled real plant;
Microcontroller controlled real system.

To apply this methodology, several mathematical models of thermal devices such as heat cell, proportional valves, mixing valves, bypass valves, pipes, splits and reservoirs were developed to simulate the system's dynamics of different configurations' TGWHs. Real experiences were performed to parameterize the developed models.

Two case studies were considered, one dedicated to the virtual bench concept validation, and the other dedicated to the control and monitoring of a TGWH.

Figure 1 presents the hardware of the developed virtual test bench.

Keywords—Thermal systems; controller; hardware-in-the-loop; virtual test bench.

Figure 2: Virtual test bench.

ACKNOWLEDGMENT

The present study was developed under the scope of the **Smart Green Homes** Project [POCI-01-0247-FEDER-007678], a co-promotion between **Bosch Termotecnologia S.A.** and the **University of Aveiro**. It is financed by Portugal 2020 under the Competitiveness and Internationalization Operational Program, and by the European Regional Development Fund.

Cofinanciado por:
COMPETE 2020 PORTUGAL 2020 UNIÃO EUROPEIA Fundo Europeu de Desenvolvimento Regional

TOPIC

2) a.: Technologies for the Wellbeing – Multiscale technologies and devices for medicine, environment and energy

REFERENCES

[1] Y. Jaluria, *Design and Optimization of Thermal Systems*. 2007.

[2] A. F. Quintã, J. A. F. Ferreira, A. Ramos, N. A. D. Martins, and V. A. F. Costa, Simulation models for tankless gas water heaters, *Applied Thermal Engineering*, 148, A1-A2, pp. 944-952, 2019.

[3] J. A. F. Ferreira, *Modelação de Sistemas Hidráulicos para Simulação com Hardware-in-the-loop*, PhD Thesis, Univerdidade de Aveiro, 2003.

Effect of porosity variation on the physical properties of porous silicon

H. Lachenani
Laboratoire de Physique des Techniques Expérimentales et ses Applications de Médéa LPTEAM, Département Science de la Matière, Faculté des Sciences, Université de Médéa Algérie

H. Lachenani, A. Larabi, N. Gabouze
Centre de Recherche en Technologie des Semi-conducteurs pour l'Energétique (CRTSE)
02 Bd, Frantz Fanon, B.P. 140, Alger, Algérie

***Abstract*— Porous silicon (PS) is a promising material for several applications in significant and varied fields (photoluminescence (PL), electroluminescence (EL), gas and (bio) sensing, depollution, etc.). In this work, structural, electronic and vibrational properties investigations of PS were performed using ab-initio pseudo potential plane wave (PP-PW) method founded on Density Functional Theory (DFT) described by the generalized gradient approximation (GGA) included in the CASTEP program (Cambridge Serial Total Energy Package) [1, 2]. Furthermore, the computation of Infrared Radiation absorption spectra needs the calculation of atomic vibrational modes, which was performed by the Density-Functional Perturbation Theory (DFPT).**

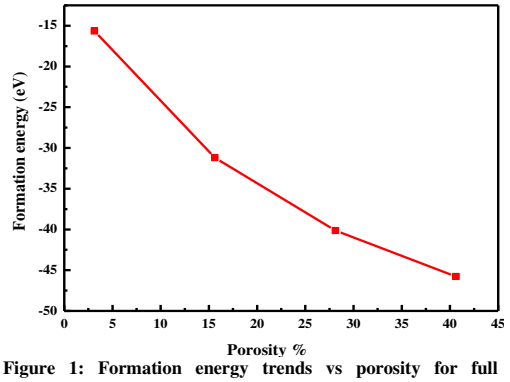

Figure 1: Formation energy trends vs porosity for full H passivation.

The formation energies obtained (Fig. 1) from Density Functional Theory (DFT) calculation confirm that the stability of Porous Silicon structure is related to its porosity and high porosities have the lowest energy formation values. In addition, the electronic band structure of all Porous Silicon structure shows direct band gap semiconductors for all studied porosities. The measured Infrared Radiation (IR) (Fig.2) spectra obtained from an elaborate sample of Porous Silicon layers was compared with the calculated spectra.

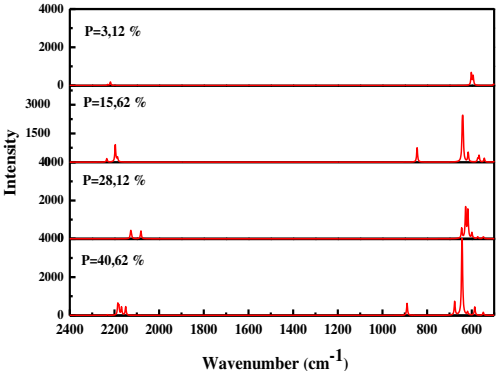

Figure 2: IR vibrational spectra for porous silicon with different porosities.

The calculated Infrared Radiation in the energy range of 2000-2300 cm^{-1}, showed for all porosities the presence of relatively high intense peaks with some shifting, corresponding to Si-H_x stretching band, characteristic of porous silicon, in good accord with the experimental one and with literature.

Keywords*— *Porous silicon, IRFT, Ab-initio, Hydrogen passivation

ACKNOWLEDGMENT

The authors are grateful to Mr Mazari Redha from university of Medea for his helpful contribution in informatics assistance.

TOPIC

2) a.: Technologies for the Wellbeing – Multiscale technologies and devices for medicine, environment and energy.

REFERENCES

[1] S. J. Clark, M. D. Segall, C. J. Pickard, P. J. Hasnip, M. I. J. Probert, K. Refson and M.C. Payne, First principles methods using CASTEP, Z. Kristallogr, 220 (2005) 567–570.

[2] M D Segall, P. J. D Lindan, M. J. Probert, C .J. Pickard, P .J .Hasnip, S. J .Clark and M .C. Payne, First-principles simulation: ideas, illustrations and the CASTEP code, J. Phys.: Condens. Matter, 14 (2002) 2717.

Electrical Properties of Pd/Ag Nanoparticles Modified Silicon Nanowires for CO_2 Detection

Naama Sabrina, Hadjersi Toufik
Research Center in Semiconductors Technology for Energetic
Division TESE, CRTSE
2 bd Frantz Fanon Algiers, Algeria
naamasabrina@crtse.dz

Naama Sabrina
University of Science and Technology USTHB
FGMGP Department of process engineering
BP 32, El Alia, Bab Ezzouar, Algeirs, Algeria
sabrina.naama@gmail.com

***Abstract*— One dimensional nanostructures play an important role in nanotechnology due to their good properties for future nanoelectronic device [1-2], photonic and optoelectronic devices [3] and more particularly as chemical or biological sensors [4-5].**

In this study, a silicon-based nanowire from silicon wafer medium doped with crystallographic orientation (100) was prepared by metal assisted chemical etching (MACE) [6]. The modification of silicon nanowires (SiNWs) by palladium (Pd) and silver (Ag) nanoparticles was performed by electroless metal deposition method.

Electrical properties of different structures Al/Pd/SiNWs/Al and Al/Ag/SiNWs/Al were studied to evaluate the performance of the sensors for CO_2 detection. The electrical characterization (I-V), response sensor, response and recovery time were performed in primary vacuum at different concentration of CO_2 (0.5, 1 and 2mbar). It was shown that the sensor response depends strongly on the modification metal type.

We have found that Pd modified structure behave as an Ohmic contact. However, Ag modified structure exhibits Schottky contact. The two structures reveal that the forward current increases with increasing CO_2 concentration, which can be explained by the decrease in the height barrier leading to an increase in the total current that flows through the device.

Also, the results reveal that the response is higher for Pd modified structure with voltage (0.05V) for high concentration (2mbar), while for Ag modified structure the response is higher with voltage (1.05V) for low concentration (0.5mbar). Operating at low voltage and low concentration of gas allows low power consumption.

Finally, the best response time and recovery time were recorded of Ag modified silicon nanowires for all CO_2 concentration. In addition, the response time is greater than recovery time indicating that the duration of the adsorption is greater than desorption time. This study shows that Ag nanoparticles can be used as catalyst for CO_2 detection. This result is very interesting since silver (Ag) is considered as relatively ductile, very malleable metal, available and less expensive.

Keywords*— *silicon nanowires; chemical etching; palladium nanoparticals; silver nanoparticles; CO_2 sensor.

ACKNOWLEDGMENT

The authors gratefully acknowledge the financial support from General Direction of Scientific Research and of Technological Development of Algeria (DGRSDT/MESRS).

TOPIC

2) a.: Technologies for the Wellbeing – Multiscale technologies and devices for medicine, environment and energy.

REFERENCES

[1] J. Goldberger, A.I Hochbaum, R. Fan, and P. Yang. "Silicon vertically integrated nanowire field effect Transistors," J. Nanolett. Vol 6, No.5, pp 973-977, February 2006.

[2] Y. Cui., and C.M. Lieber, "Functional nanoscale electronic devices assembled using silicon nanowire building blocks," Scien. American. Vol 291, pp 851-853, February 2001.

[3] C. Yang, C.J Barrelet, F. Capasso, and C.M Lieber. "Single p-type/Intrinsic/n-type Silicon Nanowires as Nanoscale Avalanche photodetectors,". J. Nanolett. Vol 6, No.12, pp 2929-2934, December 2006.

[4] Y. Cui, Q. Wei, H.K Park, and C.M. Lieber. " Nanowire nanosensors for highly sensitive and selective detection of biological and chemical species," scien. American. Vol 293, pp 1289-1292, August 2001.

[5] L.M. Lechuga, M. Alarz, L.G. Carrascosa, A. Yafera, R. Doldan, and A. Bernard. "A highly sensitive microsystem based on nanomechanical biosensors for genomics applications,". J. Sensors and Actuators, Vol 118, pp 2-10, June 2006.

[6] K-Q. Peng, X. Wang, and S-T. Lee, "Gas sensing properties of single crystalline porous silicon nanowires," J. Appl. Phys. Lett. Vol 95, pp 243112-243114, December 2009.

From the beginning of life to nanotechnology: the vital role of carbon

Gil Gonçalves
Centre for Mechanical Technology and Automation (TEMA), Aveiro, Portugal
ggoncalves@ua.pt

***Abstract*— Carbon is one of the key elements for the beginning of life on earth. Based on the recent theories carbon was one of the atomic components on the molecular precursors for build up the first forms of life. Although the impact of carbon on the evolution of human species, nowadays carbon have been also extensively explored in order to improve the quality of life in the society. Nanotechnology have been providing the necessary tools for development of new synthetic methods in order to obtain novel carbon nanomaterials with different conformations. These novel nanomaterials bring new exotic properties that can be explored as functional materials in different areas, with particular relevance in health and environmental fields. Several new carbon-based high-tech nanosystems have been developed and explored as an advance biosensor, multifunctional therapeutic agents, smart scaffolds and highly efficient nanomaterials for environmental applications. Importantly, carbon was considered the source for the creation of life and maybe will play a crucial role to avoid the extinction of human species.**

Keywords*— *Carbon; nanomedicine ; nanosensors; water remediation; tissue engeneering.

APPLICATION OF CARBON NANOSTRUCTURES FOR CANCER THERAPY AND BIOIMAGING

Carbon is considered a biogenic element (H, C, N, O, P, and S), originated from the Big Bang theory for the formation Universe. This element performed a long journey in the complex cosmic history, playing an important role in the increasing complexity of abiotic molecular precursors until the appearance of the first forms of life. [1] Indeed, the current theories about the origin of life considered that carbon is a key element for the formation of precursors essential for the beginning of biological evolution of cells.[2] It is predicted that this carbon molecular precursors were involved in the formation of the first macromolecules, essential for building blocks of the first forms of life.[3]

Carbon's discovery dates from the prehistoric humans in the form of charcoal. Curiously, one of the pioneer applications of carbon by humans consisted of artistic expression on caves. [4] Currently, coal has been explored as one of the most important sources of energy worldwide and in the production of steel. Graphite is another important allotropic form of carbon, highly explored in several industrial applications. The high temperature and chemical stability make graphite an excellent candidate for refractory material and lubricant. Diamonde, the hardest material known, still one the most requested and expensive carbon material with applications in jewelry and other industrial hi-tech applications.

Nanotechnology brought a new perspective to explore carbon materials. The run for development of novel carbon nanostructures started in 1985 with Harry Kroto et al. by the discovery of fullerenes. In 1993 Ijima et al reported a new cylindrical 1D carbon nanostructure, Single Walled Carbon Nanotubes (SWCNT). The scientific advances in the field of carbon nanomaterials started to happen in a very chaotic way. The recent highest scientific achievement was marked by the discovery of 2D graphene nanosheets that culminates in the 2010 Nobel Prize in Physics to Andre Geim and Konstantin Novoselov. [5]

The exciting advances in the preparation of carbon-based nanomaterials have led to accomplish new challenges in the design of smart materials capable to face several societal challenges. New synthetic strategies have been widely explored for the development of advanced functional carbon materials, showing a high potential for many different applications that range from the environment to healthcare. [6] This work covers the recent progress on the development of new synthetic strategies for nanoengineering carbon materials in the field of of cancer diagnosis and therapeutics. Carbon nanodots are an emerging material that have been gain high interest on the field, due to his high biocompatibility and interesting optical properties. Our work reveals the possibility to modulate the optical properties of graphene oxide carbon dots by exploring their chemical structure.

ACKNOWLEDGMENT

Gil Gonçalves is grateful to FCT for financial support through the FCT programme Stimulus of Scientific Employment – Individual Support - CEECIND/01913/2017.

TOPIC

2) a.: Technologies for the Wellbeing – Multiscale technologies and devices for medicine, environment and energy.

REFERENCES

[1] S. Pizzarello, Looking for the origin of life in cosmochemistry asteroids and their carbon-rich meteorites, Metode Science Studies Journal, (2016) 161-165.

[2] G.A. Olah, T. Mathew, G.K.S. Prakash, Chemical Formation of Methanol and Hydrocarbon (“Organic”) Derivatives from CO2 and H2—Carbon Sources for Subsequent Biological Cell Evolution and Life’s Origin, Journal of the American Chemical Society, 139 (2017) 566-570.

[3] P.B. Rimmer, O. Shorttle, Origin of Life's Building Blocks in Carbon- and Nitrogen-Rich Surface Hydrothermal Vents, Life-Basel, 9 (2019).

[4] R. Moliner, From active carbon to graphene: Evolution of carbon materials, Bol. Grupo Esp. Carbon, (2016) 2-5.

[5] A.K. Geim, K.S. Novoselov, The rise of graphene, Nat. Mater., 6 (2007) 183-191.

[6] Graphene-based Materials in Health and Environment, Springer International Publishing2016.

Impact of the storage system through batteries in the finite networks with penetration of wind energy

Jorge Mendes Tavares
Faculty of Science and Technology
University of Cape Verde
Praia, Cape Verde
jorgemendestavares@ua.pt

Fernado Neto
Centre for Technology and Automation, TEMA
University of Aveiro,
Aveiro, Portugal
fneto@ua.pt

***Abstract*— Through dynamical analysis (Generation Adequacy Analysis), with the help of DIgSILENT Powerfactory software, and applying the Monte Carlo Probabilistic Method it was possible to evaluate the impact of the storage system with batteries in finite networks, with the penetration of non-dispatchable energies, namely the energy coming from the wind power source, and to propose an appropriate model for island regions, as is the case of the Cape Verde Islands. The adequacy of the power system refers to the capacity of generation to meet the demand of the system, also considering the typical system restrictions, such as (i) generation unavailability due to fault or maintenance requirements, (ii) variation in system load on a monthly, hourly and/or minute by minute basis, (iii) variations in renewable output - notably wind power production - which in turn affects the available generation capacity[1]. Therefore, it is possible to determine the contribution of wind power generation to the overall capacity of the system and to determine the Loss of Load Probability (LOLP) and Expected Demand Not Supplied (EDNS) for centralized and decentralized generation scenarios, with a view to maximum utilization of the wind resource[1]. Storage by means of a battery bank contributes greatly to the reduction of critical system parameters, ie, it contributes to the reduction of LOLP and EDNS, since, in addition to storing energy, it helps the generators in the flow control of power in the system[2]. According to the World Wind Energy Association [3], the total capacity of wind turbines installed worldwide by the end of 2017 has reached 546.4 GW. However, this value is very far from the 53000 TWh/year estimated global wind power potential [4]. Battery storage can help to improve this scenario, as shown.**

Keywords*— *Wind power, generation adequacy storage, stability.

METHODOLOGY AND RESULTS

For a power grid, whose main characteristics are represented in Table 1, in a perspective of penetration of 61.5% of wind power, six scenarios were evaluated, namely:

C1: Centralized diesel and wind generation without battery;

C2: Centralized diesel and wind generation with battery;

C3: Centralized diesel and decentralized wind generation without battery;

C4: Centralized diesel and decentralized wind generation with battery;

C5: Decentralized diesel and wind generation without battery;

C6: Decentralized diesel and wind generation with battery.

	Maximum power	Power factor
Diesel Generator	3 x 5 MW	0,9
Wind generator	12 x 2 MW	0,9
Load 1	13 MW	0,9
Load 2	3 MW	0,9
Load 3	10 MW	0,9
Battery	3 x 1.6 MVA	0,9

Table 1: Generation and load characteristics.

Observing the critical values (LOLP and EDNS) of the adequacy analysis of the generation of each scenario, it has been concluded that the most appropriate model for energy systems with wind energy penetration is the C4: Centralized diesel and decentralized wind generation with battery. Finally, this model is applied to the electric grid of the island of Santiago, where it is possible to increase the participation of energy through this strategy. The results show that increasing the storage capacity by means of batteries is required to achieve high penetration rate of wind energy in the systems and to guarantee their stability

ACKNOWLEDGMENT

This work was supported by the Calouste Gulbenkian Foundation.

Thanks are due for the financial support to TEMA through projects UID / EMS / 00481/2013-FCT and CENTRO-01-0145-FEDER-022083.

TOPIC

2) a.: Technologies for the Wellbeing – Multiscale technologies and devices for medicine, environment and energy.

REFERENCES

[1] DIgSILENT GmbH, PowerFactory 2018. DIgDILENT GmbH, 2018.

[2] J. Stanojevic, A. Djordjevic, and M. Mitrovic, “Influence of battery energy storage system on generation adequacy and system stability in hybrid micro grids,” 4th Int. Symp. Environ. Friendly Energies Appl. EFEA 2016, pp. 1–6, 2016.

[3] WWEA, “Wind Power Capacity in 2017,” 2018. [Online]. Available: https://wwindea.org/blog/2018/02/12/2017-statistics/. [Accessed: 20-Jun-2019].

[4] T. E. Drennen, “Renewable Energy: Sources for Fuels and Electricity,” Journal of Environment Quality, vol. 23, no. 3. p. 622, 2010.

Innovative architecture optimization of electromagnetic energy harvesters

Pedro Carneiro, Marco P. Soares dos Santos, Jorge A. F. Ferreira
Department of Mechanical Engineering, University of Aveiro
Aveiro, Portugal

***Abstract*— This paper provides a new concept of electromagnetic energy harvester to maximize the energy efficiency for time-varying excitations: the self-adaptive electromagnetic energy harvester. This optimization tool to design electromagnetic harvesters will allow (1) geometrical optimization to a priori known excitations; and (2) controlled geometrical optimization to variable excitations. This research work aims to theorically analyse the potential of adjusting the generator length to its optimal as variations in the excitation patterns occur.**

The design of optimized motion-driven energy harvesting systems is of upmost importance for high-performance self-powering ability. Nevertheless, the rational design of energy harvesters is hard due to time-varying external excitations. Up to date, no effective technological solution was proposed to optimize such harvesters for optimization prior to fabrication and throughout its operation [1]. This work provides, for the first time, a methodology with ability to perform such optimization by adjusting the harvester length. The optimization procedure was established considering a well-known architecture, since it readily highlights the transduction process and it is a basic configuration suitable to validate the concept of customizable harvester (Figure 1a). An analytical solution of the levitating magnet dynamics was previously calculated by Mann and Sims [2] and good experimental validation results were already achieved [3]. The influence of the harvester length on dynamic response of the levitating magnet was intensively analyzed for variable excitations patterns and load resistances using the analytical solution of Mann and Sims [2]. Intensive computation was performed using Matlab R2016a (v9.0, Mathworks) to correlate the architecture and load parameters with external excitation. The parametric analysis was conducted considering the length change (Δd) in the range [$-d_0/2$, $d_0/4$], as illustrates Figure 1b. The acceleration frequency and magnitude were considered in the 0-100 [Hz] and 0.1-8.4 [m/s^2] ranges, respectively. Two load resistances with 1 MΩ and 188 Ω were tested. As is well known, low excitation magnitudes drive a linear behave of the levitating magnet, resulting in a single periodic attractor for velocity. However, increasing the external acceleration will cause multiple periodic attractors and hysteresis. By consequence, optimization here proposed was carried out by analysing how the highest velocity achievable in both trajectories (ascending and descending) changes for different system parameters.

When Δd is increased from $-d_0/2$ to 0, a frequency decrease is observed for the highest velocity, but no significant differences are observed in the maximum values. However, considerable increases on either the frequency, for the maximum velocity or the maximum velocity/current/power are noticed when Δd evolves from 0 to $d_0/4$. Figure 2a highlights the overall system response taking into account the effects of frequency and five excitations on maximum power (considering the optimum Δd) under 188 Ω load. The power variations regions are emphasized: lower resolutions of Δd (<93μm) would result in lower peak-to-peak values. In order to achieve such maximums, Figure 2b describe the values that Δd must take to ensure the best performance of the harvester. The best Δd for any excitation is always positive and follow a highly non-linear pattern.

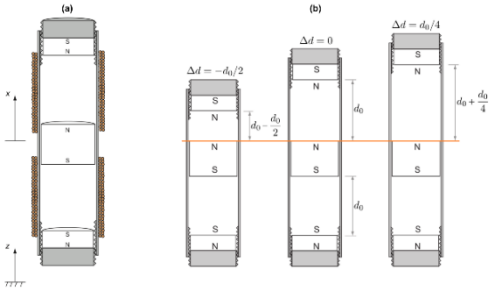

Figure 1: (a) schematic representation of the electromagnetic harvester [1]; (b) schematic representation of the length change.

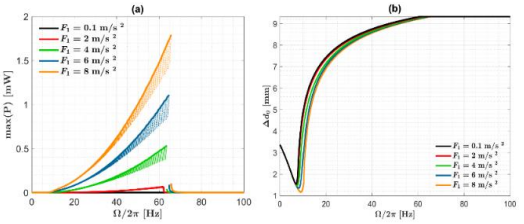

Figure 2: (a) maximum electric power considering the best harvester length; (b) optimized Δd.

Keywords—electromagnetic energy harvesting, magnetic levitation, electric powering, architecture optimization, self-adaptability.

TOPIC

2) a.: Technologies for the Wellbeing – Multiscale technologies and devices for medicine, environment and energy.

REFERENCES

[1] M. P. Soares dos Santos, et al., Sci. Rep., 6, 18759.

[2] B. P. Mann, N. D. Sims, J. Sound Vib., 319, pp.515-530.

[3] W. Wang, et al., Energy Convers. Manag., 132, pp.189-197

Interaction between motor vehicles and bicycles at two-lane roundabouts: a driving volatility based analysis

Ph.D. Mechanical Engineering – Transportation

Behnam Bahmankhah, Paulo Fernandes, João Teixeira, Margarida C. Coelho
Department of Mechanical Engineering
Centre for Mechanical Technology and Automation (TEMA)
Aveiro, Portugal
behnam.bahmankhah@ua.pt, paulo.fernandes@ua.pt, jpteixeira@ua.pt, margarida.coelho@ua.pt

***Abstract*— Although safety benefits of roundabouts for motor vehicles are well-documented [1], these are not always extensive to bicycles [2]. One of the main reasons may be the unexpected driving volatility of motor vehicle (MV)-bicycle interaction at roundabouts. Drivers' instantaneous decisions regarding speed and acceleration/deceleration, as well as the time rate of acceleration change (jerk) can result in a volatility driving behavior with significant impact on cyclist safety [3, 4]. The main objective of this paper is the assessment of driving volatility in MV-bicycle interactions at two-lane roundabouts and its impacts on safety, pollutant emissions and traffic performance. Traffic flow and bicycle GPS data were collected from two two-lane roundabouts in the city of Aveiro, Portugal. Based on field measurements, a description of the different operational and behavior variables, such as entry and exit traffic flows, bicycle volumes, acceleration-deceleration rates and unexpected maneuvers experienced by drivers and cyclists was developed. Then, traffic (VISSIM), emissions (VSP) and safety (SSAM) models were used to evaluate volatility impacts on above transportation-related outputs. The concept of vehicular jerk (derivative of acceleration) was explored [3, 4]. The findings showed the trend of vehicular jerk variation was identical for both bicycles and MVs regardless of roundabout design with a higher amplitude of variation for MVs. It was also found that the impact of MVs and bicycles speeds on driving volatility, as well as roundabout design was more important than bicycle volumes at roundabouts. Finally, the results of emissions dictated good relationships ($R^2 > 0.70$) between acceleration and VSP modes distributions. The potential applications of this paper can be used for proving real-time information for drivers, or warning surrounding cyclists using emerging connected vehicle technologies. This paper also supplied relevant information for transportation experts to better understanding in how MV-bicycle interactions can affect traffic performance, safety, and emissions at circular intersections.**

Keywords*— *Driving volatility; Cyclists; Roundabout; Safety; Emissions.

ACKNOWLEDGMENT

The authors acknowledge to the following projects: Centre for Mechanical Technology and Automation Strategic Project UID/EMS/00481/2019-FCT and CENTRO-01-0145-FEDER-022083; @CRUiSE (PTDC/EMS-TRA/0383/2014), funded within Project 9471 – Reforçar a Investigação, o Desenvolvimento Tecnológico e a Inovação (Project 9471 – RIDTI) and supported by European Community Fund FEDER; MobiWise (P2020 SAICTPAC/0011/2015), co-funded by COMPETE2020, Portugal2020 - Operational Program for Competitiveness and Internationalization (POCI), European Union's ERDF (European Regional Development Fund), CISMOB (PGI01611, funded by Interreg Europe Programme) and FCT – Portuguese Science and Technology Foundation. The bicycle used in the data measurements was given by Orbita Bikes. The authors also acknowledge to Toyota Caetano Portugal, which allowed the use of vehicles and Pavlos Tafidis for his cooperation in data collection. This work was finally supported by the project POCI-01-0145-FEDER-029463, funded by FEDER, through COMPLETE2020-Portuguese Operacional Competitividade e Internacionalização (POCI), and by national funds (OE), through FCT/MCTES.

TOPIC

2) b.: Technologies for the Wellbeing – Innovative technologies for Smart Cities.

REFERENCES

[1] S.U. Jensen, "Safe roundabouts for cyclists," Accident Analysis & Prevention, vol. 105, 2017, pp. 30-37.

[2] E. Ferguson, J. Bonneson, L. Rodegerdts, N. Foster, B. Persaud, C. Lyon, and D. Rhoades, "Development of Roundabout Crash Prediction Models and Methods," 2018 (No. Project 17-70).

[3] J. Liu, A.J. Khattak, and X. Wang, "A comparative study of driving performance in metropolitan regions using large-scale vehicle trajectory data: Implications for sustainable cities," International Journal of Sustainable Transportation, vol. 11(3), 2017, pp. 170-185.

[4] X. Wang, A.J. Khattak, J. Liu, G. Masghati-Amoli, and S. Son, "What is the level of volatility in instantaneous driving decisions?," Transportation Research Part C: Emerging Technologies, vol. 58, 2015, pp. 413-427.

Life Cycle Thinking of Active Mobility

From the Concept to the Use, under a Mechanical Technology and Automation Perspective

Margarida C. Coelho, Aliaksandr Shaula, António Completo, Carlos Relvas, Eloísa Macedo, Fábio Fernandes, Fernando Neto, Jorge Bandeira, José Paulo Santos, Paulo Fernandes, Pukazh Selvan

Mechanical Engineering Department / Centre for Mechanical Technology and Automation
University of Aveiro
Aveiro, Portugal
margarida.coelho@ua.pt

***Abstract* - The efficiency of the road transportation network is a matter of concern to governments and other sectors of society, whether for economic or environmental reasons. The externalities associated with this sector (namely, traffic congestion, safety, and emissions) are increasingly a source of global concern, with many cities implementing traffic restriction programs and emphasizing the use of alternative modes of mobility. Therefore, active mobility is an increasingly attractive option, especially for short distances. Today there is a greater interest in walking, biking and other modes (such as e-scooters) and there is an attempt to introduce more attractive products on the market, including the use of new and more sustainable materials, with the aim to improve wellbeing avoiding other more polluting transportation means. However, it is important to understand the impact of the production of these new products.**

In addition, one of the arguments against bicycle or scooters (namely, electric ones) is the feeling of being unsafe in the road environment (both the cyclist or scooter user, but also from the pedestrian perspective). All these topics are research significant and their integration will, as an ultimate objective, increase the quality of life and the mobility of the population inside the cities.

Mechanical technology and automation related research could have an important role to increase awareness of decision makers and citizens as well as to provide information that can influence decision-making processes.

The main objective of this proposal is to develop a complete life cycle thinking platform for active mobility, including:

1) the concept of innovative products to support walking, cycling and other active modes (e.g., scooters);

2) the manufacturing of these products namely, the raw materials and the processes used in the design and production of the different components);

3) the use of active modes in the cities, with the analysis of the user behavior, as well as his/her interaction with the remaining road traffic elements (including safety issues).

The research topics to be addressed will be (but not limited to:

• To explore the needs of product development under this domain;

• To evaluate cycling and scooters ergonomics;

•To assess life cycle impacts of active mobility related products;

• To assess how conflicts and crashes between diferente road users (namely, pedestrians, cyclists and scooters' users) can be mitigated;

• To quantify the impacts of the penetration of innovative products for active mobility on traffic congestion, global network emissions and energy consumption.

• To study the effectiveness of ICT in active mobility related products.

This mobilizing project will include the organization of a workshop/conference where the subject of active mobility in cities will be discussed and the developed methodology and methods will be presented. An important feature of this discussion will be the inclusion of transportation decision makers in the discussions, from National to regional and local representatives (transportation institutes, authorities, agencies, municipalities and companies).

The proposal builds on a continuing and productive work focused on different topics of active mobility developed by TEMA members over the past 10 years (including MSc. Dissertations, PhD Theses, research projects, cooperation with the local industry and participation in UA technological platforms) and will benefit from a collaboration and an effective integration of different domains.

Keywords—active mobility; life cycle thinking; sustainable mobility

ACKNOWLEDGMENT

This work is supported by the projects UID/EMS/00481/2019-FCT - FCT - Fundação para a Ciência e a Tecnologia; and CENTRO-01-0145-FEDER-022083 – Centro Portugal Regional Operational Programme (Centro2020), under the PORTUGAL 2020 Partnership Agreement, through the European Regional Development Fund.

TOPIC

2) b.: Technologies for the Wellbeing – Innovative technologies for Smart Cities.

Low GWP heat pump water heaters
Component modelling and validation

Francisco Bispo Lamas
Departamento de Engenharia Mecânica
Universidade de Aveiro
Aveiro, Portugal
francisco.lamas@ua.pt

V. A. F. Costa
Departamento de Engenharia Mecânica
Universidade de Aveiro
Aveiro, Portugal
v.costa@ua.pt

***Abstract*—Vapor compression cycles used in heat pumps water heaters (HPWH) are a well-established technology. In particular, electrical-driven HPWH have reached an unparalleled state of technological development and energy performance, unachievable for similar equipment based on other technologies. However, the use of alternative fluids to the conventional refrigerants, mainly due to recent environmental restrictions, resulted in a significant setback. Equipment using natural and synthetic low global warming potential (GWP) refrigerants detain some still unsolved safety and energy efficiency issues. The development of accurate numerical models for establishing fundamental design parameters of safe and high performant HPWH using CO_2, propane, and R1234ze(E), will cooperate on the global effort to accelerate the phasedown of high-GWP refrigerants and increase the energy-efficiency of domestic hot water systems, and consequently, contributing to the EU goals and United Nations Agenda for 2030.**

With regard to the purpose end use of HPWH systems, the most important heat exchanger is at the higher temperature, *i.e.*, condenser (subcritical systems), or gas cooler (transcritical CO_2 systems). All models are being developed using the finite-volume method, retaining the physical meaning of the problem and surpassing some of the hindrances of the classical heat exchanger engineering approaches (LMTD, ε – NTU), particularly for the gas cooler design, due to the sudden variations of the supercritical CO_2 thermodynamic properties. Experimental data available from the literature ascertained the high accuracy of the gas cooler model. Also following a segment-by-segment analysis, evaporator models allow the simulation of arbitrary tube circuitries, considering different flow patterns along this cold-side heat exchanger. Moreover, models accounting with all possibilities for the operational conditions - fully dry, fully wet and partially wet (contrarily to the majority of the models found in the literature), result on a rigorous analysis for heat and mass transfer processes. These models are being developed considering different configurations (parallel- / counter-flow, upper / lower feed, multi-circuitry, and staggered / in-line arrangement), allowing the assessment of their impact on the overall performance. Beside the main heat exchangers, also the compressor is a key component on the energy performance of these systems. It is the equipment with the largest impact on the energy consumption, presenting large irreversibility losses, and thus, strongly contributing to the overall exergy destruction. Nevertheless, its isentropic efficiency is often overestimated, usually considered constant for the entire operation range, or even unitary (ideal compression). Indeed, it is an approach quite far from reality, particularly for rolling piston compressors, commonly used in low capacity systems such as the HPWH for domestic use. Simple black-box type models based on bi-cubic polynomials and regression coefficients, obtained from the compressor data and brief thermodynamic analyses using experimental data, reveal isentropic efficiencies lower than the expected ones, worsening as the pressure ratio increases. For closing the cycle and reestablishing the low-pressure level, the use of thermostatic expansion valves is the common throttling practice. However, their models are frequently undetailed isenthalpic evolutions, having no ability to modulate the refrigerant mass flow rate and considering constant superheat at the evaporator's outlet, resulting in ineffective control strategies and poor energy efficiencies.

Keywords—Heat pump; water heating; heat exchanger; compressor; expansion device; numerical model; validation.

ACKNOWLEDGMENT

The present study was developed in the scope of the **Smart Green Homes Project** [POCI-01-0247-FEDER-007678], a co-promotion between **Bosch Termotecnologia S.A.** and the **University of Aveiro**. It is financed by Portugal 2020 under the Competitiveness and Internationalization Operational Program, and by the European Regional Development Fund. The authors acknowledge the Portuguese Foundation for Science and Technology for the financial support provided through project UID/EMS/00481/2019-FCT, and CENTRO-01-0145-FEDER-022083.

Cofinanciado por:
COMPETE 2020 PORTUGAL 2020 UNIÃO EUROPEIA Fundo Europeu de Desenvolvimento Regional

TOPIC

2) a.: Technologies for the Wellbeing – Multiscale technologies and devices for medicine, environment and energy.

Modelling of NOx degradation in a continuous stirred-tank reactor

Tatiana Zhiltsova[1], Nelson Martins[1], Mariana R. F. Silva[2], Mirtha A. O. Lourenço[2], M. Paula Seabra[2], David M. Tobaldi[2], Carla F. Da Silva[2], Paula Ferreira[2]

[1]Centro de Tecnologia Mecânica e Automação, Mechanical Engineering Department
[2]CICECO – Aveiro Institute of Material, Department of Materials and Ceramic Engineering
University of Aveiro
Aveiro, Portugal

***Abstract*— People spend 90% of their time indoors, where concentrations of volatile organic compounds (VOCs) and other toxic substances as nitrogen oxides may be several times higher than outside. These harmful substances, emitted by several sources including, but not limited to, paints, solvents, carpets and furniture, cleaning agents, exhaust of motor vehicles, cigarette smoke and even by humans, are unlikely to be removed efficiently by conventional air filtration systems. Heterogeneous photocatalysis, already widely used for water purification, can provide an alternative solution for destruction of VOCs [1]. This process is based on irradiation of photocatalyst, generally an inorganic semiconductor such as TiO2 by UV or and visible light. When the TiO2 coating is illuminated, strong oxidants are formed which decompose the VOCs into water and other harmless substances. Photocatalytic oxidation (PCO) process has been proved as a promising technology for air purification both VOCs [2-7] and nitrogen oxides (NOx) [8, 9]. However, there is constant demand in development of new, more efficient photocatalytic materials demanding for refined numerical methodologies for simulation of the PCO process. Taking this into consideration, the authors have focused on the development of numerical methodologies towards modelling and simulation of the NOx photocatalytic oxidation process kinetics. The latter was analyzed in terms of the Langmuir-Hinshelwood (LH) mechanism. Thereafter, the rate of reaction of NOx on the surface of the catalyst was modeled and simulated in ANSYS/Fluent using the User-Defined Functions. To set the limits of validity, the proposed numerical solution was compared with the data obtained from the experimental tests. It was found out that for various concentration tested, the simulated degradation was underestimated about 20%. The main reason for that is not clear yet. However, the authors believe it is a consequence of the perfect mix assumption considered through the entire space of the reactor, disregarding non-uniformity of the NOx concentration in the vicinity of the photocatalytic surface. More precise identification of the LH model parameters is currently under investigation.**

Keywords—CFD modelling; Photocatalytic Oxidation Process; User Defined Function; ANSYS/Fluent; Langmuir-Hinshelwood (LH) mechanism; NOx.

ACKNOWLEDGMENT

The present study was developed in the scope of the Smart Green Homes Project [POCI-01-0247-FEDER-007678], a co-promotion between Bosch Termotecnologia S.A. and the University of Aveiro. It is financed by Portugal 2020 under the Competitiveness and Internationalization Operational Program, and by the European Regional Development Fund.

TOPIC

2) a.: Technologies for the Wellbeing – Multiscale technologies and devices for medicine, environment and energy.

REFERENCES

[1] Boyjoo, Y., M. Ang, and V. Pareek, *Some aspects of photocatalytic reactor modeling using computational fluid dynamics.* Chemical Engineering Science, 2013. **101**: p. 764-784.

[2] Einaga, H., S. Futamura, and T. Ibusuki, Heterogeneous photocatalytic oxidation of benzene, toluene, cyclohexene and cyclohexane in humidified air: comparison of decomposition behavior on photoirradiated TiO2 catalyst. Applied Catalysis B: Environmental, 2002. **38**(3): p. 215-225.

[3] Einaga, H., et al., Kinetic analysis of TiO2-catalyzed heterogeneous photocatalytic oxidation of ethylene using computational fluid dynamics. Chemical Engineering Journal, 2015. **263**: p. 325-335.

[4] Mohseni, M. and F. Taghipour, Experimental and CFD analysis of photocatalytic gas phase vinyl chloride (VC) oxidation. Chemical Engineering Science, 2004. **59**(7): p. 1601-1609.

[5] Chong, S., et al., Simulations of photodegradation of toluene and formaldehyde in a monolith reactor using computational fluid dynamics. AIChE Journal, 2011. **57**(3): p. 724-734.

[6] Nakahara, K., et al., Computational fluid dynamics modeling and parameterization of the visible light photocatalytic oxidation process of toluene for indoor building material. Sustainable Cities and Society, 2017. **35**(Supplement C): p. 298-308.

[7] Queffeulou, A., et al., Kinetic Study of Acetaldehyde Photocatalytic Oxidation with a Thin Film of TiO2 Coated on Stainless Steel and CFD Modeling Approach. Industrial & Engineering Chemistry Research, 2010. **49**(15): p. 6890-6897.

[8] Bianchi, C.L., et al., Pigmentary TiO2: A challenge for its use as photocatalyst in NOx air purification. Chemical Engineering Journal, 2015. **261**: p. 76-82.

[9] Bianchi, C.L., et al., NOx degradation in a continuous large-scale reactor using full-size industrial photocatalytic tiles. Catalysis Science & Technology, 2016. **6**(7): p. 2261-2267.

Multifunctional lightweight cellular materials

Susana C. Pinto[1], Isabel Duarte[1], Romeu Vicente[2] and Paula A.A.P. Marques[1]
[1]TEMA, Department of Mechanical Engineering
[2]RISCO, Department of Civil Engineering
University of Aveiro
3810-193 Aveiro, Portugal
scpinto@ua.pt, isabel.duarte@ua.pt, romvic@ua.pt, paulam@ua.pt

***Abstract*— Cellular materials are fascinating structures composed by two phases, a continuous solid phase (cell walls) and a continuous or discontinuous gaseous phase corresponding to the air trapped within it (pores or cells). This arrangement results in an interconnected porous network of solid struts or plates, which form the edges and faces of pores/cells [1,2]. The low weight and unique mechanical properties make this kind of structures suitable for a wide range of engineering applications, namely in the areas of biomedical, acoustic and thermal insulation, and crashworthiness. With the significant advances in manufacturing industry, cellular materials can be designed, based on engineering optimization process, or be nature inspired. Metallic open-cell foams are one of the most interesting multifunctional materials which cellular structure is easy to control ensuring the fabrication of high-quality foams. They can be used for example, as filters, catalysts, heat exchangers and in biomedical applications and are characterized by high thermal and electrical conductivities and high internal surface area. Furthermore, they are recyclable and non-flammable Recently, special attention is being dedicated to hybrid foams based on aluminum open-cell [3,4].**

Based on the hybrid material concept, we developed and tested new hybrid foams by combining the open-cell aluminum foams with different polymers. The open-cell foam specimens were completely impregnated with specific polymers to explore possible synergies and therefore enhance their performance, thus creating a multifunctional material. Foamed polymers (cellulose and polyurethane) and bulky polymers (epoxy and silicone) have been chosen as filling materials. These were prior combined with graphene-based materials, GBMs (graphene and graphene oxide) at low loading values to ensure the final hybrids with fire-retardancy and enhance mechanical properties, as reported in literature [5].

The aluminum hybrid foams were characterized by a set of complementary techniques and special focus was address to mechanical, acoustic, energetic, thermal and fire-retardancy features. Globally, this type of structures present significant reduction in weight associated with other benefits such as good acoustic and thermal insulating properties, impact energy absorption and fire-retardancy.

Keywords—Aluminium open-cell foams, Polymers, Graphene based materials, Hybrid foams, Mechanical, Acoustic and Thermal properties, Fire-retardancy.

ACKNOWLEDGMENT

The authors thank to FCT for the PhD grant SFRH/BD/111515/2015, and IF/00917/2013/CP1162/CT0016. Also, TEMA (UID/EMS/00481/2019).

TOPIC

2) a.: Technologies for the Wellbeing – Multiscale technologies and devices for medicine, environment and energy.

REFERENCES

[1] M.F. Ashby and Y.J.M. Bréchet, “Designing hybrid materials”, Acta Mater., vol. 51, pp. 5801–5821, 2003.

[2] I. Duarte, N. Peixinho, A. Andrade-campos and R. Valente, “Special Issue on Cellular Materials,” Sci. Technol. Mater., vol. 30, no. 1, pp. 1–3, 2018.

[3] I. Duarte and J.M.F. Ferreira, “Composite and Nanocomposite Metal Foams”, Materials (Basel)., vol. 1, pp. 1–34, 2016.

[4] I. Duarte, M. Vesenjak, L. Krstulović-Opara and Z. Ren, (2018) “Crush performance of multifunctional hybrid foams based on an aluminium alloy open-cell foam skeleton”, Polym. Test., vol. 67, pp. 246–256, 2018.

[5] Sang, Z. Li, X. Li, L. Yu, and Z. Zhang, “Graphene-based flame retardants: a review”, J. Mater. Sci., vol. 51, pp. 8271–8295, 2016.

.

New magnetic stimulator for instrumented implants

Rodrigo Bernardo, Marco P. Soares dos Santos, António Lopes, João Sequeira Amaral
Department of Mechanical Engineering, University of Aveiro
Department of Physics, University of Aveiro
Aveiro, Portugal.

***Abstract*— This work provides, for the first time, a new small-scale magnetic stimulation system that requires lower excitation of electrical current.**

Previous studies have found promising results to enhance osseointegration through the use of multifunctional instrumented implants that include therapeutic actuators based on inductive stimulation to promote and control bone regeneration [1]. Recent studies highlight the ability of inductive architectures to deliver therapeutic magnetic stimuli to target tissues and to be embedded into small-scale intracorporeal medical devices [1-3]. However, current small-scale (up to micro-scale) implantable magnetic devices require high electrical currents (usually exceeding 1 A) flowing in the stimulation coils to ensure the delivery of efficient therapeutic magnetic flux densities [2,3]. This is a critical problem as advanced implantable devices demand self-powering, stand-alone and long-term operation.

Computational models were developed in COMSOL Multiphysics 5.3a to analyse the magnetic stimuli distributions and densities delivered to cellular tissues during *in vitro* experiments. A planar (Fig. 1a) and two quasi-planar (Fig. 1b) architectures were designed for the delivery of magnetic stimuli to bone cells in culture during the first two stages of bone remodeling (proliferation and differentiation).

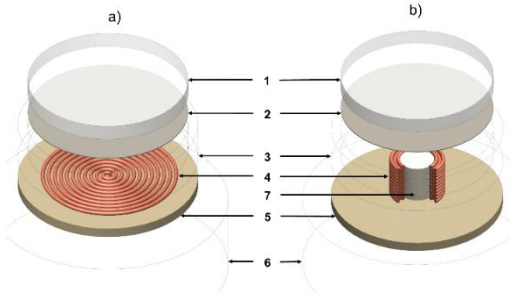

Figure 1: Computational models of inductive architectures: a) schematic representation of the planar architecture; b) schematic representation of the quasi-planar architectures. Domains: 1 - Culture medium (a liquid solution); 2 - Cellular layer (proliferation stage) or cellular tissue (differentiation stage); 3 - Culture dish; 4 - Coil; 5 - Polymeric substrate; 6 - Air; 7 - Core.

The planar architecture (P-architecture), composed by a coil shaped with a planar geometry of spiral pattern and micro-scale wire diameter (5 µm), was firstly analysed. The ability of a ring quasi-planar architecture (µM-architecture) comprising a cylindrical-shaped core surrounded by a helicoidal-shaped single-layer coil with few turns (20) and micro scale wire diameter (5 µm) to deliver magnetic field stimuli was also explored, according to Bonmassar *et al.* [2]. A new insight is here provided to significantly minimize the electric current supply by using a quasi-planar architecture (µM-kT-architecture) composed by a cylindrical core surrounded by a helicoidal-shaped multilayered coil with a large number of turns (1000) and micro-scale wire diameter (5 µm) with 1 mm of height.

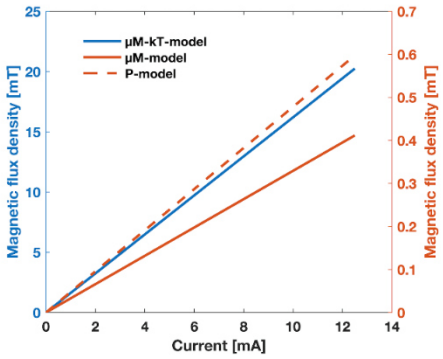

Figure 2: Magnetic flux densities delivered by all architectures as a function of current excitations.

The results demonstrate that this new stimulative technology is able to deliver osteogenic stimuli (0.1-7 mT range) by current excitations in the 0.06-4.3 mA range. The µM-kT-architecture requires up to 50-fold and 34-fold lower electric current excitations than required by µM- and P-arquitectures, respectively (Fig. 2). These results support the design of biomagnetic devices suitable for a wide range of high-sophisticated therapeutic applications.

Keywords—Medical device; Biomagnetic device;; Implantable devices; Magnetic stimulation.

TOPIC

2) a.: Technologies for the Wellbeing – Multiscale technologies and devices for medicine, environment and energy.

REFERENCES

[1] M. P. Soares dos Santos et al., Sci. Rep., vol. 6, no. February, p. 30231, 2016.

[2] G. Bonmassar et al., Nature Communications 3 (2012) 921.

[3] H.-J. Park et al., Nature Communications 4 (2013) 246.

PCM in thermal energy storage – a CFD approach

Bruno Daniel Cordeiro Pereira
Departamento de Engenharia Mecânica
Universidade de Aveiro
Aveiro, Portugal
bdcp@ua.pt

Fernando Neto
Departamento de Engenharia Mecânica
Universidade de Aveiro
Aveiro, Portugal
fneto@ua.pt

***Abstract*— The use of renewable energy has been steadily rising over the years, with efforts to reduce emissions reinforcing this trend. However, renewable energy production is intermittent and a bridge over production/demand gap is required [1], with energy storage becoming increasingly needed. For thermal energy storage (TES), Phase Change Materials (PCM) represent a safe and inexpensive technique to match solar or residual heat availability to thermal requirements [2], [3]. To design and operate latent heat-based TES, adequate tools must be developed and tested. One of the main questions regarding the thermal storage capacity of PCMs is related to the low thermal conductivity of these materials, which limits the amount of heat that can be stored in a volume of PCM. This characteristic limits the response time of the heat transfer for these systems, as low thermal transfer coefficient can lead to low heat transfer if the system is not properly designed [4]. Additionally, PCMs need high values of latent heat densities, this being an important factor to the amount of energy that the PCM is theoretically able to store. Scientific developments are generally focused in the improvement of the heat transfer surface area, with reduced emphasis on the improvement of the intrinsic characteristics of the PCMs. While several advances in this area are visible in literature, the impact of these approaches on the values of energy stored is still somewhat unclear. Both the heat transfer coefficient and the total energy stored are vital for the optimization of systems that include PCMs, and as such a deeper analysis of its interaction is required. The main goal of the present work is the development a flexible numerical tool capable of the analysis of the behaviour of PCMs in transient thermal energy storage systems, intending on understanding the interaction between heat storage capacity and the velocity of heat release or take up and its impact on the system performance.**

Keywords—Phase Change Materials; CFD; TRNSYS; Energy storage.

ACKNOWLEDGMENT

The present study was developed in the scope of the **Smart Green Homes Project** [POCI-01-0247-FEDER-007678], a co-promotion between **Bosch Termotecnologia S.A.** and the **University of Aveiro**. It is financed by Portugal 2020 under the Competitiveness and Internationalization Operational Program, and by the European Regional Development Fund.

Cofinanciado por:
COMPETE 2020 PORTUGAL 2020 UNIÃO EUROPEIA Fundo Europeu de Desenvolvimento Regional

TOPIC

2) a.: Technologies for the Wellbeing – Multiscale technologies and devices for medicine, environment and energy.

REFERENCES

[1] A. Sharma, V. V. Tyagi, C. R. Chen, and D. Buddhi, "Review on thermal energy storage with phase change materials and applications," *Renewable and Sustainable Energy Reviews*, vol. 13, no. 2. Pergamon, pp. 318–345, 01-Feb-2009.

[2] G. Wei *et al.*, "Selection principles and thermophysical properties of high temperature phase change materials for thermal energy storage: A review," *Renewable and Sustainable Energy Reviews*, vol. 81. pp. 1771–1786, 2018.

[3] A. Abhat, "Low temperature latent heat thermal energy storage: Heat storage materials," *Sol. Energy*, vol. 30, no. 4, pp. 313–332, Jan. 1983.

[4] N. Sarier and E. Onder, "Organic phase change materials and their textile applications: An overview," *Thermochimica Acta*, vol. 540. pp. 7–60, 2012.

Photocatalytic reduction of CO_2 using amorphous SiC thin films

S. Kaci[1], K. Benfadel[1], L. Talbi[1], A. Boukezzata[1], I. Bozetine[1], R. Rahmoune[1], A. Keffous[1], Y. Ouadah[1], S. Achacha[1], S. Belaid[1], O.Manseri[1], H. Menari[1].

[1]*Research Center on Semiconductor Technology for Energetic, CMSI Division, CRTSE*
2 Bd Frantz Fanon, PB 140, 7M, Algeria

***Abstract* — Global warming due to rising levels of greenhouse effect gases, such as atmospheric carbon dioxide, and energy consumption are the major challenges in the energetic field. Decreasing carbon dioxide emissions is a key issue but not the only one; thus, it is becoming compulsory to capture and reuse this gas in an efficient mode as a new source of fuels. One of the best means of solving the carbon dioxide (CO_2) problem is to photocatalytically convert the CO_2 to hydrocarbons using solar energy, a process which simultaneously generates renewable energy. In this work, p-type amorphous silicon carbide a-$Si_{1-x}C_x$ thin films were deposited by magnetron sputtering method. The as-prepared amorphous thin films were used for photo-electrochemical (PEC) CO_2 reduction as photocathode catalyst. The XRD, Raman, UV-Visible Spectroscopy (UV-Vis) and cyclic voltammetry experiments were done to characterize the catalyst. Linear sweep voltammetry (LSV) was employed to evaluate the visible light (λ>400 nm) effect of this catalyst for CO_2 reduction (fig. 1).**

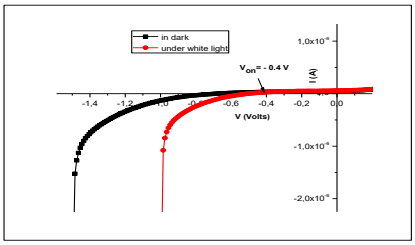

Figure 1: LSV of a-$Si_{1-x}C_x$ thin film in 0.1M K_2CO_3.

The band gap energy of the catalyst was found 1.80 eV with the VB and CB edges at 0.58V and -1.23 V vs Ag/AgCl, respectively, calculated from UV-Vis and I-V characterizations (fig. 2).

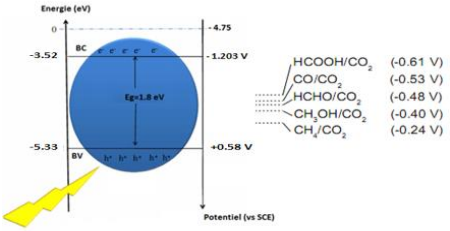

Figure 2: Energy band edge diagram.

The a-$Si_{1-x}C_x$ thin films photocathode exhibited a strong cathodic peak at -0.77 V and -1.12V with an onset potential of -0.51 V versus Ag/AgCl under the illumination of visible light. Under light irradiation in the CO_2-saturated K_2CO_3 solution, a remarkable current development associated with CO_2 reduction was found during LSV representing the occurrence of CO_2 reduction reactions (fig. 3). In addition, the mechanism of PEC was proposed for the photocathode.

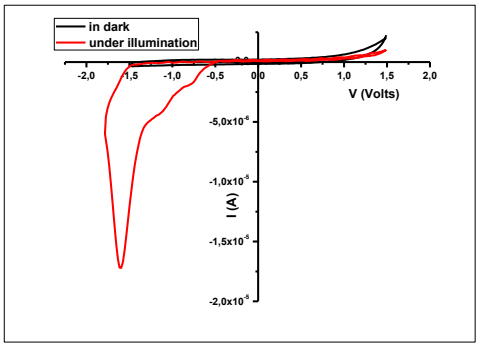

Figure 3: Cyclic voltammetry of a-$Si_{1-x}C_x$ thin film in 0.1M K_2CO_3 solution saturated with CO_2.

Keywords—a-$Si_{1-x}C_x$, thin film, CO_2 photoelectrochemistry reduction.

ACKNOWLEDGMENT

This work was completed thanks to the National Funds of Research, DGRSDT/MESRS (Algeria). We thank the TEMA for the organisation of this event.

TOPIC

2) a.: Technologies for the Wellbeing – Multiscale technologies and devices for medicine, environment and energy.

REFERENCES

[1] C.S.Jeffrey, "photocatalytic reduction of carbon dioxide (CO2)", Carbon Dioxide (Co2) Storage and Utilisation, vol. 2, 2010, pp. 463-501.

Predictive control for tankless gas water heaters

André Quintã[1], Nelson Martins[1], Jorge Ferreira[1]
[1]TEMA, Department of Mechanical Engineering, University of Aveiro
Aveiro, Portugal

***Abstract*— Presently there is a growing consciousness and concern with the scarceness of natural resources, associated with the noticeable increase in energy consumption and harmful emissions. Water heating is a relevant part of buildings energy consumption and tankless gas water heaters (TGWH) are extensively used. TGWH is the most efficient conventional method of generating heat from natural gas in a domestic hot water application [1]. One of the most relevant drawbacks of TGWH is the difficulty to control the outlet hot water temperature as changes in hot water flow rate can be quick and unpredictable [2]. Some of the more recent and advanced TGWH appliances have electronic control units with feedback controllers, connected to flow rate and temperature sensors and gas modulation actuators. However, the demand for faster and more robust control persists. One of the most promissory approaches for advanced control strategies is the model based predictive control (MPC), as already demonstrated by [3,4], for electric tankless water heaters. Advanced control strategies, like MPC and adaptive techniques, can increase safety and comfort indicators by reducing water temperature undershoots and overshoots. As the best known by the authors, there aren't any successful implementations of adaptive predictive control in TGWH in the literature.**

Predictive control is today one of the most popular and efficient strategies of advanced control, with plentiful successful applications ranging from industrial processes and consumer appliances, where aspects such as operative constraints are particularly important [5]. Although MPC has been in development over some decades, its application to embedded appliances and consumer goods is rather recent. Some of the adversities in the adoption of MPC are the difficulty in obtaining a sufficiently accurate system model, the complexity of the controller design and the large computational resources required for solving optimization problems in each iteration. The large computational resources used in MPC implementation is particularly challenging for domestic appliances, like TGWH, with discrete control embedded on microcontrollers with limited computational resources.

The purpose of this work programme is to develop predictive control methodologies and algorithms for instantaneous domestic hot water appliances. By improving thermal control stability, reducing water temperature overshot and undershoot, improved safety and comfort indicators will be achieved, in addition to higher sustainability and lower environmental impact, due to energy and water consumption optimization and reduction of gaseous emissions. A lumped space approach is proposed to model individual components, parametrized with experimental data, to build TGWH models. The developed MPC algorithms are presented and discussed. Preliminary results are encouraging, showing significant performance gains compared to classic control systems.

The development of new TGWH configurations and control strategies must be supported by simulation techniques. Hardware-in-the-loop-simulation (HILS) methodologies are state-of-the-art procedures for evaluation of embedded control systems, with multiple levels of hardware virtualization. The methodology for the development of a virtual-test-bench platform and some details of its implementation are presented. This platform will allow assessing and accelerating the development of advanced control strategies for TGWH and other water heating technologies.

Keywords*— *Tankless gas water heaters, Domestic hot water, Model predictive control, Embedded control.

ACKNOWLEDGMENT

The present study was developed in the scope of the **Smart Green Homes Project** [POCI-01-0247-FEDER-007678], a co-promotion between **Bosch Termotecnologia S.A.** and the **University of Aveiro**. It is financed by Portugal 2020 under the Competitiveness and Internationalization Operational Program and by the European Regional Development Fund.

TOPIC

2) a.: Technologies for the Wellbeing – Multiscale technologies and devices for medicine, environment and energy.

REFERENCES

[1] D. Bohac, B. Schoenbauer, M. Hewett, M.S. Lobenstein, T. Butcher, Actual savings and performance of natural gas tankless water heaters., in: ASHRAE Trans., Las Vegas. NV, 2011.

[2] V. Costa, J. Ferreira, D. Guilherme, Modeling and simulation of tankless gas water heaters to reduce temperature overshoots and undershoots, in: Proceddings 12th Int. Conf. Heat Transf. Fluid Mech. Thermodyn. (HEFAT 2016), Málaga, Spain, 2016: pp. 1404–1409.

[3] G.P. Henze, A.H. Coward, D.P. Yuill, Development of a Model Predictive Controller for Tankless Water Heaters., HVAC&R Res. 15 (2009) 3–23.

[4] E.M.G. Rodrigues, R. Godina, E. Pouresmaeil, J.R. Ferreira, J.P.S. Catalão, Domestic appliances energy optimization with model predictive control, Energy Convers. Manag. 142 OP-(2017) 402.

[5] J.A. Rossiter, A first course in predictive control, Second ed, CRC Press, 2018. doi:10.1201/9781315104126.

Project Ghisallo: A mobile multi-sensor in the city

P. Nunes, J.P. Santos, J. Januário, A. Completo
Department of Mechanical Engineering
University of Aveiro
Aveiro, Portugal
pnunes@ua.pt

***Abstract*— Project "Ghisallo" aims the development of an electrically assisted mobility solution conceived to be practical, stylish and safe. In addition to the three-wheel electric vehicle, the solution includes a connectivity platform, an intelligence unit (IU), a smart lock, and an interface based on the user's smartphone, developed to give cyclists more comfort and security during their bicycle trips.**

The IU includes features as an Inertial Measurement Unit (IMU), vandalism detection, GPS and a connectivity module. The engine control unit (ECU) is wired connected to the battery management system (BMS), in order to get battery features as the percentage of charge and number charging cycles. The ECU is an I2C [1] slave of IU and sends it messages containing the battery and engine data. ECU is also wired connected to a Human Machine Interface (HMI) with buttons, in which the user can choose the engine assistance level and control the illumination system. The IU connectivity module allows the exchange of messages between the bicycle and the connectivity platform using the mobile network. The connectivity platform includes an MQTT [2] (Message Queuing Telemetry Transport) broker which is an intermediary in the process of communication between the connectivity platform and the IU. The communication is of the type publisher/subscriber. The bicycle (IU) can be the publisher when it sends data from sensors, battery and electric motor to the platform and can be subscriber when it requires data from the databases. The connectivity platform allows "Ghisallo" to be integrated into a bike sharing system since it includes services as payment methods and dashboards that facilitate the management and automation of the process of booking / renting a bicycle.

The user interface is based on smartphone use. The communication is made through the connectivity platform, i.e., the IU sends data to the connectivity platform and the user can monitor the bicycle with his smartphone who connects the platform using the mobile network. This allows the user to monitor the vehicle anywhere. He can check if the bicycle was disturbed and in case of theft, he knows where to search it because IU keeps sending GPS information to the platform. In the bike sharing use case, the user can rent a bike in the smartphone interface and pay for it, then the platform will publish the authorization to unlock the bike in the broker and the bikes IU will subscribe that service, in order to activate the smart lock. The user interface also allows him to search for route recommendation, since it has integrated an innovative routing engine algorithm that suggests the optimal route to a cyclist between two points, according to a chosen criterion. The algorithm considers the existence of cycle paths, type of surface, type of highway, the existence of intersections, traffic signals, roundabouts, road slope and uses the data sent to the platform in order to detect bad quality road surface or roads with many obstacles to improve the quality of the suggested routes, transforming "Ghisallo" in a mobile multi-sensor in the cities.

Keywords—connectivity platform; intelligence unit; sensors.

ACKNOWLEDGMENT

POCI-01-0247-FEDER-033769-"Ghisallo – Investigação e Desenvolvimento de uma nova solução de comutação urbana, assente num novo conceito de veículo elétrico de próxima geração" – "Ghisallo - Research and Development of a new urban commuting solution, based on a new concept of a next-generation vehicle".

TOPIC

2) b.: Technologies for the Wellbeing – Innovative technologies for Smart Cities.

REFERENCES

[1] Addressing - I2C Bus [Internet]. [visited 2019 Jun 7]. Available from: https://www.i2c-bus.org/addressing/.

[2] MQTT Version 5.0. Edited by Andrew Banks, Ed Briggs, Ken Borgendale, and Rahul Gupta. 07 March 2019. OASIS Standard.

Project Ghisallo: Mecahnical development of a new smart soft-mobility concept

J. Januário, A.Completo, P. Nunes, J. Santos
Department of Mechanical Engineering
University of Aveiro
Aveiro, Portugal
joaojanuario@ua.pt

***Abstract*— Bicycles are traditionally unstable vehicles. This fact keeps away many people from using them on a daily basis, both for commuting or for short trips in-town: some of them because they never learned how to use/stand on a two-wheeled vehicle, others are afraid to share the roads with cars and trucks or fear steep slopes uphill. Also, for a cyclist who lives in a crowded world where space is at a premium at home and in the workplace, storing a bicycle could present a challenge because of its size [1]. Three-wheeled cycles offer many benefits including safety, stability and comfort, however their increased size can present storage and maneuverability challenges. For the same reason, it is often not practical to carry a either a two or three-wheeled bicycle on buses, trains, taxis, small boats, and planes, thus limiting its use for the commuting or touring cyclist. Project "Ghisallo" aims to develop an electrically assisted mobility solution conceived to be compact, practical, stylish, safe and fun to use, bringing the stability of a three-wheeled vehicle and the tilting of a bicycle. The tilting mechanism is adaptative: the user can choose a more stable (less tilting, more stability) configuration and gradually adopt a funnier configuration (more tilting, less stability). The vehicle is foldable, fitting on elevators and capable of being transported on public transports (train, bus…) and stored inside an office or building. The frame is low, easing the hop-in hop-off movement, and the vehicle can even be ride by users wearing dresses, since every part of the transmission system is covered. The front is detachable from the rest of the vehicle (can be used as a shopping trolley) and has storage to carry a load up to 25kg. To help with the cargo weight or just to ease out uphills, an electrically assisted 8-speed powertrain will be installed, along with a Li-Ion battery and energy-recovering system for deceleration and braking. The vehicle is intended to weight less than 16kg. The target groups for this solution are adult users that need a compact and foldable vehicle for their journeys in town but don't want to sweat on their way or leave their fashionable clothes at home, bike sharing companies and elderly people that have balance problems and cannot ride a normal bike. This solution also targets everyone that is afraid of riding bicycles due to safety or comfort reasons. Currently, a prototype of the tilting system is being tested to reveal the influence of geometric conditions on the dynamics and stability of the vehicle. The frame is being designed according to an adapted version of the ISO 4210-2 [2] and -6 [3] safety norms, since there are currently any safety requirements specifically for this type of vehicles. The technical specifications of the vehicle are already defined after anthropometric and competition studies. The technical specifications of structural components are also already defined after FEM simulations. A full prototype is expected to be built in 2020.**

Keywords—three wheeled cycles; tilting; urban trike, e-assist.

ACKNOWLEDGMENT

POCI-01-0247-FEDER-033769-"Ghisallo – Investigação e Desenvolvimento de uma nova solução de comutação urbana, assente num novo conceito de veículo elétrico de próxima geração" – "Ghisallo - Research and Development of a new urban commuting solution, based on a new concept of a next-generation vehicle".

TOPIC

2) b.: Technologies for the Wellbeing – Innovative technologies for Smart Cities.

REFERENCES

[1] J. Fuentes, K. Newling, L. Ferreira, L. Gannon, P. Faria, T. Gamboa, "ME310: spring documentation 2016" pp. 162-167, June 2016, unpublished.

[2] International Organization for Standardization. Safety requirements for bicycles -- Part 2: Requirements for city and trekking, young adult, mountain and racing. ISO 4210-2.

[3] International Organization for Standardization. Safety requirements for bicycles -- Part 6: Frame and fork test methods. ISO 4210-6.

Real-time Prevention Tool Integrating Volatility and Environmental Impacts

Elisabete Ferreira[1], Eloísa Macedo[1], Paulo Fernandes[1], Ricardo Tomás[1], Jorge M. Bandeira[1], Margarida C. Coelho[1]*

[1]*Department of Mechanical Engineering*
Center for Mechanical Technology and Automation
University of Aveiro, Portugal
*elisabetedsf@ua.pt, macedo@ua.pt, paulo.fernandes@ua.pt, ricardotomas@ua.pt, jorgebandeira@ua.pt, margarida.coelho@ua.pt

***Abstract*— In Europe, the number of road traffic deaths and injuries is still far too high and the European Union is committed in improving road safety and move closer to the target of approaching zero road fatalities by 2050. For that purpose, new strategies based on the Safe System approach to preventing deaths and serious injuries for all road users should be developed. Road transport is a major source of pollutant emissions. In particular, it is responsible for the emission of harmful pollutants such as nitrogen oxides (NOx) and carbon dioxide (CO_2), which has serious impacts in global warming [1].**

It is known that driver behavior can play a key role in what concerns road crashes and pollutant emissions. Such impacts increase when associated to aggressive behavior, experiencing high and extreme levels of fuel consumption, speed and acceleration. A deep understanding of driver behavior should be an important step to improve road safety. Various studies have been conducted to identify driver's behavior under many contexts such as, traffic, roadway and weather conditions. An issue that has not been so explored is an analysis of drivers' volatility [2-3]. Volatility can be defined as the extent of variations in driving, which can be characterized by accelerations/braking, lane change and also unusual high speed for roadways conditions. Therefore, particular attention should be given to developing preventive tools, anticipating dangerous situations and warning the driver that may be efficient solutions to avoid an occurrence.

In [4], an advisory system was developed on a driver's simulator to warning the driver. However, there is no preventive tool in the literature that integrates volatility and environmental impacts. The main objective of this work is to develop a decision support system to evaluate driver volatility and provide instantaneous and integrated information on safety and emission impacts to the driver. To validate our application, we used real traffic, dynamic and on-road emissions data collected from probe vehicles on two highways of different specificities (e.g., slope, relief and traffic volumes). A simulation-based approach through Vissim COM API using Matlab was constructed in order to give to the driver warnings regarding safety and emissions. Markov Decision Process (MDP) was used to support the decision on safety and the Vehicle Specific Power (VSP) methodology was used for estimating pollutant emissions.

Keywords — driving behavior; safety; emissions; Markov Decision Process.

ACKNOWLEDGMENT

The authors acknowledge the support of the projects: UID/EMS/00481/2019-FCT - Fundação para a Ciência e a Tecnologia (FCT); CENTRO-01-0145-FEDER-022083 - Centro2020 Regional Operational Programme, under the PORTUGAL 2020 Partnership Agreement, through the European Regional Development Fund; DICA-VE (POCI-01-0145-FEDER-029463); Mobiwise (P2020 SAICTPAC/0011/2015); and InFLOWence (POCI-01-0145-FEDER-029679).

TOPIC

2) b.: Technologies for the Wellbeing – Innovative technologies for Smart Cities.

REFERENCES

[1] Air quality in Europe - 2018 report. (European Environment Agency, Ed.), EEA Report No 12/2018.

[2] Kattak, A.J. and Walli, B. Wali. Analysis of volatility in driving regimes extracted from basic safety messages transmitted between connected vehicles. *Transportation Research Part C.* 2017. 84: 48-73.

[3] Walli, B., A. J. Khattak, H. Bozdogan and M. Kamrani. How is driving volatility related to intersection safety? A Bayesian heterogeneity-based analysis of instrumented vehicles data. *Transportation Research Part C: Emerging Technologies.* 2018. 92: 504-524.

[4] Li, Q., F. Qiao, X. Wang and L. Yu. Drivers' smart advisory system improves driving performance at STOP sign intersections. *Journal of Traffic and Transportation Engineering.* 2017. 4(3): 262-271.

Statistical Methodologies to Support Road Safety Analysis involving Vulnerable Road Users

Mariana Vilaça, Eloísa Macedo, Margarida Coelho
Mechanical Engineering Department
University of Aveiro
Aveiro, Portugal
mvilaca@ua.pt; macedo@ua.pt; margarida.coelho@ua.pt

***Abstract*— Urban areas rapid growth often leads to adverse effects such as traffic congestion and increasing crash risk due to the expansion in transportation systems. In the frame of smart cities, walking and cycling are considered active modes that are being promoted as sustainable, healthy, environmentally friendly and inexpensive. Despite these benefits, pedestrians and cyclists are exposed to a higher risk of injury and fatality in road crashes and are therefore considered vulnerable road users (VRUs).**

Road crashes are among the leading cause of death, disability, property loss and yield costs to society, representing 1-3% of gross domestic product (GDP) worldwide [1]. More than one million people lose their lives every year in road crashes and 20 to 50 million people are injured [1]. In 2017, the percentage of VRUs fatalities in Portugal was 25% of the total crash involved injuries (21% corresponding to pedestrians and 4% to cyclists) [2].

The main objective of this work is to present statistical methodologies to support identification of risk factors that possibly affect the severity of a VRU injured when involved in a motor vehicle crash. Additionally, it is important to explore spatial and temporal patterns considering this type of road accident between cities with different social and demographic conditions. Machine learning techniques (multinomial logistic regression and decision tree) were applied to road crash records from Aveiro, Porto and Lisbon – Portugal. A GIS-based approach (Kernel density estimation) was applied to identify blackspots based on injury severity levels. Afterward, in an attempt to obtain a more accurate analysis regarding sample classification, three different resampling techniques were applied to deal with imbalanced data in terms of injury severity level and understand how it may influence the classifier performance.

Results revealed that road markings, road conditions and luminosity can significantly affect the injury severity of pedestrians. On the other hand, age group and temporal variables (month, weekday and time) showed to be relevant to predict the severity of cyclist injury. Spatial analysis revealed that the most injuries occur in surrounding areas of high attraction places, such as train stations, shopping and touristic points, where the speed limits are relatively low. More than 40% of the pedestrian crashes occur in the vicinity of crosswalks.

This work will be useful for policy and decision makers, as well as road safety managers, in order to recognize blackspots and develop road safety measure strategies to improve VRUs safety. This is even more important in an era where driverless vehicles are about to be implemented, and the way they will circulate and interact in the urban space.

Keywords*— *road crashes; vulnerable road users; statistical analysis; spatial and temporal patterns; injury severity.

ACKNOWLEDGMENT

The authors acknowledge the Portuguese National Authority of Road Safety (ANSR) for providing crash data and Pavlos Tafidis for the support in the development of this work.

We also acknowledge the financial support of TEMA (CENTRO-01-0145-FEDER-022083), and the projects: Strategical Project (UID/EMS/00481/2019—FCT), @CRUiSE project (PTDC/EMS-TRA/0383/2014, funded within Project 9471—Reforçar a Investigação, o Desenvolvimento Tecnológico e a Inovação and supported by the European Community Fund FEDER), MobiWise (P2020 SAICTPAC/0011/2015, cofunded by COMPETE2020, Portugal2020—Operational Program for Competitiveness and Internationalization, European Union's ERDF and FCT), and CISMOB (PGI01611, funded by the Interreg Europe Programme), project POCI-01-0145-FEDER-029463 (DICA-VE) and POCI-01-0145-FEDER-029679 (InFLOWence), funded by FEDER through COMPETE2020—Programa Operacional Competitividade e Internacionalização (POCI), and by national funds (OE) through FCT/MCTES.

TOPIC

2) b.: Technologies for the Wellbeing – Innovative technologies for Smart Cities.

REFERENCES

[1] WHO. Global Status Report on Road Safety 2018; License: CC BY-NC-SA 3.0 IGO; World Health Organization: Geneva, Switzerland, 2018.

[2] ANSR. Annual Report 2017 (30 Days Victims)—National Authority of Road Safety; Portuguese National Authority for Road Safety: Lisbon, Portugal, 2017. (In Portuguese).

The relevance of on-road emission monitoring in different type of roundabouts in rural roads

Francesco Acuto, Anna Granà
Department of Engineering
Civil, Environmental, Aerospace and Materials Engineering
Palermo, Italy
francesco.acuto@unipa.it, anna.grana@unipa.it

Paulo Fernandes, Margarida C. Coelho
Department of Mechanical Engineering
Centre for Mechanical Technology and Automation - TEMA
Aveiro, Portugal
paulo.fernandes@ua.pt, margarida.coelho@ua.pt

***Abstract*— Road traffic significantly contributes to urban air pollution as means of particulate matter (PM) and nitrogen oxides (NO_X) emissions [1]. Despite the deployment of clean powertrains, internal combustion engines are the most widely used technology in the European Union; gasoline- and diesel-fueled represented around 90% of passenger cars sold between 2014 to 2017 [2].**

The amount of exhaust gases emitted by motor vehicles depend on speed profile, vehicle type, traffic volumes and intersections [3]. Roundabouts have been considered and built around the world to replace intersections previously controlled by traffic lights as a means of improving operational performance, at least in certain flow range [4]. These latter ones are considered pollution hotspots locations, due to speed changes cycle around them [5] [6]. Despite the demonstrated benefits in terms of traffic flow, delay reducing and safety [7], roundabouts raised some doubts concerning emissions performance [8].

Bearing this in mind, this paper compares vehicle activity and on-road emission data in three different roundabouts in rural roads: a compact two-lane, a multi-lane and a single lane roundabout in Aveiro, Portugal. It was hypothesized that carbon dioxide (CO_2) and NO_x emissions, engine speed and the relative positive acceleration (RPA) are impacted by the differences in the approaching and conflicting traffic volumes, the volume-to-capacity ratio and the roundabout layout.

Input data such as approaching and circulating traffic volumes, and queue length were collected by videos cameras installed at the studied locations. Field measurements were carried out with two light duty vehicles (gasoline and diesel), using a Portable Emissions Measurement System (PEMS) to measure CO_2 and NO_X volumetric concentrations. Alongside, an OBD-II scan interface record vehicle speed data, engine speed and acceleration. After that, a relationship between congestion level of roundabouts and occurrence of each speed profile (no stop – I, stop once – II and multiple stops – III) was established, using discrete choice models. Finally, discrete choice models obtained from single-lane, compact two-lane and multi-lane roundabouts were compared.

The methodology and models developed used in this paper can be applied by simply measuring roundabout traffic volumes by means of discrete choice models that allows simultaneously detecting differences in location and variability characteristics of the distributions of the observations taken at roundabouts. It also allows to identify some relevant operational and design features of a rural roundabout prior its implementation to enhance capacity and emissions fields.

***Keywords*— *Roundabouts, Traffic, Exhaust emissions, Portable Emissions Measurement System; Light duty vehicles*.**

ACKNOWLEDGMENT

The authors acknowledge the financial support of the following projects: TEMA – CENTRO 01-0145-FEDER-022083; Strategical Project UID/EMS/00481/2019-FCT (FCT-Portuguese Science and Technology Foundation); @CRUiSE project (PTDC/EMS-TRA/0383/2014), funded within Project 9471 – Reforçar a Investigação, o Desenvolvimento Tecnológico e a Inovação and supported by European Community Fund FEDER; MobiWise (P2020 SAICTPAC/0011/2015), co-funded by COMPETE2020, Portugal2020 - Operational Program for Competitiveness and Internationalization (POCI), European Union's ERDF (European Regional Development Fund), and FCT; CISMOB (PGI01611, funded by Interreg Europe Programme); DICA-VE (POCI-01-0145-FEDER-029463), Driving2Driverless (POCI-01-0145-FEDER-031923) and inFLOWence (POCI-01-0145-FEDER-029679) projects funded by FEDER through COMPETE2020 - Programa Operacional Competitividade e Internacionalização (POCI), and by national funds (OE), through FCT/MCTES.

TOPIC

2) b.: Technologies for the Wellbeing – Innovative technologies for Smart Cities.

REFERENCES

[1] EEA, Air quality in Europe — 2018 report, European Environment Agency, Copenhagen, Denmark, 2018.

[2] ACEA, ACEA Pocket Guide 2018 - 2019, European Automobile Manufacturers' Association, Brussels, Belgium, 2019.

[3] C. Meneguzzer, M. Gastaldi, R. Rossi, G. Gecchele, and M. V. Prati. "Comparison of exhaust emissions at intersections under traffic signal versus roundabout control using an instrumented vehicle". Transportation Research Procedia, Vol. 25, 2017, pp. 1597-1609.

[4] Rodegerdts, L., et al. *Roundabouts: An Informational Guide - Second Edition.* Publication NCHRP 672, Transportation Research Board, Washington, DC., 2010.

[5] S. Gokhale, "Impacts of traffic-flows on vehicular-exhaust emissions at traffic junctions". Transportation Research Part D: Transport and Environment, Vol. 17, January 2012, pp. 21-27.

[6] P., Fernandes, K. Salamati, N. M. Rouphail, and M. C. Coelho. "Identification of emission hotspots in roundabouts corridors". Transportation Research Part D: Transport and Environment, Vol. 37, June 2015, pp. 48-64.

[7] Rodegerdts, L., et al. Roundabouts: An Informational Guide - Second Edition. Publication NCHRP 672, Transportation Research Board, Washington, DC., 2010.

[8] [8] P. Fernandes, T. Fontes, M. Neves, S.R. Pereira, J.M. Bandeira, M.C. Coelho, and N.M. Rouphail, "Assessment of corridors with different types of intersections: An environmental and traffic performance analysis". Transportation Research Record, Vol. 2503, 2015, pp. 39-5

Posters

Structural and optical study of evaporated cerium-doped silicon layers

BRIK Afaf[1], BEKHEDDA Kheira[1], BENYAHIA Badra[1],MENARI Hamid[1],MANSERI Amar[1]

[1]Centre de Recherche en Technologie des Semi-conducteurs pour l'Energétique (CRTSE) 2 Bd Frantz Fanon, B.P.140 Alger-7 Merveilles, Algiers (Algeria), Tel & Fax: +213 21433511

Email : brikafaf@yahoo.com

Abstract

The study of semiconductors doped with trivalent rare earth ions (TR3 +) has attracted a lot of interest and appears promising for applications in optoelectronics, notably thanks to the optical properties of rare earth ions. Our choice was cerium because it has several thin emission bands in a spectral range from near UV to infrared and it acts as a good antireflection coating.

The present study focused on evaporation of cerium (Ce) layers on silicon substrates (Si). Next, the applied doping process consists of high temperature annealing to be effective in the incorporation and activation of rare earth ions in silicon. The effect of heat treatment temperature was examined and studied using scanning electron microscopy (SEM) for structural characterizations and UV-Visible optical reflectance spectroscopy for optical characterizations.

Keywords: Cerium, Silicon, evaporation.

Introduction

In this work, the structural and optical characteristics of silicon doped with Ceruim ions were studied. We used a physical vapor phase deposit. Next, the applied doping process is followed by high temperature annealing to be effective in the incorporation and activation of rare earth ions into the silicon.
In a vacuum chamber connected to a pumping unit, capable of reaching a residual pressure of the order of 10-7 mbar, the 12 mg cerium (CeO2) oxide to be evaporated is charged into a crucible (see FIG. 1).
We used several means of characterization. We began by presenting SEM characterization results, and UV visible reflectance spectroscopy for optical characterization. it is a preliminary study to define the deposits for a photovoltaic application.

Experimental technique

The cerium was deposited using a vapor phase physical technique on p-type Si (100) substrates followed by a thermal annealing at different temperatures [1]

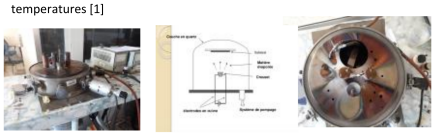

Fig 1 : Physical vapor phase image (Evaporation Edwards) used for thin film development at CRTSE

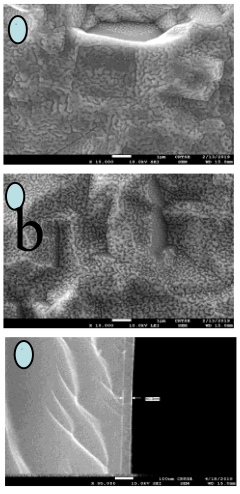

✓ small particles spread uniformly over the surface are in agglomerates.

✓ the higher the temperature or the duration of annealing, the higher the density of the agglomerates.

✓ CeO2 thickness

Fig 2 : **SEM** images of a Ce deposit on Si and annealing a t different temperatures for 1 h under N2 a)900C° b)1000C°

Experimental Results

The most direct technique for demonstrating the presence of Ce in annealed samples is Scanning electron microscopy.

The first observations were made on a thin film Ce deposited directly on a Si substrate.
These observations demonstrate the presence of a high density of Ce in a Si layer after annealing at 900-1000 ° C for 1 h with a surrounding thickness of 50 nm as shown in Figure 2 a, b and c.

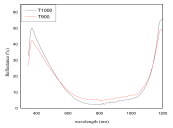

✓ a minimum reflectance around 2,5% is procured for the 1000° C sample.

Fig.3 Plot of reflectance of Si + CeO2 versus wavelength for two temperatures annealing

CONCLUSION

Thin layers of cerium oxide are deposited by the evaporation technique. The development procedure is simple, reproducible and inexpensive because it does not require expensive equipment. The elaboration is carried out at room temperature and atmospheric pressure after using different temperature annealing under N2 ambient . This simple procedure could be introduced in the solar cell manufacturing steps for efficiency improvement.

Com o apoio dos projetos:
UID/EMS/00481/2019 - FCT
CENTRO-01-0145-FEDER-022083

Effect of porosity variation on the physical properties of porous silicon

H. Lachenani, **A. Larabi**, N. Gabouze.

Centre de Recherche en Technologie des Semi-conducteurs pour l'Energétique (CRTSE), 02 Bd, Frantz Fanon, B.P. 140, Alger, Algérie.

Laboratoire de Physique des Techniques Expérimentales et ses Applications de Médéa LPTEAM, Département Science de la Matière, Faculté des Sciences, Université de Médéa Algérie

Resumo

Porous silicon (PS) is a promising material for several applications in significant and varied fields (photoluminescence (PL), electroluminescence (EL), gas and (bio) sensing, depollution, etc.). In this work, structural, electronic and vibrational properties investigations of PS were performed using ab-initio pseudo potential plane wave (PP-PW) method founded on Density Functional Theory (DFT) described by the generalized gradient approximation (GGA) included in the CASTEP program (Cambridge Serial Total Energy Package) [1, 2]. Furthermore, the computation of Infrared Radiation absorption spectra needs the calculation of atomic vibrational modes, which was performed by the Density-Functional Perturbation Theory (DFPT). The formation energies obtained from Density Functional Theory (DFT) calculation confirm that the stability of Porous Silicon structure is related to its porosity and high porosities have the lowest energy formation values. In addition, the electronic band structure of all Porous Silicon structure shows direct band gap semiconductors for all studied porosities. The measured Infrared Radiation (IR) spectra obtained from an elaborate sample of Porous Silicon layers was compared with the calculated spectra. The calculated Infrared Radiation in the energy range of 2000-2300 cm^{-1}, showed for all porosities the presence of relatively high intense peaks with some shifting, corresponding to Si-H_x stretching band, characteristic of porous silicon, in good accord with the experimental one and with literature.

Descrição

- Structural, electronic and vibrational properties investigations of PS were performed using ab-initio pseudo potential plane wave.
- Supercell model was used to simulate nanopores in porous silicon structure by taking out columns of atoms in the [0 0 1] direction on c-Si crystal. We begin from a supercell of 32 atoms formed by connecting four cubic cells, each with eight Si-atoms and lattice constant a = 5.43 Å. The lattice constants of the supercell (2x2x1) are of A = B = 2a and

To obtain different porosities P (ratio between the number of removed atoms to their total in the supercell), number of 1, 5, 9, 13 and 15 central Si atoms were removed from the supercell, which produced a porosity of 3.12, 15.62, 28.12, 40.62 and 46.87% successively as illustrated.

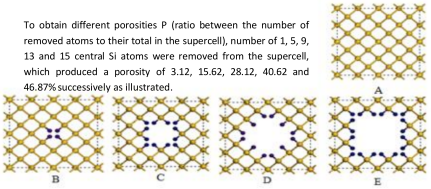

Fig 1 :Porous silicon model where yellow and blue spheres represent Si and H atoms, respectively.
A represents 32 atoms supercell of c-Si, and B, C, D and E are full H passivated porous silicon with 3.125%, 15.625%, 28.125%, and 40.625% of porosity, respectively.

- Porous silicon (PS) was achieved by electrochemical etching of (001) p-type silicon wafer (1–10 Ohm cm resistivity).
- The **Ohmic** contact on the back side of the Si anode has been achieved by rubbing GaIn

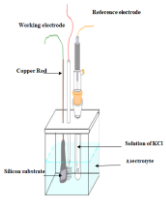

- Anodization of p-type substrates was performed under galvanostatic conditions in a simple O-ring cell in the dark, with a Pt wire as counter electrode and saturated calomel electrode as reference (SCE) using a Biologic VMP3 potentiostat/galvanostat.
- The etching solution was prepared by adding 30 vol. % of ethanol to 70 vol. % of HF aqueous solution (49 wt.%). The wafer was etched at a current density **of 10 mA/cm²** and etching time **of 5mn** to obtain a porosity of approximately 40 %

Fig 2: Anodization cell used for porous silicon elaboration.

- In order to confirm the ab-initio results, nanoporous silicon specimens were processed. Porous silicon (PS) was achieved by electrochemical etching of (001) p-type silicon wafer (1–10 Ohm cm resistivity).

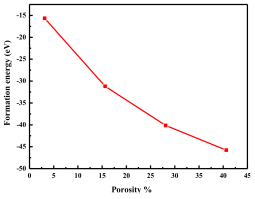

Fig 3: Formation energy trends vs porosity for full H passivation..

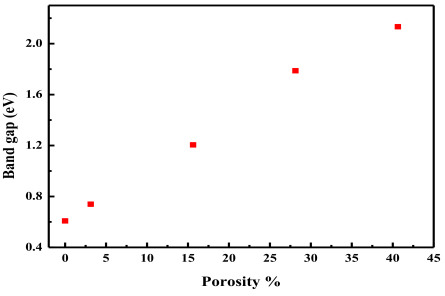

Fig 4: Evolution of band gap energy with porosity.

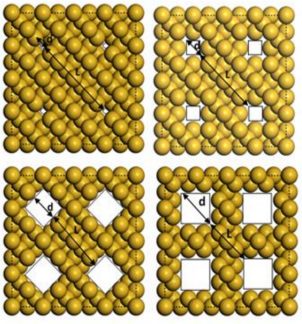

Fig 5 : Pores width (d) and confinement distance (L) between pore boundaries for different porosities for a) P=3.25%; b) P=15.62%; c) P=28.12%; d) P=40.62%.

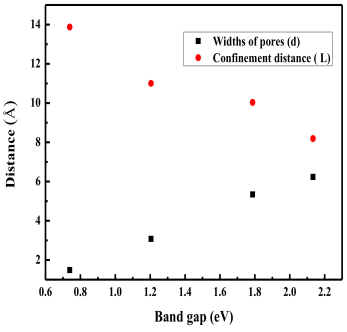

Fig 6 : Pores width (d) and confinement distance (L) between pore boundaries for different porosities for a) P=3.25%; b) P=15.62%; c) P=28.12%; d) P=40.62%.

Acknowledgement
The authors gratefully acknowledge the research unit and the research infrastructure TEMA of projects: UID / EMS / 00481/2013-FCT CENTRO-01-0145-FEDER-022083 respectively.

Com o apoio dos projetos:
UID/EMS/00481/2019 - FCT
CENTRO-01-0145-FEDER-022083

tema
centre for mechanical technology and automation

TECHNOLOGIES FOR THE WELLBEING

Electrical Properties of Pd/Ag Nanoparticles Modified Silicon Nanowires for CO_2 Detection

Naama Sabrina, Hadjersi Toufik

Abstract

One dimensional nanostructures play an important role in nanotechnology due to their good properties for future nanoelectronic device [1-2], photonic and optoelectronic devices [3] and more particularly as chemical or biological sensors [4-5].

In this study, a silicon-based nanowire from silicon wafer medium doped with crystallographic orientation (100) was prepared by metal assisted chemical etching (MACE) [6]. The modification of silicon nanowires (SiNWs) by palladium (Pd) and silver (Ag) nanoparticles was performed by electroless metal deposition method.

Electrical properties of different structures Al/Pd/SiNWs/Al and Al/Ag/SiNWs/Al were studied to evaluate the performance of the sensors for CO_2 detection. The electrical characterization (I-V), response sensor, response and recovery time were performed in primary vacuum at different concentration of CO_2 (0.5, 1 and 2mbar). It was shown that the sensor response depends strongly on the modification metal type.

We have found that Pd modified structure behave as an Ohmic contact. However, Ag modified and unmodified structures exhibit Schottky contact. The all structures reveal that the forward current increases with increasing CO_2 concentration, which can be explained by the decrease in the height barrier leading to an increase in the total current that flows through the device.

Also, the results reveal that the response is higher for Pd modified structure with voltage (0.05V) for high concentration (2mbar), while for Ag modified structure the response is higher with voltage (1.04V) for low concentration (0.5mbar). Operating at low voltage and low concentration of gas allows low power consumption.

Finally, the best response time and recovery time were recorded of Ag modified silicon nanowires for all CO_2 concentration. In addition, the response time is greater than recovery time indicating that the duration of the adsorption is greater than desorption time. This study shows that Ag can be used as catalyst for CO_2 detection. This result is very interesting since silver (Ag) is considered as very malleable metal, available and less expensive.

Description

- Silicon nanowires are the typical one-dimensional nanomaterial and attract lots of interest in recent years due to their good properties and their wide range of possible applications compared to the Si bulk.
- These properties open new perspectives in different domains such as electronic, photovoltaic, thermoelectic and sensors.....
- Here, SiNWs were synthesized by one-step process in $HF/AgNO_3$ solution.
- Low cost wet chemical etching method was used to fabricate SiNWs

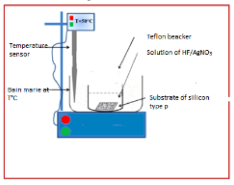

Fig 1 / Schematic of the system used for the formation of silicon nanowires (SiNWs).

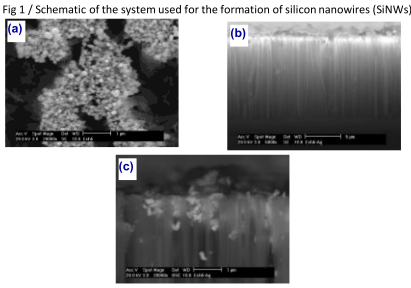

Fig 3 / (a,b and c) SEM plan and cross-sectional view images of the AgNPs modified SiNW s arrays.

- Palladium and silver nanoparticles were deposited by chemical method in solution $HF/PdCl_2$ /HCl and $HF/AgNO_3$ respectively.
- The morphology of silicon nanowires unmodified and modified with Pd, Ag was investigated by Scanning Electron Microscopy (SEM).
- The silicon nanowire arrays modified by metal nanoparticles have been employed to develop the sensors.
- The metal type used to modify the SiNWs strongly influences the I-V characteristics.
- The electrical characterization (I-V) was performed in primary vacuum and CO_2 gas at different concentrations.

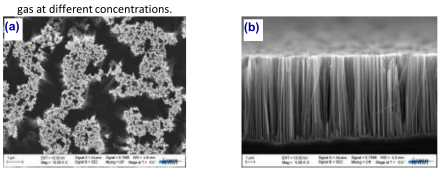

Fig 2 / (a) SEM plan view (b) SEM cross-sectional view of etched layer in HF /$AgNO_3$ solution : T= 50° C , t= 10min.

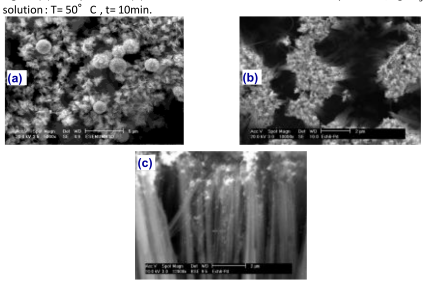

Fig 4 / (a,b and c) SEM plan and cross-sectional view images of the PdNPs modified SiNWs arrays.

- Ag is deposited uniformly as spherical shape nanoparticles of smooth surface. Their diameter is ranged from 70 to 170 nm.
- The Pd is deposited uniformly in the form of sheet and spherical shape nanoparticles of diameter about 2µm with density very important .

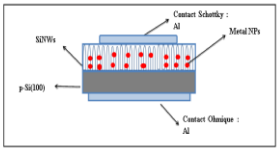

Fig 5 / Schematic of Al/MtNPs/SiNWs/Si/Al structures.

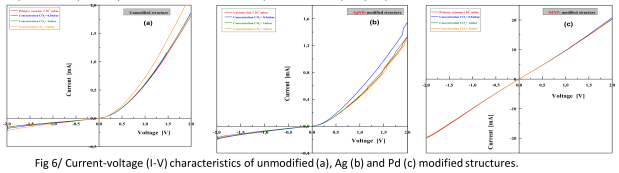

Fig 6/ Current-voltage (I-V) characteristics of unmodified (a), Ag (b) and Pd (c) modified structures.

- The I-V characteristics of Pd modified structures reveal an Ohmic contact but for unmodified and Ag modified structures a Schottky contact.

Table 1 / Response sensor of unmodified and modified structures.

Structures	Voltage(V)	Optimal sensor response (%) 0.5mbar	Voltage(V)	Optimal sensor response (%) 1mbar CO_2	Voltage(V)	Optimal sensor response (%) 2mbar CO_2
Unmodified structure	2	3.8	1.11	4.7	1.65	23
Ag modified structure	1.04	23	1.18	4.7	1.90	3
Pd modified structure	0.05	26	0.05	25	0.05	27

- The response of the sensor shows that unmodified structure is insensitive to CO_2 molecules for low concentration.
- For Ag and Pd modified structures, the maximum response is observed for low and high CO_2 concentration respectively.

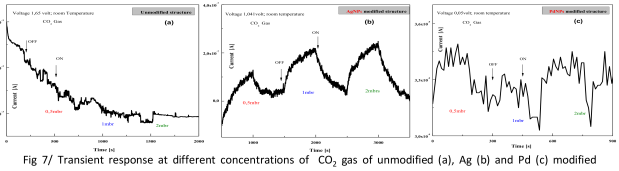

Fig 7/ Transient response at different concentrations of CO_2 gas of unmodified (a), Ag (b) and Pd (c) modified structures. at room temperature .

Table 2 / Response sensor of unmodified and modified structures.

Structures	Response time (s)			Recovery time (s)		
	0.5mbar	1mbar	2mbar	0.5mbar	1mbar	2mbar
Unmodified structure	No response	No response	No response	No response	No response	No response
Ag modified structure	272	279.75	293.69	192.31	184.25	125.28
Pd modified structure	No response	No response	No response	No response	No response	No response

Acknowledgment

The authors gratefully acknowledge the research unit and the research infrastructure TEMA of projects: UID / EMS / 00481/2019-FCT CENTRO-01-0145-FEDER-022083 respectively

Com o apoio dos projetos:
UID/EMS/00481/2019 - FCT
CENTRO-01-0145-FEDER-022083

tema
centre for mechanical
technology and automation

TECHNOLOGIES FOR THE WELLBEING

Multifunctional lightweight cellular materials

Susana C. Pinto[1], Isabel Duarte[1], Romeu Vicente[2] and Paula A.A.P. Marques[1]

[1]TEMA, Department of Mechanical Engineering, University of Aveiro

[2]RISCO, Department of Civil Engineering, University of Aveiro

Abstract

Cellular materials are fascinating structures composed by two phases, a continuous solid phase (cell walls) and a continuous or discontinuous gaseous phase corresponding to the air trapped within it (pores or cells). This arrangement results in an interconnected porous network of solid struts or plates, which form the edges and faces of pores/cells [1,2]. The low weight and unique mechanical properties make this kind of structures suitable for a wide range of engineering applications, namely in the areas of biomedical, acoustic and thermal insulation, and crashworthiness. Recently, special attention is being dedicated to hybrid foams based on aluminum open-cell (Al-OC) [3,4].

Based on the hybrid material concept, we developed and tested new hybrid foams by combining the Al-OC foams with different polymers. The Al-OC foam specimens were completely impregnated with specific polymers to explore possible synergies and therefore enhance their performance, thus creating a multifunctional material. Bulky polymers (polydimethyl siloxane, PDMS and epoxy, EP) and foamed bacterial cellulose, BC, and have been chosen as filling materials. These were prior combined with graphene-based materials, GBMs (graphene oxide, GO and/or reduced graphene oxide, rGO) at low loading values to ensure the final hybrids with fire-retardancy [5].

In the former the polymers improved the mechanical behaviour of Al-OC and in the later it will be the Al-OC to confer an appropriate structure to BC fragile foams.

Al-OC foams impregnated with PDMS and PDMS/GO composite

Fig 1 Fabricated specimens: a) Al-OC , b) PDMS, c) PDMS/GO, d) Al-PDMS and e) Al-PDMS/GO

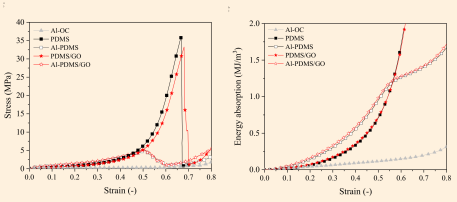

Fig 2 Mechanical behaviour: a) Stress-Strain curves and b) Energy absorption curves.

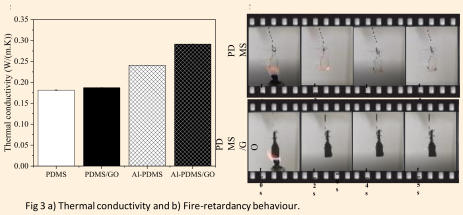

Fig 3 a) Thermal conductivity and b) Fire-retardancy behaviour.

Al-OC foams impregnated with EP and EP/GO composite resins

Fig 4 Fabricated specimens: a) Al-OC , b) EP, c) EP/GO, d) Al-EP and e) Al-EP/GO

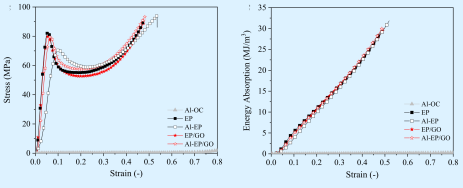

Fig 5 Mechanical behaviour: a) Stress-Strain curves and b) Energy absorption curves.

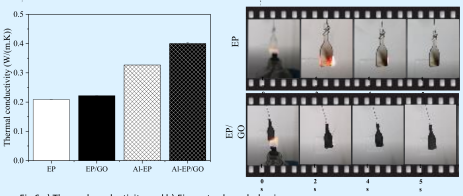

Fig 6 a) Thermal conductivity and b) Fire-retardancy behaviour.

Al-OC foams impregnated with BC, BC/GO and BC/rGO composite foa

Fig 7 Fabricated specimens: a) Al-OC , b) Al-BC, c) Al-BC/GO10% and d) Al-BC/rGO10%

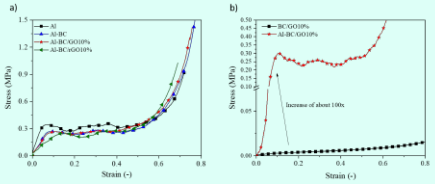

Fig 8 Mechanical behaviour. a) Stress-strain curves and b) improvement of mechanical behaviour with Al-OC.

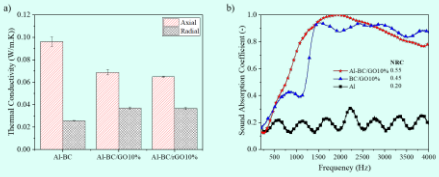

Fig 9 a) Thermal conductivity and b) sound absorption coefficient.

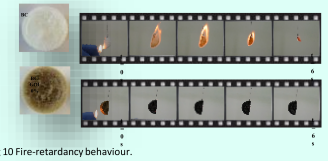

Fig 10 Fire-retardancy behaviour.

Final Remarks

- Multifunctional hybrid foams were prepared successfully;
- The incorporation of GBMs provided fire-retardancy to the polymers tested;
- The mechanical behaviour of Al-OC structures was improved by EP and PDMS incorporation;
- The Al-BC and its composites showed acoustic and thermal insulation properties provided by the cellular structure;
- The combination of BC and BC composite foams with Al-OC greatly enhanced the mechanical strength, while keeping the lightweight properties of BC and BC composites.

References

[1] M.F. Ashby and Y.J.M. Bréchet, "Designing hybrid materials", Acta Mater., vol. 51, pp. 5801–5821, 2003.

[2] I. Duarte, N. Peixinho, A. Andrade-campos and R. Valente, "Special Issue on Cellular Materials," Sci. Technol. Mater., vol. 30, no. 1, pp. 1–3, 2018.

[3] I. Duarte and J.M.F. Ferreira, "Composite and Nanocomposite Metal Foams", Materials (Basel)., vol. 1, pp. 1–34, 2016.

[4] I. Duarte, M. Vesenjak, L. Krstulović-Opara and Z. Ren, (2018) "Crush performance of multifunctional hybrid foams based on an aluminium alloy open-cell foam skeleton", Polym. Test., vol. 67, pp. 246–256, 2018.

[5] Sang, Z. Li, X. Li, L. Yu, and Z. Zhang, "Graphene-based flame retardants: a review", J. Mater. Sci., vol. 51, pp. 8271–8295, 2016.

Acknowledgments

Com o apoio dos projetos:
UID/EMS/00481/2019 - FCT
CENTRO-01-0145-FEDER-022083

Full Papers

Design and sustainability: transforming plastic waste into new long-life products

Catarina Marques[1,2], Teresa Franqueira[2], Victor Neto[1]
[1] Department of Mechanical Engineering, [2] Department of Communication and Art
University of Aveiro, Aveiro, Portugal
cpmarques@ua.pt, teresa.franqueira@ua.pt, vneto@ua.pt

Abstract— The plastic industry and the prevailing dependence on plastic has generated an excessive amount of waste, that consequently, pollutes the environment. It has been estimated that 8300 million metric tons (Mt) of virgin plastic have been produced thus far and, if the trend remains, roughly 12000 Mt of plastic waste will be in landfills or in a natural environment by 2050 [1]. This problem has rapidly grown to the point where the current era is characterized as the "Age of plastics" [2].

Overconsumption and discard habits, combined with poor material lifecycle management, contribute to the deposit of these wastes into the environment, especially in the ocean [3]. Therefore, the ocean becomes the final receiver of some plastic materials, that are considered the most abundant and the most problematic for the environment, economy, and health of ocean habitats. Thus, it's estimated that each year, 8 million tons of plastic end up in the ocean [4]. These circumstances become harmful to marine life as they may cause imprisonment or ingestion of the plastic [5]. The situation can affect the health and well-being of humans with a transmission of plastic through the food chain [6].

In this context, the challenge and goal of this work is to minimize this problem by developing products using ocean plastic or likely to get in there one day as a resource. In this sense, the work focuses on the usage of recycled Polyethylene terephthalate (PET), Polypropylene (PP) and High-density polyethylene (HDPE), considering they are the most commonly -used materials and are easily found in the ocean, according to an analysis made during the study. The work consists of doing experimental procedures with domestic and ocean plastic in two different manufacturing processes, injection molding, and 3D printing. Thus, it's possible to draw conclusions from the behavior and limitations of each material submitted to reprocessing, and consequently satisfy the requirements for each product that will be developed. The results obtained show that the material coming from the ocean presents less tensile strength than the domestic one.

Therefore, an interior plant cultivation system will be designed using domestic waste plastic and, in future works, an item of urban furniture will be developed with ocean-sourced plastic. Additionally, the products are accompanied by a service with the aim of developing a basis for the process chain, from the collection of the raw material until its new life, based on a sustainable stance.

In conclusion, the aim of this research is to design strategically so that there's an increase in the life cycle of the materials. This will be accomplished by giving them a new life, through the transformation of plastic waste, mitigating the environmental impact created from the excessive consumption of disposable products. It should be noted that the current excessive usage of products will not be sustainable unless the industry develops more innovative and ecological approaches.

Keywords— Plastic recycling; Ocean plastic; Product design; Circular economy.

TOPIC

1) c.: Sustainable Manufacturing Solutions – Manufacturing for Circular Economy

Introduction

Plastic is a synthetic polymeric and organic material, derived from petroleum - a substance that serves as raw material for the manufacture of the most varied products. It was developed in the twentieth century and since then it has been used in various applications due to its elastic properties. However, it is not biodegradable, presenting a major environmental risk to the planet [7].

The ocean is one of the ecosystems most affected by the excessive production of plastic and Europe is in second place on world ranking of its production after China. According to studies carried out by the scientific community that analyzes this global phenomenon, about eight million tons of plastic debris and its derivatives are released annually in the oceans, damaging the ecosystem [8]. These circumstances arise concerns for the health of human beings and marine animals, but also on a socio-economic level.

Figure 3 – Ocean pollution and its impacts

Currently, although it isn't yet enough for a sustainable economy, there is a growing concern at this level. This translates into the development of new projects based on reusing and recycling the plastics to utilize the available raw material. In this context, new concepts such as circular economy, eco-design, and sustainability emerged, in order to face the consequences of the excess consumption and waste adjacent to the increase of population [9]. In the European Union (EU), there is also and emersion of new agreements that restrict the use of certain single-use plastics, as this category represents about 70% of the waste that pollutes the oceans and beaches [10].

Sustainable evolution is still a daily challenge and represents a goal to accomplish on a global scale. The great difficulty presented in the recycling process is the constraints that exist in its different phases, from the collection of the raw material to its new application. Furthermore, the quality of the final product can be compromised due to the properties lost during the process. For this reason, for many companies recycling still doesn't represent a 100% reliable solution.

In such manner, the main purpose of this article is to select some thermoplastic polymers to be recycled and to proceed with the evaluation of their mechanical behavior after its life cycle has ended in the trash or the ocean. The goal is to analyze the properties, and, with this, understand the limitations of the recycled material. It's intended that this material can be well applied, according to the requirements of the product.

THEORETICAL CONTEXTUALIZATION

The proliferation of the use of plastics in combination with poor management of waste at the end of its life has resulted in pollution [11], which contributes to the increase and persistence of marine and domestic debris [12]. Nonetheless, some solutions have emerged to combat this paradigm, one of them is recycling.

Recycling is the reprocessing of materials into new products. This process presents major advantages because it avoids the excessive use of natural resources and reduces the consumption of raw material and energy, in comparison to the production of virgin material. In addition to that, it potentiates the reduction of manufacturing costs in the environmental, social and, in some cases, economic level. On the other hand, this process eliminates several stages where it's necessary to use techniques that consume energy in the process and transportation [13].

The plastic waste can be produced from different sources, which distinguish them in two large groups. Pre-consumer waste is obtained from the plastic waste of a production process. And the post-consumer waste is obtained through products and packaging that already have an associated life cycle [14].

Figure 4 – Sources of plastic waste

In this sense, the present study highlights the post-consumer waste, since these present more difficulties in the process.

I. MERO

The business model or service behind the process from collecting to producing new products is called MERO, which means "Maintain and Recover the Ocean". The project consists of the treatment and recovery of waste from the ocean or coastal areas, intending to develop products that promote sustainability by using material not currently valued.

The service includes preventive and corrective measures, corresponding to "Maintain" and "Recover", respectively. Preventive measures include gathering plastic that hasn't yet been into the sea, either domestic or lost in the city, and so preventing plastic from going to the ocean. The corrective measures are intended to collect the plastic present in the marine environment, considered marine litter.

The service includes the treatment of plastic waste, from its collection, through associations and partner companies, to the production of new products. It also includes the sale of products with MERO brand, and in this work, a product line was developed with domestic material, as an example of product that can be sold. Besides that, MERO does awareness campaigns in schools and companies interested in the sustainability approach.

Figure 5 – MERO

Raising awareness, valuing and developing projects that meet sustainability is becoming a global goal. However, there are still difficulties to overcome, one of them being the loss of mechanical properties that the recycled material present, due to the contamination

and deterioration that sometimes happens during its useful life. In this context, the next phase is the experimental process, in order to identify the variations and limitations in the mechanical properties of the recycled materials.

Methods

In this section, the experimental procedures used are outlined, as well as the methods and techniques necessary to determine the properties of the materials. The purpose is to understand the differences in the process and behavior of domestic and ocean materials in two different manufacturing processes, injection molding, and 3D printing. Injection molding because it is one of the processes most used in the plastics industry and 3D printing because it is in constant development and is accessible to the general audience. The goal is to make it so that anyone can create their products through their plastic waste. Thus, in addition to establishing a comparison between materials that have different life cycles, it also analyzes its mechanical behavior in different processes.

I. Collection of material

Firstly, it was necessary to collect both household plastics and marine litter. For this purpose, some household materials were collected as well as materials resulting from marine debris collecting campaigns by fishermen from Gafanha da Nazaré. Each material was properly separated, classified according to its typology and analyzed. In the graphs of figure 4, the variety of material collected can be observed, organized according to its mass and with that, it's possible to conclude the ones that are most relevant to the study.

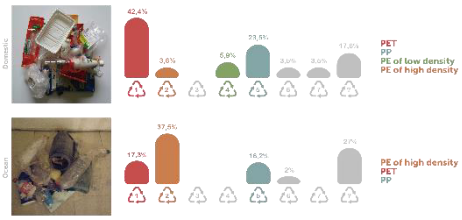

Figure 6 - Analysis of the Plastic material collection

According to the graphs, in the collection of household use, the most present materials in order are PET, PP, and PE. On the other hand, in the collection that comes from the sea, are HDPE, PET, and PP. Although it isn't shown in the same order, PET, PP, and PE represent the largest amount collected in both household and marine waste. This is probably because domestic material is the main source of marine debris. Therefore, the materials most commonly used in our houses are also the materials that will probably end up in the oceans. In this sense, the materials to be used as an object of the study are PET, PP e HDPE.

II. Injection molding

To produce injected samples, in the first instance, it was necessary to remove the labels from the packaging, proceed to the proper washing using detergent and water and finally cut the packages in pieces of 5mm x 5mm. It was still necessary to dry the PET and HDPE material using an oven for this purpose. The PET was heated to 120 degrees and HDPE to 100 degrees (figure 5).

Figure 7 - Injection process

The process was done in the Haake Minijet II machine from Thermo Fisher Scientific. And the samples were obtained according to the type 5A sample of ISO 527-2: 1996 [15] (figure 6).

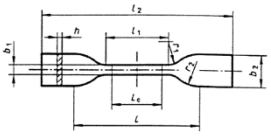

Dimensão	Valor (mm)
l_2	75,00 ± 0,05
b_2	12,70 ± 0,05
l_1	25,00 ± 0,05
b_1	4,10 ± 0,05
r_1	8,00 ± 0,05
r_2	12,5 ± 0,1
L	50,00 ± 0,05
L_0	20,00 ± 0,05
h	2,00 ± 0,05

Figure 8 - Injection of standard samples

After some experiments to establish the most favorable parameters, the ideal conditions were reached (Table 1).

Table 1 - Parameters for injection molding

	material	cylinder temp.	mold temp.	pressure	post pressure
domestic	PET	270ºC	140ºC	500 bar - 20s	300 bar - 10s
	PP	270ºC	50ºC	600 bar - 20s	600 bar - 10s
	HDPE	210ºC	75ºC	600 bar - 20s	600 bar - 10s
ocean	PET	270ºC	148ºC	500 bar - 20s	500 bar - 20s
	PP	210ºC	60ºC	600 bar - 20s	600 bar - 20s
	HDPE	210ºC	75ºC	600 bar - 20s	600 bar - 20s

Figure 7 shows the injected samples to be tested. Five samples were produced for each study because of inevitable systematic and random deviations in an experimental procedure.

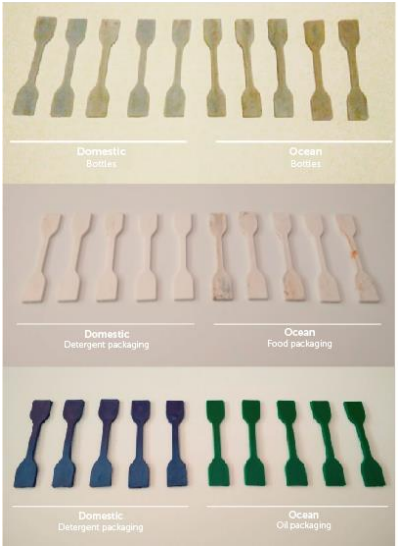

Figure 9 - Injection samples

In order to study the mechanical properties of the prepared samples, tensile tests were done in accordance to ASTM D638-10 (equivalent to ISO 527) [16,17], using Shimadzu Autograph AGS-X 10 kN universal machine (Figure 8). For each study material, five samples were done, thirty in total, with a speed of 3mm/min, L0 = 45mm, D = 4mm, and b = 2mm to perform the tests.

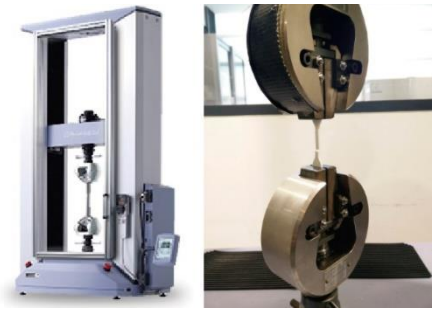

Figure 10 - Shimadzu Autograph AGS-X 10kN

Figure 9 shows the test results from the six different studies.

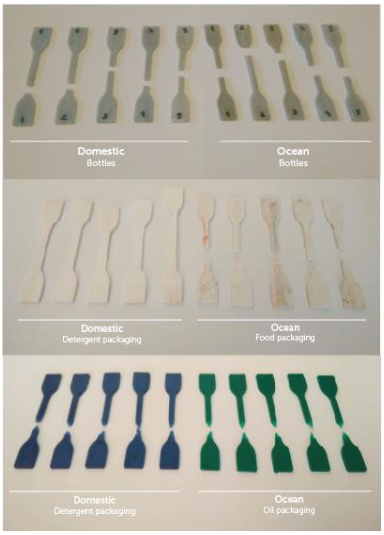

Figure 11 - Injection samples after tensile test

III. 3d printing

The same procedure was done for 3D printing, with the difference that, after the washing and drying of the material, extrusion of filament was required.

The process was done using two machines, the extruder to make the filament, in the Noztek Pro Desktop Filament Extruder machine, and the 3D printer, Beeverycreative B2X300, to print the samples (figure 10).

Figure 12 - Extruder and 3D printer

The conditions used in the extruder and 3D printing were as shown in the following tables.

Table 2 - Conditions used in extrusion

	material	temperature
domestic	PET	245ºC a 260ºC
	PP	270ºC
	HDPE	210ºC
ocean	PET	245ºC a 260ºC
	PP	200ºC
	HDPE	210ºC

Table 3 - Conditions used in 3D printing

	material	temperature	bed temp.	speed
domestic	PET	250ºC	60ºC	60 mm/s
	PP	250ºC	85ºC	15 mm/s
	HDPE	220ºC	85ºC	15 mm/s
ocean	PET	250ºC	60ºC	60 mm/s
	PP	250ºC	85ºC	15 mm/s
	HDPE	220ºC	85ºC	15 mm/s

Figure 11 shows the printed samples to be tested. Not five but three samples were produced for each study since the process of extrusion of constant filament and subsequent printing process still presents some difficulties. HDPE was the material that showed more difficulties, so because of that, it wasn't possible to print this material's samples.

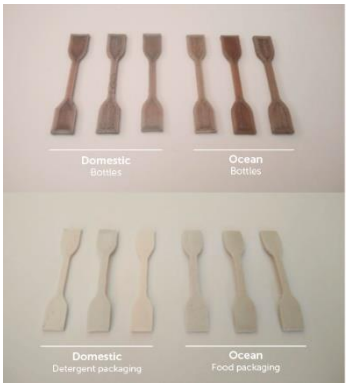

Figure 13 - Printed samples

Figure 12 shows the test results from the six different studies.

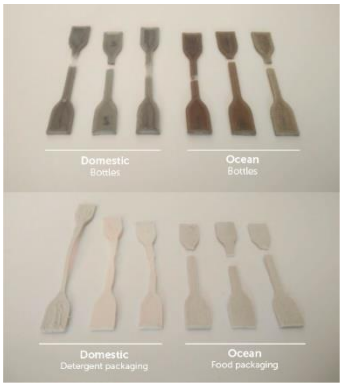

Figure 14 - Printed samples after tensile test

IV. Results

Each material had distinctions in its behavior during the process, causing problems or benefits in the two processes. The conclusions of the challenges during reprocessing are shown in the following graphs (figures 13 and 14).

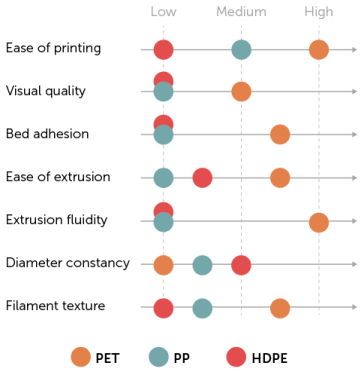

Figure 15 - Challenges of 3D printing

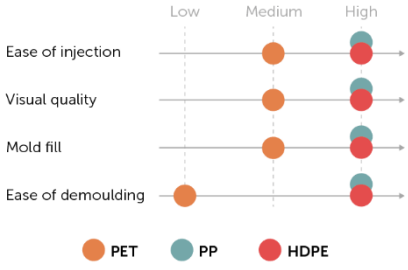

Figure 16 - Challenges of injection molding

Briefly, PP and HDPE are the easiest materials to inject, while PET is the easiest to extrude and print.

After the end of the tensile tests of the different studies, and for a better comparison of the results, it was necessary to obtain Stress-Strain diagrams (figures 15, 16 and 17). As the name implies, these diagrams present stress curves as a function of the deformation, and it's possible to analyze the behavior of the material throughout the test.

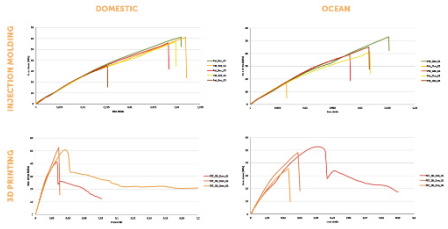

Figure 17 - Stress-Strain diagrams from PET

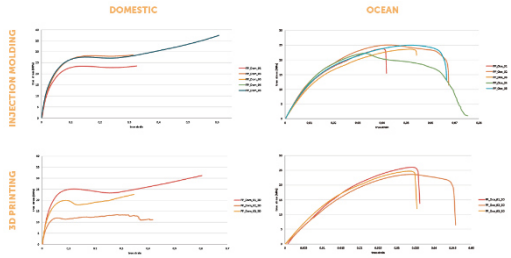

Figure 18 - Stress-Strain diagrams from PP

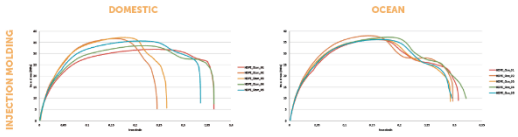

Figure 19 - Stress-Strain diagrams from HDPE

It can be observed that the curves obtained in the PET study describe a characteristic behavior of fragile materials, more conclusive in the injection samples. However, PP and HDPE show more ductile behavior.

Besides that, it was important to determine the necessary parameters in the mechanical properties' analysis in the different studies: ultimate tensile strength, deformation, Young's modulus and the breaking point [18]. At the end of each test series, the arithmetic mean of the measured values and the standard deviation shall be determined. The results obtained are shown in the following table.

Table 4 - Results of tensile strength test

material	test	ultim. strength	deformation	Young's modulus
PET	INJ. DOM.	54±10.8	0.06024±0.02	2544.2±29.6
	INJ. OCE.	39.2±13.0	0.04142±0.02	2936.4±247.7
	PRINT DOM.	48.3±6.4	0.0676±0.01	2239±117.1
	PRINT OCE.	45.7±8.8	0.0688±0.02	2126.3±159.4
PP	INJ. DOM.	29.2±4.8	0.82816±0.29	829.6±99.4
	INJ. OCE.	24±1.2	0.09698±0.02	1404.2±82.0
	PRINT DOM.	22.3±9.0	0.9152±0.38	694±130.5
	PRINT OCE.	25±1.0	0.07507±0.01	1275.7±124.5
HDPE	INJ. DOM.	35.2±2.2	0.4501±0.07	850.4±123.6
	INJ. OCE.	36.6±0.9	0.36066±0.03	993.6±40.1

PET has the highest resistance (highest ultimate strength), the highest stiffness (highest Young's modulus), and the highest hardness (lowest deformation) in both processes. While PP is less resistant and harder than all three but has the same rigidity as HDPE.

Regarding the origin of the material, PET and PP from the ocean have a lower resistance to injection than those from the domestic origin. However, this cannot be stated in 3D printing, since they have very similar or even slightly higher resistances. Thus, it was concluded that 3D printing can be a good solution for recycling materials from the ocean.

Regarding the rigidity, in general, the material from the ocean presents higher values than the domestic material.

It's important to mention that the resulting values are variable since there is a huge variability of existing products of the same typology and that have different characteristics. This not only hinders the homogeneity of the results in the recycling process but also makes comparisons between materials' difficulties, with often ambiguous and uncertain results.

product development

I. Self-watering pot

Nowadays, the human being spends 85% of its lifetime in closed spaces [19], mainly in its habitation. Thus, it's fundamental to bring nature from the outside to the inside to assure the well-being of the inhabitants of the space. For that reason, an indoor cultivation system is a good solution. Furthermore, the environmental impacts resulting from this product are a significant reduction in transport and energy resources and carbon dioxide reduction, due to the decrease in the distance between the producer and the consumer. Addicionally, it reduces the need for packaging, thereby reduceing plastic waste [20].

The development of this product goes through different phases: benchmarking, a study of kitchen ergonomics, concept generation and selection, and validation through mock-ups (figure 18).

Figure 20 - Product development

After these phases have been completed, the final proposal is an auto-irrigation system to facilitate the cultivation, shown in the figure below. The bottom container serves to store water, and through the phenomenon of capillarity, water is transported to the plant, according to its needs.

Figure 21 - Final product

It was also possible to print a component of the plant pot, through filament obtained by plastic water bottles (PET), validating the applicability of this product using 3D printing as a means of production.

Figure 22 - Printed component of the vase

Conclusions

In conclusion, the accomplishment of this study was fundamental to the point of view of the knowledge acquired in the field of recycling polymer materials.

It was concluded that the ocean material presents some complications due to degradation processes that occur in the marine environment, however, in general, the characteristics that they present are similar to the domestic materials.

The loss of mechanical properties in the reprocessing of plastics is a fact that cannot be ignored. However, the main matter is to adapt the applicability of the product to the characteristics of the material. Thus, the use of recycled materials is a solution for products with specifications of a low requirement.

Acknowledgment

The research here presented was supported by the projects UID/EMS/00481/2019-FCT - FCT - Fundação para a Ciência e a Tecnologia; and CENTRO-01-0145-FEDER-022083 - Centro Portugal Regional Operational Program (Centro2020), under the PORTUGAL 2020 Partnership Agreement, through the European Regional Development Fund. The authors also acknowledge the support of Professors Filomena Cardoso Martins and Ana Paula Gomes, from the Department of Environment and Planning, and of Catarina Lemos, from the UACopera unit, for the handling of the sea plastic residues.

References

[9] Geyer, R., Jambeck, J. R., & Law, K. L., "Production, use, and fate of all plastics ever made" *Science Advances*. vol. 3, pp. 1-5, July 2017.

[10] Moore, C. J., "How much plastic is in the ocean? You tell me!" *Marine Pollution Bulletin*. vol. 92, pp. 1-3, 2015.

[11] Martins, J., and Sobral, P., "Plastic marine debris on the Portuguese coastline: A matter of size?" *Marine Pollution Bulletin*. vol. 62, pp. 2649-2653, 2011.

[12] European Environment Agency, "*Marine Litter Watch: Citizens collect plastic and data to protect Europe's marine environment*." *Marine Litter Watch*. 2014.

[13] Allsopp, M., Walters, A., Santillo, D., & Johnston, P., "*Plastic Debris in the World's Oceans*." The Netherlands. 2006.

[14] Sobral, P. et al., "*Lixo Marinho: um problema sem fronteiras*." Parceria Portuguesa para o Lixo Marinho., Lisboa, pp. 1-65, 2015.

[15] Frias, J., Microplásticos: O presente envenenado. Lisbon: University Nova de Lisboa, 2010.

[16] Ocean Action, "Origem da poluição" unpublished

[17] Ellen MacArthur Foundation, "New Plastics Economy – Catalysing Action" *World Economic Forum*. vol. 52, pp. 1-68, 2013.

[18] EU council, "*Plásticos de utilização única: Presidência chega a acordo provisório com o Parlamento*." Brussels. 2018.

[19] Zero Waste Europe, "Plastics in the Interface between Chemicals, Products and Waste." *Rethink Plastics*. Brussels. pp. 1-6, 2015.

[20] Rios, L.M., Moore, C., Jones, P.R., "Persistent organic pollutants carried by synthetic polymers in the ocean environment" *Marine Pollution Bulletin*. vol. 54, pp. 230-1237, 2007.

[21] Mohamad, A., Abdul, H., William, D., Review of Recycling and Its Techniques. Malaysia: Engineering Conference on Energy and Environment, 2007.

[22] Gort, I., Gerrits, A., "Designing with recycled plastics handbook" *Partners for Innovation.* Amsterdam. pp. 1-48, 2015.

[23] International Organization for Standartization, Plastics - Determination o tensile properties - Part 2: Test conditions for moulding and extrusion plastics, 2nd ed. London: British Standard, 2006.

[24] ASTM International, Standard Test Method for Tensile Properties of Plastics D638. United States: Department of Defense, 2010.

[25] ASTM International, Standard Test Method for Tensile Strength and Young Modulus for High-Modulus Single-Filament Materials (D 3379). United States: West Conshohocken, 1989.

[26] Costa, A., Nanocompósitos de matriz polimérica para impressão 3D. Aveiro: University of Aveiro, 2016.

[27] Martins, J., and Sobral, P., "Interaction with indoor plants may reduce psychological and physiological stress by suppressing autonomic nervous system activity in young adults: A randomized crossover study" *Journal of Physiological Anthropology*. vol. 34, pp. 1-6, 2015.

[28] Doron, G., "Urban Agriculture: Small, Medium, Large" *Architectural Design*. vol. 75, pp. 52-59, 2005.

[29] Yücel, G., "Street Furniture and Amenities: Designing the User-Oriented Urban Landscape" *Advances in Landscape Architecture*. pp. 623-644, 2013.

Development of a cost-effective multi-axis force sensor for robotics automation

Ricardo Guincho
School of Design, Management and Production
Technologies Northern Aveiro
University of Aveiro
Oliveira de Azeméis, Portugal

Daniel Afonso
School of Design, Management and Production
Technologies Northern Aveiro
and
TEMA - Centre for Mechanical Technology and Automation
University of Aveiro, Portugal

The industry 4.0 revolution centers itself around the automation of industrial processes, with a focus on interconnected manufacturing units and autonomous process control, among others [1]. As industrial robots take the place of human workers in monotonous, repetitive and even dangerous tasks, a need appears for a robotic solution for more intuitive lines of manufacturing, which often depend on human expertise, such as polishing, grinding and assembly [2]. A cost-effective force sensor is developed as a base solution for the automation of such operations. While this sensor is being developed as a part of a mold polishing automation project, it is being designed to be able to be used in any force sensing implementation, within the sensor's own limitations.

The currently developed system is capable of detecting (linear) forces in two axes, with the possibility of detection of forces in three orthogonal axes with a slight design modification.

Force calculations are performed within a signal conditioning/controller board that can communicate directly with the industrial robot system, reducing the computational load on the latter. The use of standard, off-the-shelf, components for the signal conditioning board attempts to ensure the low cost and ease of part repair/replacement, and the controller board allows for one dimensional Analog (DAC) and Digital (PWM) output as a direct communication method with the input cards of an industrial robot controller, as well as Serial TTL, and Serial-USB communication for a more in depth control of the sensor-robot system, allowing for custom robot responses to the measured forces, as well as individual load cell gain adjustment and calibration.

The development of an active response force sensing tool is also underway. It will enable the usage of the tool as a self-correcting closed system that does not require real-time control or direct communication with the robot system, improving ease of implementation in different types of robots.

force sensor; automation; robotics; polishing; lowcost;

Introduction

Process automation is ever more present in modern factories and production lines, and as such human-robot interaction is sometimes inevitable, as well as the replacement of the human worker for a robotic one [1]. The use of robots in tasks previously only performed by humans due to characteristics such as the need for intuitive decision making, real-time adaptation of tools and tool path, requires the development of adaptive robot control techniques which analyze the robot's surroundings and the objects it is in contact with and uses that information to plan the next stage in the robot's movement. One of the main components in the implementation of adaptive behaviors in industrial robots is the force sensor. The sensor allows the robot to get feedback about its interaction with the objects and people in its surroundings. However, currently available solutions are very expensive for small scale implementations and are of proprietary nature, which forces the use of specific industrial robot models in the production line [4-7]. The force feedback loop allows the controller to adjust the position or velocity of the machine based on the intensity of the force and torque values. Some examples or applications of robotics with force sensing capabilities are assembly, grinding and polishing, material and product testing, surgery, and others. Besides the sensing ability, [2,8-10].

Although several soluctions exist for the implementation of automated systems, a large part of the manufacturing tasks are still performed by humans. While some task are perform by humans due to their cognitive and adaptive capacity, others are limited by the automation cost, skilled resources and long installation period[11].

This work focuses on the development of a cost effective and adaptable force sensor/control unit to be used in industrial robotics applications such as grinding, polishing and assembly. Such operations are heavily dependent on the senses of touch and vision, as well as, and most importantly, experience on the worker's part. Polishing is a very intuitive operation, requiring years of expertise to know the technique needed for a desired surface look. For a robot to perform such tasks, it needs the same force sensitivity capabilities to emulate the sense of touch humans have [2, 3]. The paper presents the development of a force sensor using easily assembled off-the-shelf parts, including the mechanical and electrical hardware, and tests its use on an industrial robot. Finally, a more complex sensor/actuator device concept is proposed.

Methods

The development of a multi-axis force sensor took into account the use of off-the-shelf parts, available from international component suppliers, allowing the cost reduction and ease of part replacement. Further, the use of custom parts was reduced, and parts were designed to be manufactured by simple milling operations and 3D printing, allowing for good reproducibility.

1. Sensor development

Although the developed force sensor can be used for several applications, the main goal is using it for polishing operations. The mechanical implementation focused in using a simple geometry and assembly, together with a semi-modular design that allows the adaptation of different kinds of tool, for the different tasks where force control is required.

1.1. Mechanical system

The sensor's mechanics consist in two parallel plates joined by a universal joint mounted perpendicular to the plates and at their center (Figure 24). One of the plates (flange plate) attaches to the robot's flange, and the other plate is where the work tool will be mounted (tool plate). In the case of this project, a conventional rotary grinding tool was used. The universal joint allows free rotation in two normal axes parallel to the plates' mounting plane. The flange plate contains slots for three TE Connectivity FX1901 compression load cells, and the tool plate contains three tapped holes corresponding to the positions of the three load cells. In those tapped holes, three calibration screws are placed, which contact the load cells, making the whole sensor assembly rigid. Force applied on the top plate will be almost completely transmitted to the load cells. The calibration screws allow the use of compression load cells in a compression-tension behavior through the preloading of the cells during screw tightening, therefore creating a load offset that can be used to measure "negative" loads on the cell. The geometry of the sensor enables the detection of force in a plane defined by two (X and Y) axis, the same of the universal joint for the sensor without a mounted tool. Depending on the tool's geometry, the applied force plane may rotate due to lever effect, which must be taken into account during load cell signal processing.

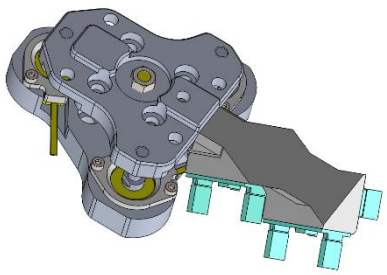

Figure 23 – Complete force sensor with load cell amplifier boards.

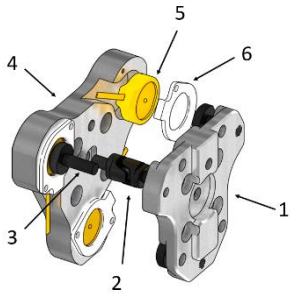

Figure 24 – Base sensor mechanics: 1 – tool plate; 2 – universal joint; 3 – load offset/calibration screw; 4 – flange plate; 5 – FX1901 load cell; 6 – Load cell lock ring.

1.2. Electronics and communications

The sensor's electronics were designed with a focus on off-the-shelf components and shifting the burden of force calculations away from the robot programming. While industrial robots can measure analog electric signals, the analog to digital conversion and processing is often highly time consuming, which compounds with any extra calculations that may be required to achieve the necessary correction trajectory. As such, the sensor itself performs any low-level signal processing and calculation, in order to return to the robot an intensity and direction of the applied force.

The brain of the tested circuit (Figure 25) consists of an ATTiny2313 MCU. The load cell signal is amplified and converted from analog to digital via the use of an HX711 load cell amplifier. This amplifier's DAC has a 24-bit precision for its digital output and the MCU communicates with the three (or more) HX711 amplifiers through serial data transfer. The MCU is also connected via serial to a computer, through the use of an FTDI cable for TTL Serial ↔ USB conversion. This computer connection at this moment serves no purpose other than debugging and supervising the sensor's output.

To communicate with the robot, the MCU uses a digital PWM signal with a duty-cycle time defined by the force intensity and direction. The PWM signal is generated via an internal 16-bit timer by activating a mode called Fast PWM. In the ATTiny2313 (and other AVR MCUs) each timer has a corresponding register or set of registers that can be used to control the PWM duty cycle. In this case the register used was a 16-bit register called OCR0B, wherein the higher byte holds the intensity of the force in the X direction, and the lower byte holds the intensity of the force in the Y direction. The force vector is therefore encoded in the time duration of the PWM pulse, with some loss of precision. The reason for the use of only one signal source for all of the force's information is due to the pin count limitation of the ATTiny2313.

In order to overcome that limit a new signal processing board was designed (Figure 26), but not yet implemented, which uses an ATMega328 microcontroller, with force data acquisition for up to 6 load cells, as well as a 5 V analog force signal output to use with the robot's analog input, and digital PWM output, the same used with the ATTiny2313 circuit. It is also capable of communicating with a computer or control device via direct Serial USB using an FTDI UB232R daughter board, and Serial TTL.

As referred in 1.1 the load cells used are TE Connectivity FX1901-0001-0010, which have a load limit of 4.54 kg (10 lbs) and a response voltage of 20 mV/V.

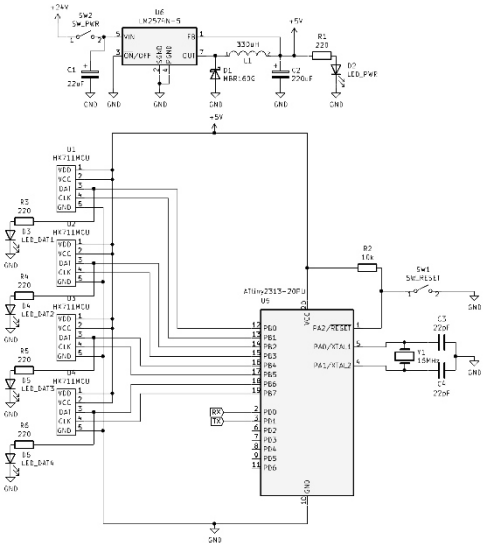

Figure 25 - ATTiny2313 test circuit with regulated power supply.

1.3. Resources

The CAD files (Solidworks Assembly), ATTiny2313 code, and demonstration video, for the tested sensor can be found at: https://osf.io/rhakt/?view_only=a49a098d49f94b2c8bd077a86e9cc7ef

1.4. Control software

The software running in the microcontroller reads the HX711 amplifiers' output and uses it to calculate a center of force via the barycentric coordinates of a triangle, given the three load cells, and sends load cell data via serial port, as well as a PWM pulse with the force data encoded within. The software is coded in AVR C for a lower memory consumption and faster low-level execution.

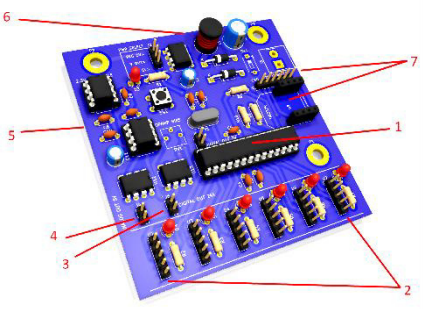

Figure 26 - ATMega328 circuit board. 1 - ATMega328; 2 - Six HX711 connections; 3 - Digital PWM output (24 V); 4 - 5V Analog output; 5 - 2.5V Reference and DAC; 6 - Regulated voltage supply; 7 – Serial TTL and UB232R Serial-USB sockets.

Each load cell is assigned to a lCell_t data structure which is formatted in a way that enables it to be directly transmitted via serial communication. It contains a 32-bit header that contains the string "CELL", followed by two 32-bit integers that contain the current measurement of the load cell value as well as a tare value obtained through averaging repeated measurements at initialization. Two 8-bit data and clock pin numbers follow, and a 16-bit cell ID is the last value sent containing, for example the relative location of the load cell, or any other extra data one might need to describe that one cell.

```
typedef struct lCell{

  uint32_t header; //data structure header

  int32_t value;   //load cell value

  int32_t centr;   //load cell tare value

  uint8_t pinDAT;  //load cell data in pin
```

The data transfer protocol consists in sending a 4 byte header with the text "DATA" followed by the load cell structures. This is transmitted in a loop during the time the microcontroller is functioning.

To communicate the force value and direction to the robot, the values from the three load cells are used to calculate a spatial center of force using barycentric coordinates whose vertex weights are the normalized load values (with respect to the maximum load a cell can withstand) of the load cells. The output is a pair of 8-bit integer coordinates, F_x and F_y, which are then OR'ed into each byte of a 16-bit PWM duty cycle length, OCR0B in the case of the ATTiny2313 implementation.

This PWM signal is detected by the robot's digital input, and the duty cycle time is counted and reverted into a force value to be used within the robot's program.

2. Sensor testing

The sensor unit was tested by running a debugging program in a computer and connecting the sensor's control board to it with an FTDI FT232 cable. Sensor data refresh rates were observed to be in the order of 40 ms at 9600 BAUD. While the load cell amplifiers (HX711) boast a 24-bit precision, only the most significant 16 bits are useable, as the lower 8 bits are too noisy to get a stable readout. It remains to be determined if that is due to mistakes in board construction or if it's intrinsic to the load cells.

A practical scenario test was performed using an ABB IRB 1600 robot system, with an IRC5 controller (Figure 28). Given that this robot system did not have any form of real-time control module installed, an attempt was made to emulate real-time control through a series of short movements and a simple PID robot position controller and try to use the test as a proof of concept for near real-time control of robots without that capability. For implementation simplicity, only the force measured in one of the cells was transmitted to the robot, which would then move vertically up or down depending on whether more or less force was measured, respectively.

At every program loop cycle the robot executes a short ranged MoveJ function with a target point. That target point's Z coordinate is constantly modified by a PID algorithm which takes as target a Z value calculated from the parsed value of the PWM duty cycle time measured by the robot, i.e., the force value.

Pressure is put on the force sensor, increasing the measured load, which is then communicated to the robot, making it move.

During testing there was a very noticeable delay between the pressure application and the robot's response, in the order of 500 ms. This issue was not fixed by increasing the sample rate of the digital card being used and deactivating all the other input cards, to avoid timesharing with unused inputs. It was also noticed that PWM frequencies higher than 2 Hz made the pulse undetectable by the robot due to factors such as the execution time of the MoveJ function, and the sampling speed of the digital card.

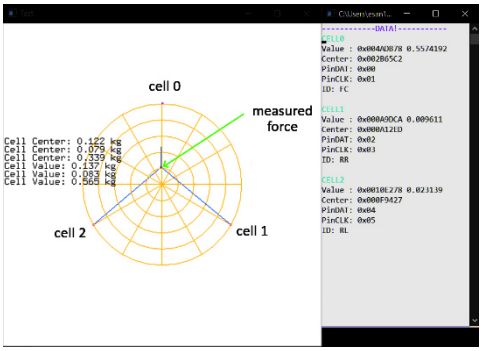

Figure 27 - Debug software running on laptop showing center of force and load cell data structure.

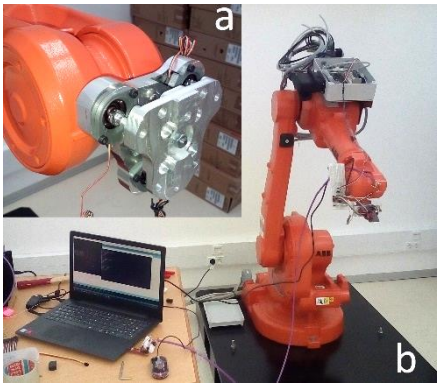

Figure 28 - a) Sensor mounted on an ABB IRB1600. b) Experimental setup with debug computer.

Conclusions

The force sensor is able to measure an applied force's magnitude as well as where on the tool plate that force is being applied, with a reasonable refresh rate, well within range of real-time applications, however it needs some form of calibration procedure for accurate force measurement, which will depend on the tool geometry and where the force is applied.

Conclusive testing of the sensor's ability to control a robot was impossible due to limitations in the robot system's real-time control capabilities. A succession of short ranged joint motion (MoveJ) functions proved ineffective at emulating a real-time system.

As the goal is the development of a cost-effective solutions, the use of real time control modules from the industrial robot manufacturers is not suitable. Thus, current work focus on the addition of actuators, allowing and autonomous force-position control. Two designs are being conceptualized using pneumatic actuators and servomotors.

The pneumatic system (Figure 29) has the advantage of offering passive force control, with the actuators doubling as dampers for smaller applied forces, but it suffers from actuation delays as well as requiring a dedicated air compressor unit. The current design uses a single pneumatic actuator and two load cells for one dimensional force compensation.

The servomotor actuated unit (Figure 30) has the advantage of being a more compact solution and keeps the whole system electrically actuated. However, it lacks the passive force control capabilities of the pneumatic system. The unit being developed keeps the two-dimensional force detection capabilities, using four load cells and two servomotors actuating a gimbal structure where the tool is attached to. In order to make this system more compact, a more complex part design is required, which makes it impossible to mill the parts, therefore this sensor's components will need to be 3D printed.

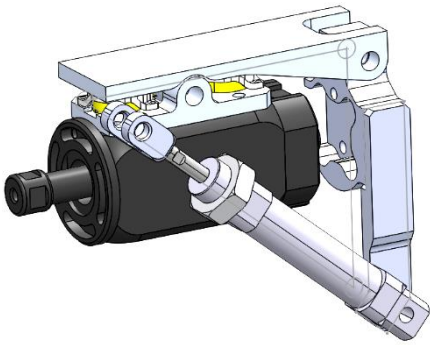

Figure 29 - Pneumatic actuated force-position control system concept.

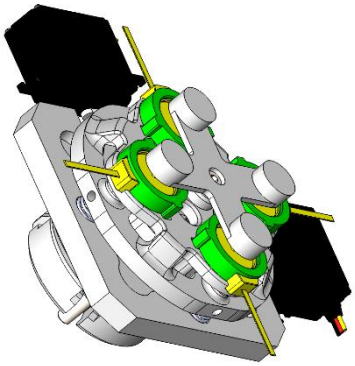

Figure 30 - Servomotor actuated force-position control system concept.

Acknowledgment

The authors would like to acknowledge the Simoldes S.A. company for supporting the project.

The authors would also like to acknowledge the projects UID / EMS / 00481/2019-FCT and CENTRO-01-0145-FEDER-022083

Topic

1) Sustainable Manufacturing Solutions
   a. Manufacturing processes & Simulation

References

[30] Pranab K. Muhuri, Amit K. Shukla, Ajith Abraham, “Industry 4.0: A bibliometric analysis and detailed overview”, Engineering Applications of Artificial Intelligence, vol. 78, pp. 218-235, 2019.

[31] Abd El Khalick Mohammad, Jie Hong, Danwei Wang, Design of a force-controlled end-effector with low-inertia effect for robotic polishing using macro-mini robot approach, Robotics and Computer-Integrated Manufacturing, vol. 49, pp. 54-65, 2018.

[32] Kalt, Eugene & Monfared, Radmehr & Jackson, Michael, “Towards an automated polishing system - Capturing manual polishing operations”, International Journal of Research in Engineering and Technology, vol. 5, pp. 182-192, 2016.

[33] ABB-Robotics, “Integrated force control”, 2015.

[34] Yaskawa-Motoman, “Force control assembly”, 2015.

[35] Fanuc, “Force sensor”, 2017.

[36] Kuka-Robotics, “Kuka.forcetorquecontrol 3.0”, 2013.

[37] Aljaž Kramberger, Andrej Gams, Bojan Nemec, Dimitrios Chrysostomou, Ole Madsen, Aleš Ude, “Generalization of orientation trajectories and force-torque profiles for robotic assembly”, Robotics and Autonomous Systems, Vol. 98, pp. 333-346, 2017.

[38] Hussein Alalem, Asma Eshahiry, “Force & Compliance Detection on Robot Gripping Manipulator”, International Journal of Computing Academic Research, Vol. 6, no 2, pp. 83-91, 2017.

[39] Bruno Siciliano, Oussama Khatib, “Springer Handbook of Robotics”, Springer, 2008.

[40] Michael Hu, Prasad Akella, Bharat Kapoor, Dave Prager, “The State of Human Factory Analytics”, A.T. Kearney, 2018

Impact of the storage system through batteries in the finite networks with penetration of wind energy

Jorge Mendes Tavares
Department of Mechanical Engineering
University of Aveiro
Aveiro, Portugal
jorgemendestavares@ua.pt

Fernando Neto
Center for Technology and Automation, TEMA
University of Aveiro,
Aveiro, Portugal
fneto@ua.pt

Abstract — Through dynamical analysis (Generation Adequacy Analysis), with the help of DIgSILENT Powerfactory software, and applying the Monte Carlo Probabilistic Method, it was possible to evaluate the impact of a storage system composed by batteries in finite networks, taking into account the penetration of non-dispatchable energies, namely wind energy , and to propose an appropriate model for island regions, as is the case of the Cape Verde Islands. The adequacy of the power system refers to the capacity of generation to meet the demand of the system, also considering the typical system restrictions, such as (i) generation unavailability due to fault or maintenance requirements, (ii) variation in system load on a monthly, hourly and/or minute by minute basis, (iii) variations in renewable output - notably wind power production - which in turn affects the available generation capacity [1]. Therefore, it is possible to determine the contribution of wind power generation to the overall capacity of the system and to determine the Loss of Load Probability (LOLP) and Expected Demand Not Supplied (EDNS) for centralized and decentralized generation scenarios, taking into account the objective of maximizing the wind resource utilization[1]. Storage by means of a battery bank contributes greatly to the reduction of critical system parameters, ie, it contributes to the reduction of LOLP and EDNS, since, in addition to storing energy, it helps the generators in the flow control of power in the system[2][3]**. The total capacity of wind turbines installed worldwide (which, in terms of available power, had reached 546.4 GW by the end of 2017 [4]) could be better fulfilled much to the point much when an estimated global wind energy production potential of 53000 *TWh/year* were achieved** [5] **if battery storage could be used.**

Keywords: Wind power, generation adequacy storage, stability.

TOPIC

2) a.: Technologies for the Wellbeing-Multiscale technologies and devices for medicine, environment and energy.

INTRODUCTION

Wind energy has been adopted by many nations as a fundamental strategy to nullify energy from fossil and nuclear sources. According to statistics released by WWEA, the total capacity of wind turbines installed worldwide by the end of 2017 reached 546.4 *GW*, with 60 *GW* added in 2017, representing an increase of 14.33% in relation to the year of 2016, when 51.402 *GW* were made available. The wind potential exploited around the world by the end of 2017, could cover more than 5% of the global electricity demand [4]. However, this accomplishment is still far from the 53000 *TWh* / year estimated globally for the wind power potential[5]. The penetration of energies from intermittent sources in the electricity network, globally, has positive impacts on the environment and the economy. However, there are several challenges (political, economic, technical, geographical, etc.) that must be overcome in order to make the most of this important resource. Technically, an efficient operation of this type of systems is determined by aspects such as (i) the inertial response to the occurrence of disturbances, (ii) the severity of disturbances (iii) the availability of rotating reserve of the system, (iv) the variability of the renewable sources and, (v) the lack of interconnection to neighbouring systems[6][7]. One of the strategies to maximize the use of renewable resources and, to a certain extent, to guarantee the stability of such systems, is the controlled storage of surplus energy from renewable sources. One of the possible solutions is the storage of wind production surplus in battery banks. This operation, in addition to storing energy, assists the generators in the control of power flow in the system, that is, contributes to the adequacy of the generation, understood as the generation capacity to meet the system demand, also considering the typical restrictions of the system such as, (i) generation unavailability due to fault or maintenance requirements;, (ii) variation in system load on an monthly, hourly and minute by minute basis; and (iii) variations in renewable output (notably wind generation output), which in turn affects the available generation capacity. Therefore, considering the adequate storage capability, it is possible to determine the contribution of wind power generation to the overall capacity of the system and to determine the Loss of Load Probability (LOLP) and Expected Demand Not Supplied (EDNS) for centralized and decentralized generation scenarios, with a view to maximize the utilization of the wind resource[4].

METHODS

The system shown in Figure 1 served as the basis for the study. The proposed network presents a ring (mesh) topology with radial exploration. It allows the decentralization of the generation so that it fits in globally the needs of distribution mainly in islands like the

island of Santiago in Cape Verde. Several scenarios were analysed in order to obtain the most efficient model. On this power grid, whose main characteristics are represented in Table 1, in a perspective of penetration of 61.5% of wind power, six scenarios were evaluated:

- M1: Centralized diesel and wind generation without battery;
- M2: Centralized diesel and wind generation with battery;
- M3: Centralized diesel and decentralized wind generation without battery;
- M4: Centralized diesel and decentralized wind generation with battery;
- M5: Decentralized diesel and wind generation without battery;
- Decentralized diesel and wind generation with battery.

Table 1: Generation and load characteristics.

	Maximum power	Power factor
Diesel Generator	3 x 5 *MW*	0.9
Wind Generator	12 x 2 *MW*	0.9
Load 1	13 *MW*	0.9
Load 2	3 *MW*	0.9
Load 3	10 *MW*	0.9
Battery	3 x 1.6 *MVA*	0.9

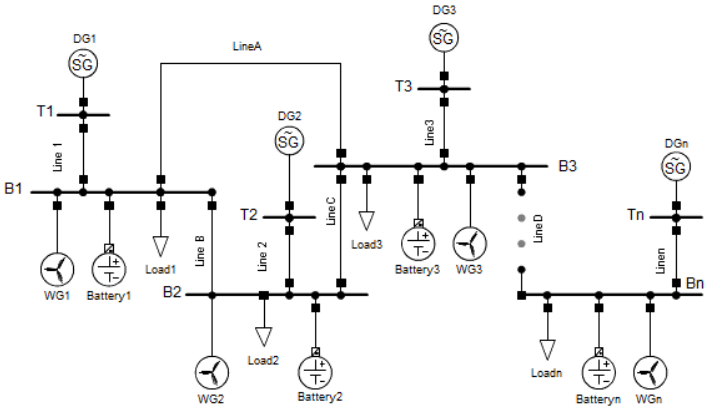

Figure 3: System with n busbars.

For the different scenarios (centralized / decentralized, with and without battery), applying the Monte Carlo Method, the value of the Demand Not Supplied (DNS) was calculated for a certain random state according to equation 1[4].

$$DNS = \sum Demand - \sum Generation \quad (1)$$

At the end of the simulation, the values of the Loss of Load Probability (LOLP), Loss of Load Expectancy (LOLE), Expected Demand Not Supplied (EDNS) and Loss of Energy Expectancy (LOEE) values are calculated as mean values of all the iterations executed. The indexes of Loss of Load Probability (LOLP) and Expected Demand Not Supplied

(EDNS) are the critical measures and are calculated by equations 2 and 3 respectively[4].

$$LOLP = \frac{N_{DNS}}{N} \times 100\% \quad (2)$$

$$EDNS = \frac{\sum DNS}{N} \quad (3)$$

where N_{DNS} is the number of iterations with $DNS>0$ and N is the total number of iterations.

Figure 1 represents the most complex scenario of the system with all forms of decentralized generation. Each remaining scenario will be derived from this one by adjustment of the generating and storage elements in or out of service, changing their parameters as desired.

Battery Control Method

For a generic system with n Busbars, knowing the energy flow through the power line from each of the *n* Thermal Plants or from an equivalent non-renewable source, the power balance between the wind subsystem and the AC load in each of the Busbar (B_j, with *j* ranging from 1 to *n*) as shown in Figure 1, can be determined in Busbar j by the following equation:

$$P_{GE_i} + P_{Load_i} = P_{Line_i} - P_{Battery_i} = P_{Meas_i} \quad (4)$$

The total power balance of the system is given by the equation:

$$P_{Meas\,Total} = \sum_{i=1}^{n} P_{Meds_i} \quad (5)$$

With *i* varying from 1 to *n*, and *n* is the number of elements connected on each busbar of the system. One strategy for controlling the battery bank is to check the P_{Meas} energy transfer rate. A positive P_{Meas}, means that the wind system is generating more energy than the energy being consumed; hence, in these occasions the battery bank can be charged so that it can fulfil the load in periods when P_{Meas} is negative. Under these circumstances, the production of energy from the thermal power stations would be minimized. Storage limits will be used to avoid unwanted battery behavior[4].

Generation Adequacy Analysis

The generation adequacy requires that each generator in the system is assigned to a number of probabilistic states that determine the probability of the generator operating at various output levels. For intermittent sources the probabilistic output power models must be developed based on historical data [4]. Thus, in the case of wind turbines, the probabilistic time series of wind velocity data and turbine power curve are used, and for each of the system load, a time-based characteristic is assigned, which determines the real level of system load for any instant of time[8][9]. Figure 2 represents the power curve of the wind turbines of the test systems.

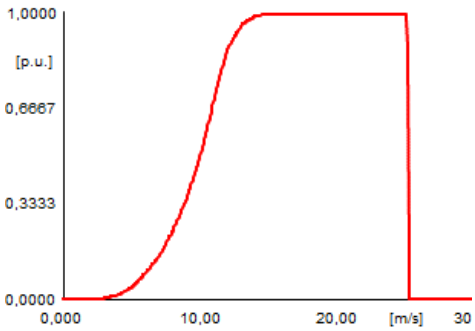

Figure 4: Power curve of wind turbines.

Definition of the stochastic multi-state model

For dispatchable and non-dispatchable generation, it is possible to assign a stochastic multi-state model to define the availability of each unit. For wind generators, stochastic wind models are defined using the Weibull distribution. The average wind speed and the form factor (*Beta*) of the distribution can be adjusted to obtain the desired wind characteristic for each wind generator. For this purpose, in order to achieve an average wind speed close to the average speed of the island of Santiago (8.0 *m/s*)[14] it is necessary to assign in the Weibull distribution the value 2 for the beta parameter. In this case in software for β = 2 the average wind speed is 8.86 *m/s*. Thus, the transformed distribution achieved is represented in Figure 6 and, therefore, the production of the turbines will be modelled based in these data associated with those of the Meteorological Station[1].

Definition of load curves e Monte Carlo method

A time-varying demand curve is defined for each load of the system according to Figures 3, 4 and 5. This variation comes as a function of the percentage of each of the maximum loads of the system. Thus, in the generation adequacy analysis the numerous iterations allow to determine the critical parameters of the system as back referenced. This way one can apply the Monte Carlo method, where, using uniform random numerical sequences, a random system state is generated at random time points.

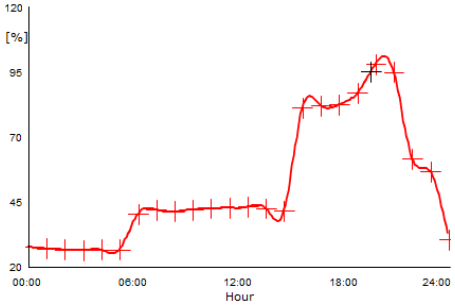

Figure 3: Load Curve 1.

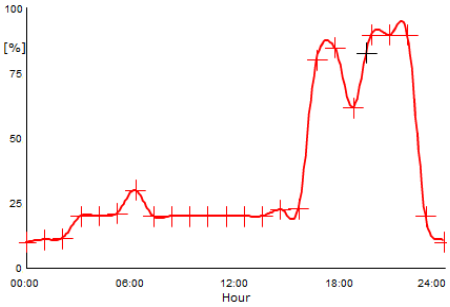

Figure 4: Load Curve 2.

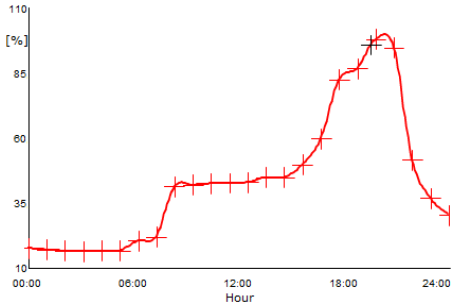

Figure 5: Load Curve 3.

The generated operating states will have corresponding generation power, while the time points will have a corresponding power demand. The value of the non-supplied demand (DNS) is then calculated for that state. This process is done for a specific number of draws (iterations), usually 100,000 iterations. At the end of the simulation, the values of the Probabilities of Loss of Load (LOLP) and Expected Demand Not Delivered (EDNS) are calculated[1].

Results of generation adequacy

The comparative results of the six scenarios are presented in Table 2. The best scenario is the one with the lowest LOLP value and the lowest EDNS value. Thus, among the analysed cases, the scenario most favourable to the maximize the utilization of the wind resource, is the one with the decentralized wind generation with storage by means of bank of batteries and the centralized diesel generation, whose average value of LOLP is 6.6760% and the average value of EDNS is 0.212 *MW*.

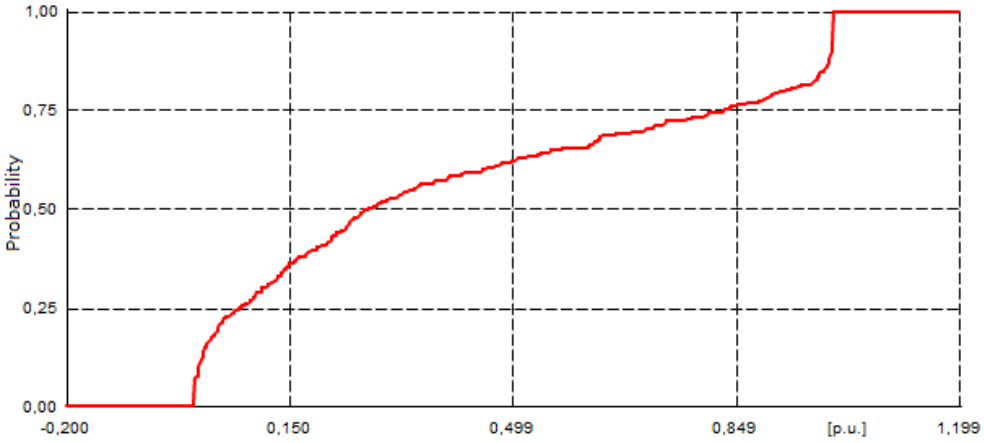

Figure 6: Probabilistic time series of wind velocity data.

Table 2: Result of the models.

LOLP [%]			EDNS [*MW*]		
	Confidence levels			Confidence levels	
Average	Lower	Upper	Average	Lower	Upper
M1: Centralized diesel and wind generation without battery					
11.512	11.3459	11.678	0.583	0.573	0.593
M2: Centralized diesel and wind generation with battery					
6.7470	6.6165	6.8774	0.215	0.210	0.220
M3: Centralized diesel and decentralized wind generation without battery					
11.3540	11.1889	11.5190	0.582	0.572	0.592
M4: Centralized diesel and decentralized wind generation with battery					
6.6760	6.5461	6.8058	0.212	0.207	0.217
M5: Decentralized diesel and wind generation without battery					
11.2730	11.1084	11.4375	0.582	0.572	0.592
M6: Decentralized diesel and wind generation with battery					
6.8010	6.67	6.9319	0.213	0.207	0.217

Characterization of the case study

The electrical system of the island of Santiago in Cape Verde, where the electrical grid is characterized by a ring topological structure, but with radial exploration, mainly in urban areas with high density of load, is considered as case of study, where normally open (NO) switches are used which can
be closed to ensure continuity of operation of the electrical network if a line fault occurs[10]. The system consists of 715 busbars, of which 467 are loads, 26 transformers, 18 thermal generators, a wind farm and a photovoltaic park[11].

Power plants of the Santiago Island

With the restructuring of the island's electrical system, the Assomada and Gamboa PS's were gradually deactivated, and therefore, the island currently has the Palmarejo Single Power Plant with installed capacity of 76,411 *MW* of power from thermal generators, a Wind Farm and a Photovoltaic Park. The characteristics of the thermal machines installed in the Central Station of Palmarejo are represented in Table 3[11].

Data provided by Electra, SA, show that in 2017, 82.2% of all energy produced was from thermal power stations and only 16.4% was produced from wind turbines.

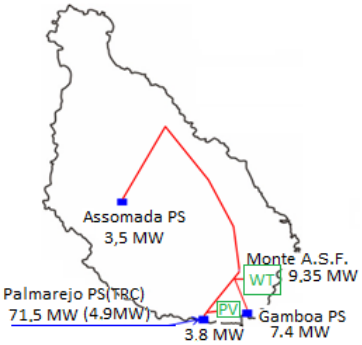

Figure 5: Power supply installations, adapted [12].

Table 3: List of thermal machines installed in Palmarejo.

Station Name	Units	Capacity [*MW*]
Palmarejo	CAT1	5.582
Palmarejo	CAT2	5.582
Palmarejo	CAT3	7.437

Palmarejo	CAT4	7.437
Palmarejo	War5	11.350
Palmarejo	War6	11.350
Palmarejo	War7	11.384
Palmarejo	War8	11.384
Palmarejo (TRC)	MAN	3 x 1.635
TOTAL		76.411

Current and additional wind installation

In the wind farm located in Monte S. Filipe, 11 Vestas (V 52) 850 *kW* turbines are installed. Their power curve is represented in Figure 8[13].

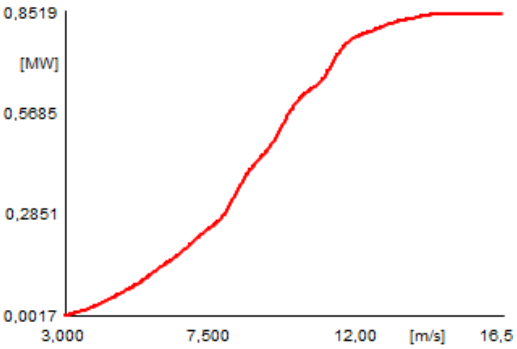

Figure 6: Turbine power curve V 52.

Taking as a reference the Government's goal of reaching 54% of renewable penetration in the network by 2030, and considering the already identified Renewable Energy Development Zones (REDZ)[14], it is proposed, in the scope of this work, the installation of two more wind farms located with connection in Assomada and Calheta according to Figure 9.

Figure 7: Wind REDZ. Source: Ad. from [14].

The island of Santiago, in 2017, was responsible for the consumption of 49% of all electric energy consumed in the archipelago, having recorded in the period in question the peak power equal to 39.2 *MW*[15]. The projection points to a consumption in the order of 47% and 40% for the years 2020 and 2030 respectively. To ensure renewable penetration by 54% in the archipelago until 2030, in parallel with other strategies, on that island the installed wind capacity should be approximately equal to 36.5 *MW* [16]. Based on these arguments, and applying the best scenario as identified in 3.3, the generation adequacy analysis is performed considering a wind penetration rate of 63.7% according to the data in Table 4. The maximum requested power to the grid (peak power) is 40*MW*.

Table 4: Capacity of units in service.

Installation	Technology [*MW*]		
	Wind	Diesel fuel	Battery
Praia	11 × 0.85	2 × 5.58 × 100% 1 × 7.43 × 32%	9.9
Assomada	9 × 0.85	0	7.2
Calheta	9 × 0.85	0	9.0
Total	24.7	14.0	26.1

Loading curve of the island of Santiago

The consumption profile of the island was classified by two regions: North Santiago where the wind farms of Santa Catarina (Assomada) and Calheta will be installed, and South of Santiago where the current wind park is located. The load curves typical of the rejects are represented in the figures respectively[15].

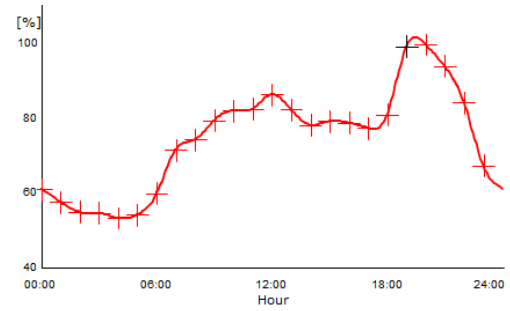

Figure 8: Load diagram South Santiago

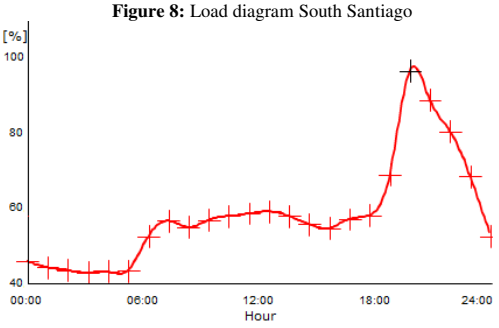

Figure 9: Load diagram North Santiago.

Generation Adequacy

The graphs in Figure 12, results of the simulation of the system in reference are essentially the data of the Monte Carlo draws graphs (total available capacity, dispatchable and non-dispatchable capacity, generation reserve, total demand and residual demand) ordered by descending order[1]. The total available capacity, with the machines out of service, varies over time and there is an 80% chance of being equal to 74.3 MW. While available dispatched capacity remains strategically constant, non-dispatchable capacity varies over time, as does total system demand. Of course, reserves vary at all times.

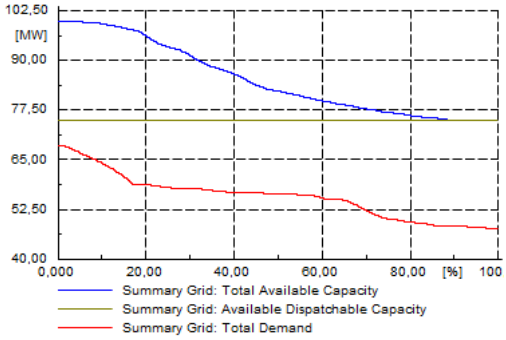

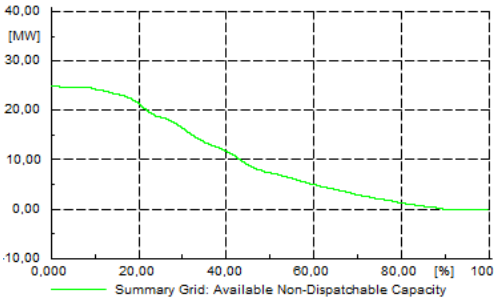

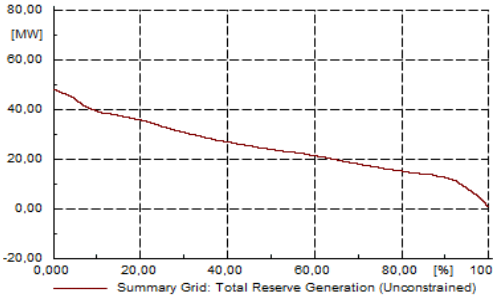

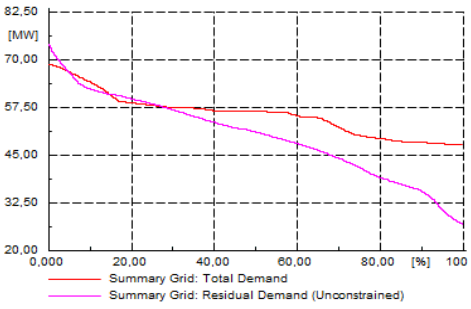

Figure 10: Cumulative Probability Distribution.

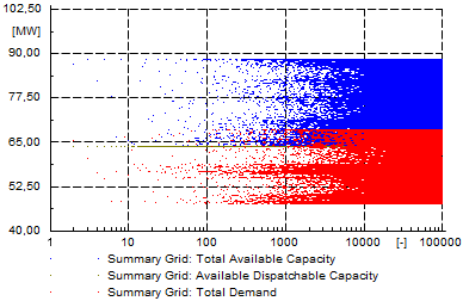

Figure 313: Monte Carlo iteration.

The Figure 13 represents the Monte Carlo iterations for total available capacity, available dispatchable capacity and total demand. Each of the data points in the graphs according to Figure 12 represents a single Monte Carlo simulation. In the linear or logarithmic scale, for iteration values close to 100000 (standard value), a large density of points is observed, confirming that the number of interactions was sufficient for the

analysis of the random data of the system.

The convergence graphs for Loss of Load Probability and Demand Not Supplied, according to Figure 14, indicate that as the number of iterations becomes large, the LOLP index will converge to its final value, in the same way for the EDNS. They are one way to visualize this process. Note that, in this case, that close to 100 000 iterations, convergence is total.

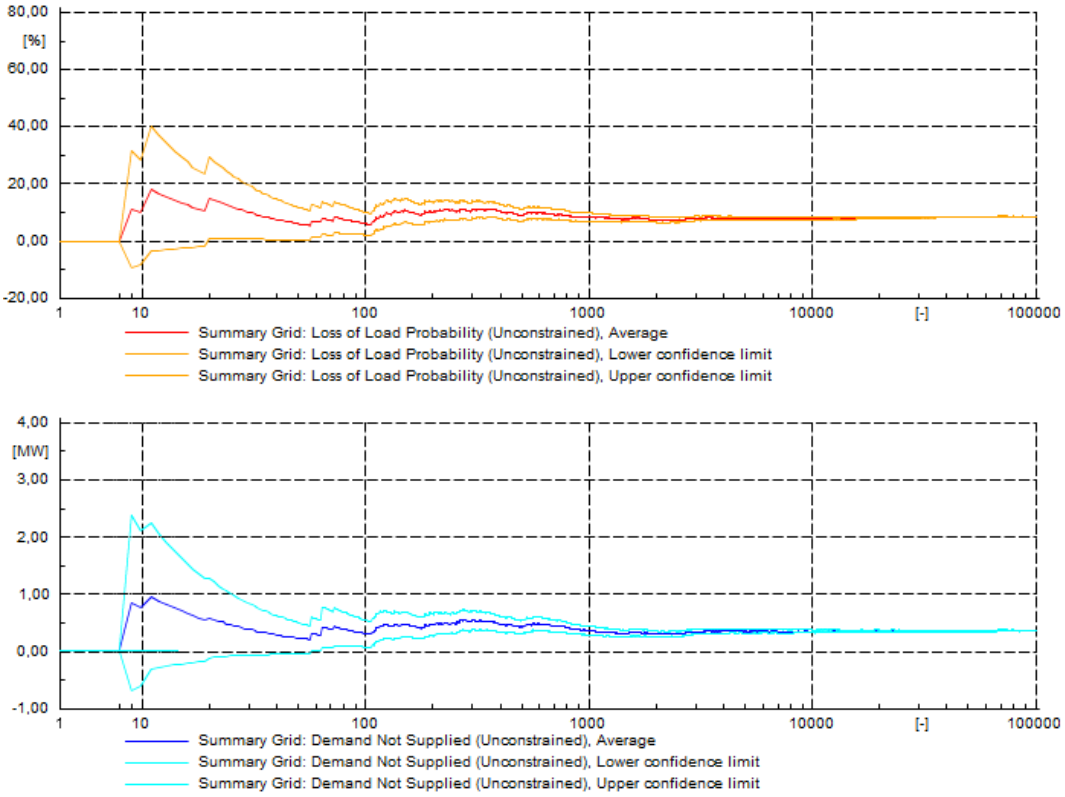

Figure 14: The convergence graphs.

RESULTS

In Table 5 are the main results of the analysis of the adequacy of the generation, after the 100000 iterations performed, considering the already mentioned conditions and 8% of losses in the system.

Table 5: Main results.

Technology			Critical Values	
Wind [*MW*]	Diesel fuel [*MW*]	Battery [*%*]	LOLP [*%*]	E [*MW*]
24.7	14.0	67.4	0	0
24.7	14.0	38.6	8.33	0.35

There is no Loss of Load Probability and no Expected Demand Not Supplied in the system when there is a battery storage system whose capacity equals 67.4% of the total generation (dispatchable and non-dispatchable), i.e. the storage allowed to meet all loads regardless of their conditions. For a storage system with capacity equals 38.6% of the total generation, there is an average of 8, 33% of Loss of Load Probability and 0.35 MW of Expected Demand Not Supplied.

CONCLUSION

The critical values of the generation suitability analysis (LOLP and EDNS) show that the most suitable model for energy systems with wind energy penetration is the centralized diesel production, decentralized wind generation accompanied by a storage system by means of batteries decentralized. Applying this model to the electricity grid of the island of Santiago in Cape Verde, we conclude that with a battery storage system with capacity equivalent to 67.4% of the total production, where the wind contribution is equals at 63.7% and diesel 36.3% it is possible to power, under all load conditions, a time-varying load system whose maximum point is 40MW. For the same system, but with a storage capacity of less than 39%, the Loss of Load Probability rate increases to values greater than 8% and therefore the system begins to become technically and economically unsustainable. Therefore, technically, storage by bank of batteries contributes to the penetration of high rates of wind power in the grid. However, it is important to evaluate the behavior of the grid in relation to the energy quality, which will be dealt with in a future work through the transient stability study of the grid, in order to establish the limits to the integration of wind power into an electric power system.

ACKNOWLEDGMENT

This work was supported by the Calouste Gulbenkian Foundation. Thanks are due for the financial support to TEMA through projects UID / EMS / 00481/2013-FCT and CENTRO-01-0145-FEDER-022083.
Thanks to the Faculty of Science and Technology of the University of Cape Verde.

REFERENCES

[1] DIgSILENT GmbH, PowerFactory 2018. DIgDILENT GmbH, 2018.

[2] J. Stanojevic, A. Djordjevic, and M. Mitrovic, “Influence of battery energy storage system on generation adequacy and system stability in hybrid micro grids,” 4th Int. Symp. Environ. Friendly Energies Appl. EFEA 2016, pp. 1–6, 2016.

[3] M. C. Argyrou, P. Christodoulides, and S. A. Kalogirou, “Energy storage for electricity generation and related processes: Technologies appraisal and grid scale applications,” Renew. Sustain. Energy Rev., vol. 94, no. July, pp. 804–821, 2018.

[4] WWEA, “World Wind Energy Association – Wind Power Capacity in 2017,” 2018. [Online]. Available: https://wwindea.org/blog/2018/02/12/2017-statistics/. [Accessed: 20-Jun-2019].

[5] T. E. Drennen, “Renewable Energy: Sources for Fuels and Electricity,” Journal of Environment Quality, vol. 23, no. 3. p. 622, 2010.

[6] F. Pereira, “Energy Storage Systems (Sistemas de Armazenamento de Energia),” pp. 17–28, 2013.

[7] ERSE - Energy Services Regulatory Authority, “Connections to Consumer Power Grids,” pp. 1–23, 2013.

[8] R. R. Micky, R. Lakshmi, R. Sunitha, and S. Ashok, “Generation adequacy assessment for microgrid with ESS,” 2016 IEEE 7th Power India Int. Conf. PIICON 2016, pp. 1–6, 2017.

[9] H. Ibrahim, M. Ghandour, M. Dimitrova, A. Ilinca, and J. Perron, “Integration of wind energy into electricity systems: Technical challenges and actual solutions,” Energy Procedia, vol. 6, pp. 815–824, 2011.

[10] J. P. S. Paiva, Eccentric Energy Networks: A Systemic Analysis, 2a. Portugal: IST Press, 2007.

[11] Electra - Electricity and Water Company, “Annual Report 2008 a 2017.” [Online]. Available: http://www.electra.cv/index.php/2014-05-20-15-47-04/relatorios-sarl. [Accessed: 10-Jan-2019].

[12] Japan International Cooperation Agency, “The Study of Information Collection and Verification Survey for Renewable Energy Introduction and Grid Stabilization in the Republic of Cabo Verde,” no. August, 2016.

[13] Vestas, “Vestas V52 - 850,00 kW - Wind turbine.” [Online]. Available: https://en.wind-turbine-models.com/turbines/71-vestas-v52#powercurve. [Accessed: 23-Jun-2019].

[14] G. Energy, “Atlas and renewable energy projects of Cape Verde”, 2011.

[15] Electra, “Electra Annual Report 2017,” Cabo Verde, 2017.

[16] Government Cape Verde, “Electric Sector Master Plan 2018-2040,” Cabo Verde, 2018.

Prediction of performance of cutting environments in turning process of Ti-6Al-4V alloy

C. Veiga[1, 2 *], J. Paulo Davim[2], A.J.R. Loureiro[3]

1. ISEC, Polytechnic Institute of Coimbra, Rua Pedro Nunes - Quinta da Nora, 3030-199 Coimbra, Portugal.
2. Department of Mechanical Engineering, University of Aveiro, Campus Santiago, 3810-193 Aveiro, Portugal.
3. 4CEMUC, Department of Mechanical Engineering, University of Coimbra, Pólo II, Pinhal de Marrocos, P-3030 788 Coimbra, Portugal.

* Corresponding author: E-mail: veiga@isec.pt / celestino@ua.pt

***Abstract* — The purpose of this work is to evaluate the performance of cutting environments in the turning process of the most used titanium alloy (Ti-6Al-4V) with cemented carbide insert (ISO-K20), using simulations carried out with the commercial software AdvantEdge FEM™.**

Three simulations were modeled and executed, being the modeling based on the cutting speed Vc = 90 m/min, feed rate f = 0.254 mm/rev, depth of cut doc = 1.27 mm, rake angle α = -5°, relief angle β = 10°, insert edge radius r = 0.02 mm, and three different cutting environments, respectively dry, emulsion and liquid nitrogen (LN2).

The results obtained show the following: the chips are serrated and the maximum plastic strain are similar for all the three cutting environments; the extension of maximum plastic strain decreased substantially from dry to emulsion and LN2 environments; Similarly, the magnitude of cutting and trust forces, the tool tip temperature, and the tool wear rate decreased from dry to other two environments; the distribution of temperature and plastic strain on the machined surface are similar for all the cutting environments.

Keywords* — *Cutting environments; FEM simulation; Titanium alloys; Turning process.

TOPIC

1) a.: Sustainable Manufacturing Solutions (Manufacturing processes & Simulation).

Introduction

Because of their unique mechanical properties, titanium alloys are widely used in industrial applications, namely in the aerospace, automotive and biomedical parts [1]. However, machining these materials is difficult due to their low thermal conductivity and elastic modulus, high hardness at elevated temperature, and high chemical reactivity [2]. These factors cause rapid tool wear, low material removal rate, and degradation of surface integrity of machined parts. [3-5].

Researchers have employed several strategies to overcome the limitation associated to the titanium cutting and most of them is based on the application of cooling/lubrication methods to reduce temperature and friction at the tool-chip interface. **Fig. 1** presents common cutting environments used in the machining processes.

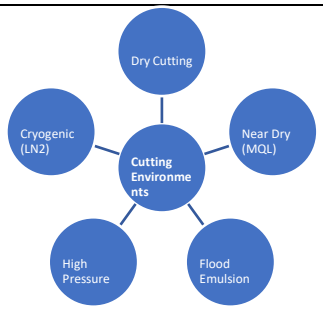

Figure 1: Common cutting environments.

Dry cutting reduces environment degradation and health risk for machine operator. However, the absence of cutting fluids causes limitation in the cutting speed and may results in high cutting temperature, rapid tool wear, and worsening of the workpiece surface integrity [6, 7]. Minimum quantity lubrication (MQL) reduces the cutting temperature, surface roughness, and cost, but this technique includes health hazard due to mist generation [8, 9]. Flood emulsion decreases the cutting temperature but increases the cost of the cutting process and results in environmental pollution [10, 11]. High-pressure coolant permits high cutting speed, segmented chips, lower cutting force, better tool life and acceptable surface finish, but the equipment is expensive [12]. Cryogenic cooling based on liquid nitrogen (LN2) is an efficient way to maintain the cutting temperature below the softening temperature of the tool material [13, 14]. This technique increases tool life and productivity, and is friendly in terms of health and environment.

Despite a lot of research devoted to cutting processes and important progress achieved, machining titanium and its alloys is still limited. Because experimental testing is expensive, finite element

method (FEM) is widely used for modeling of metal cutting [15]. Various software packages based on FEM were developed for machining simulation. One of them is AdvantEdge FEM™.

AdvantEdge FEM™ software is an explicit dynamic, thermo-mechanically coupled finite element model based on advanced technology, namely [16]: a) resolution of multiple length scales, including cutting edge radius, secondary shear zone and chip load; b) multiple body deformable contact for tool-workpiece interaction; c) transient thermal analysis; d) adaptive re-meshing techniques to ensure accurate finite element configuration during large deformations inherent to the machining processes. It integrates multiple constitutive models for modeling the material behavior, namely the power law model and the Drucker Prager model, and uses a friction coefficient based on Coulomb friction law, constrained between 0 and 1.

The purposes of this work are modeling and simulation of turning process of Ti-6Al-4V alloy with different cutting environments (Dry, Emulsion, and Liquid nitrogen – LN2), and compare the performance of these cutting environments in terms of chip morphology, machining forces, cutting temperature, tool wear and life, and workpiece strain and temperature. The motivation for this research are the difficulties on machining a material with interesting properties (Ti-6Al-4V), the cost of experimental testing, and the demands for Sustainability.

Methods

The AdvantEdge FEM™ software was selected as modeling tool because it allows rapid simulation setup and provides interesting outputs, namely the chip morphology, cutting forces, cutting temperatures, tool wear, and distributions of strain and temperatures on the tool and on the workpiece.

This work was based on 2D modeling, which requires setup of workpiece model (**Fig. 2**), cutting tool model (**Fig. 3**), cutting parameters (**Fig. 4**) and meshing parameters (**Table 1**).

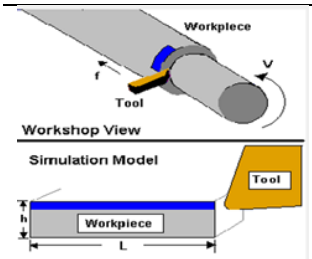

Material: Ti-6Al-4V
Yield Strength: 1050 MPa
Length (L): 8 mm
Height (h): 3 mm

Figure 2: Workpiece Model (material and geometry).

The cutting parameters was extracted from literatures [17- 19] that provides at least one measured result for comparison. With regards to cooling/lubrication, the simulation software provides three options for cooling area, namely: a) Immersed, b) Exclude tip vicinity and c) Focused location. The option selected for this work was the second one, as illustrated in **Fig. 5** and the details for different cutting environments are presented in **Table 2**.

The material behavior was modeled with power law constitutive model, according to **Table 3**.

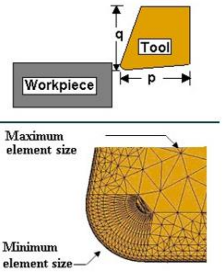

Material: Carbide-Grade-K
Edge radius: 0.02 mm
Rake angle: -5 [°]
Relief angle: 10 [°]
Relief length (p): 2 mm
Rake length (q): 2 mm

Figure 3: Parameters for tool Model.

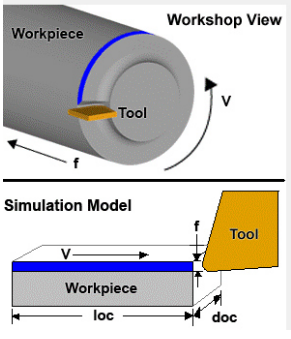

Depth of cut (doc) 1.27 [mm]
Length of cut (loc) 6 [mm]
Cutting speed [m/min] 90
Feed rate 0.254 [mm/rev]

	Environments
	Dry; Emulsion; LN2

Figure 4: Cutting parameters for simulation modeling.

Tool	Maximum element size [mm]	0.1
	Minimum element size [mm]	0.02
	Mesh Grading	0.4
Workpiece	Maximum element size [mm]	0.10
	Minimum element size [mm]	0.02
	Cutting edge radius [mm] (*)	0.6
	Feed fraction [mm] (*)	0.1
	Mesh refinement factor	2
	Mesh coarsing factor	6
Maximum number of nodes: 24000		
(*) – Used to determine minimum element size.		

Table 1: Parameters for meshing Model.

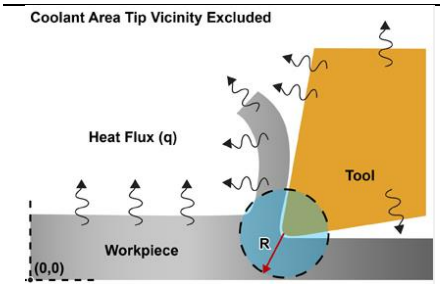

Figure 5: Cooling area for emulsion and LN2 cutting.

Environment	T [°C]	H [W/(m2 K)]	R [mm]	μ	
Dry		25	-	-	0.5
Emulsion		25	8.75 x 104	0.6	0.3
LN2		-180	4.827 x 104	0.6	0.3
		650	7.495 x 10-4	0.6	0.3

T - fluid temperature; H - heat transfer coefficient; R - distance from cutting edge for thermal flux exclusion (chip-tool contact length);

Table 2: Details on the cutting environments.

$\sigma(\varepsilon^p, \dot{\varepsilon}, T) = g(\varepsilon^p) \times \Gamma(\dot{\varepsilon}) \times \Theta(T)$	
$g(\varepsilon^p)$	Strain Hardening
$\Gamma(\dot{\varepsilon})$	Strain Rate Sensitivity
$\Theta(T)$	Thermal Softening
ε^p	Plastic strain
$\dot{\varepsilon}$	Strain rate
T	Temperature

Table 3: Power Law, constitutive model.

Fig. 6 provides the AdvantEdge FEM™ menu (a) and the steps needed for setting a simulation (b). Each step requires inserting and/or selecting a set of parameters.

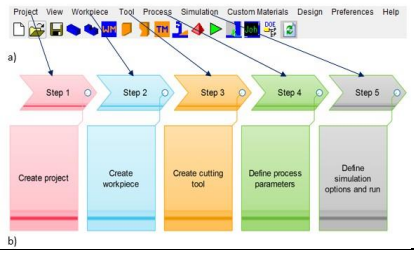

Figure 6: Steps to setup and run a simulation.

Step 1 is for specification of the project name, project description, cutting process (turning) and modeling dimension (2D/3D). Step 2 defines the workpiece geometry and material (**Fig. 2**). Step 3 is devoted to specification of geometry, boundary conditions and tool material (**Fig. 3**). The right side (1) and top side (2) of the tool are fixed in the X and Y directions. These sides have a default thermal boundary condition set to 20ºC. Step 4 is for specification of the process parameters (**Fig. 4**). Step 5 focuses on the selection/setup of simulation options, namely the workpiece meshing (**Table 1**).

Results and discussion

Fig. 7 provides the chip obtained from the simulations. All chips are segmented with maximum plastic strain (ε) close to 3.43, but the extension of such maximum (red area) decreased from dry cutting to other environments.

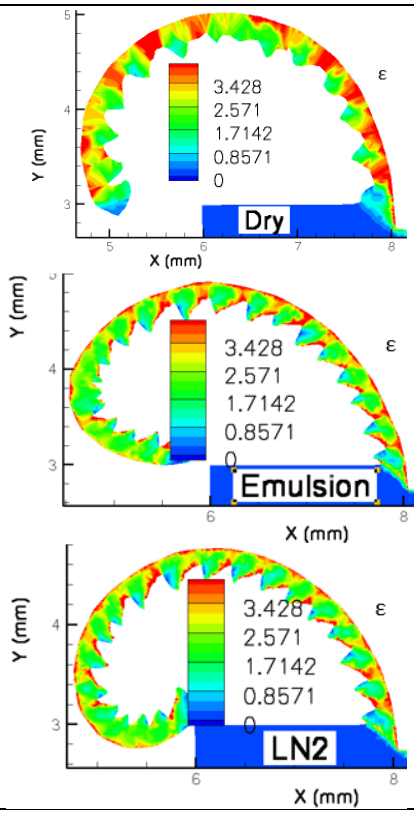

Figure 7: Chip morphology for different cutting environments.

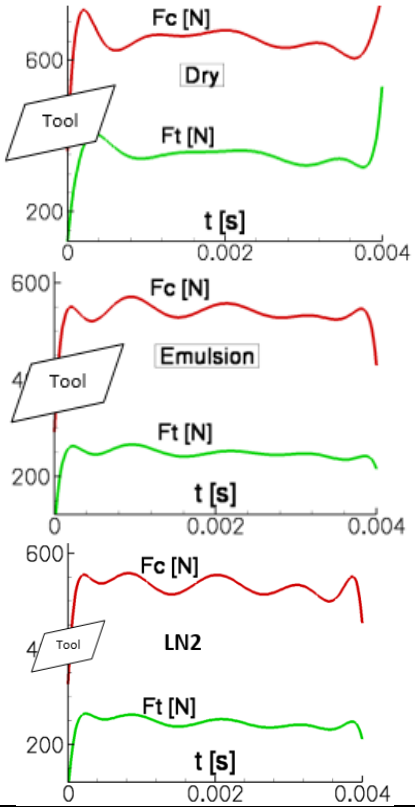

Figure 8: Machining forces versus cutting time.

Possible reasons for this decrease is lower cutting temperature and friction at the tool/chip interface for emulsion and LN2 fluids. This behavior agrees with the experimental results from literature obtained for similar cutting conditions [18].

For each cutting environment, the magnitudes of cutting force (Fc) and thrust force (Ft) reach maximum in the early stage then decrease and progress with some fluctuation (**Fig. 8**), being this behavior in accordance with common descriptions in literature [20].

The emulsion and the LN2 environments reduced the various components of machining forces relatively to the dry cutting, especially the cutting component, according to **Fig. 9** (**max** – maximum; **ave** – average). However, comparison of the emulsion and LN2 environments with each other shows no relevant dissimilarities in terms of the machining forces.

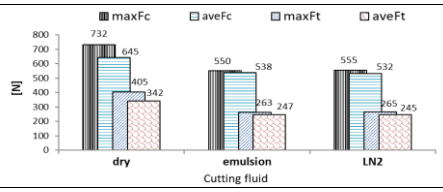

Figure 9: Maximum and average machining forces.

Fig. 10 shows that the maximum cutting temperatures at the tool tip were 906 (865) ºC for dry, 839 (335) ºC for LN2 and 829 (524) ºC for emulsion. Inside the parentheses are the measured values found in literatures [17 - 19] for similar cutting conditions. The discrepancies

between the simulation and the literature values may have several origins, including the differences in the input parameters and the inaccuracy associated with the finite element method and the experimental method. Emulsion and LN2 reduced similarly the cutting temperature.

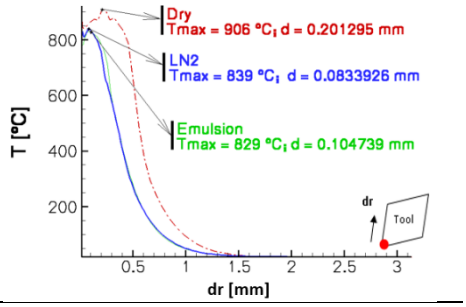

Figure 10: Cutting temperature versus distance from tool tip.

According to **Fig. 11**, LN2 and emulsion environments increased the tool life, relatively to the dry environment, by about 34% and 41% respectively. Possible reason for such increase is lower cutting temperatures.

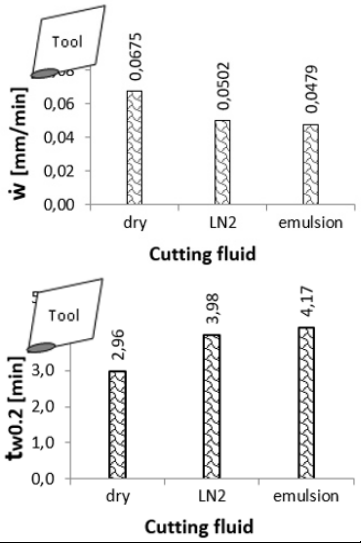

Figure 11: Tool wear rate and tool life for wear of 0.2 mm.

The variation of plastic strain (ε) with the distance (dx) is large and random, and the maximum value is close to 2.5 for all the three cutting environments (**Fig. 12**).

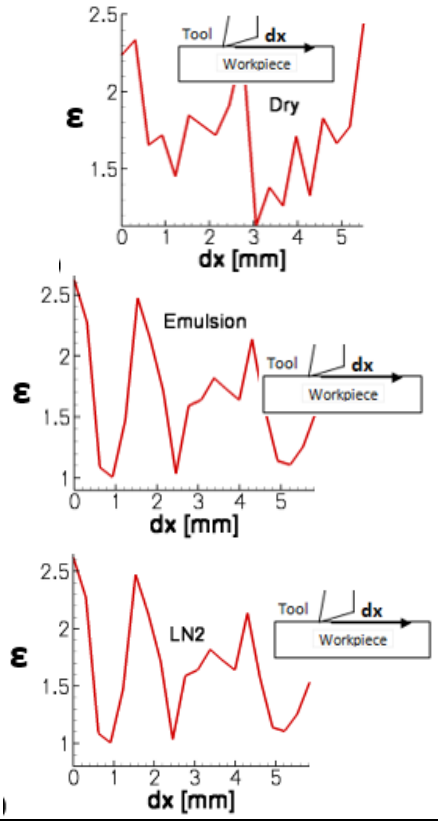

Figure 12: Plastic strain along the workpiece surface.

For all the cutting environments (**Fig. 13**), the surface temperature (T) decreases rapidly with the distance from cutting tool along the machined surface (dx). Such temperature gradient is an important source of the workpiece distortion and residual stress.

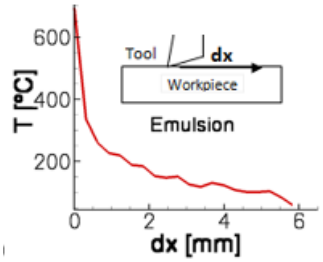

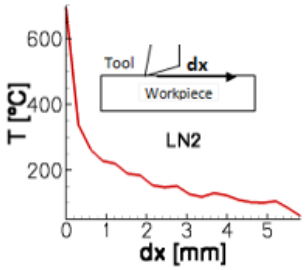

Figure 13: Temperature along the workpiece surface.

Fig. 14 indicates that the temperature decreases quickly in depth from the machined surface, which result in a very small thickness affected by high temperature and possible metallurgical transformations. The LN2 and emulsion environments reduced substantially the maximum temperature on the machined surface.

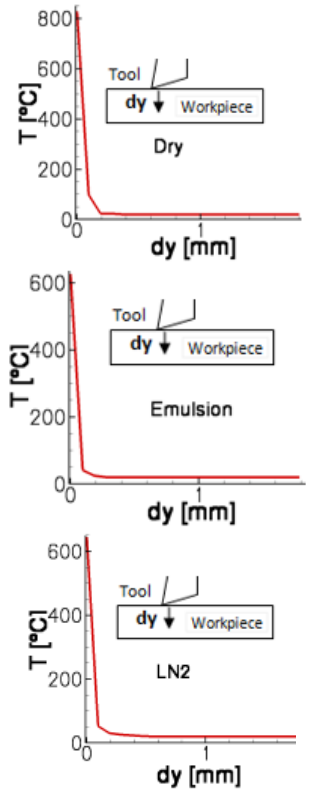

Figure 14: Temperature along the workpiece depth.

According to literature [21-23], rapid cooling of Ti-6Al-4V alloy from α+β field above martensitic start temperature (800 ˚C), leads to martensitic transformation of β phase, which results in a very fine needle-like microstructure. Therefore, considering the result of **Table 3**, it is possible to infer that the dry and LN2 cutting would result in martensitic transformation upon rapid cooling.

Cutting fluid	Dry	LN2	Emulsion
T_{max}[°C]	880	810	765

Table 3: Maximum workpiece surface temperatures.

Conclusions

Three simulations of turning process of Ti-6Al-4V alloy, based on three different cutting environments, were modeled and executed. The main conclusions obtained are presented next.

CHIP MORPHOLOGY: the chips are serrated with maximum plastic strain close to 3.43 for all the three cutting environments, but the emulsion and LN2 environments reduced the area of maximum plastic strain.

MACHINING FORCE: the cutting and trust forces decreased from dry to emulsion and to LN2.

CUTTING TEMPERATURE: the tool tip temperature decreased for emulsion and LN2.

TOOL WEAR: emulsion and LN2 environments reduced the tool wear.

WORKPIECE STRAIN: distribution of plastic strain on the machined surface are similar for the three cutting environments.

WORKPIECE TEMPERATURE: the maximum temperature on the machined surface were 880 °C (Dry), 810 °C (Emulsion) and 765 °C(LN2). Martensitic transformation of β phase during rapid cooling may occur for dry and LN2 environments.

Globally, the emulsion and LN2 environments provided similar performances and showed advantages over dry cutting in terms of reduction of machining forces, cutting temperature and tool wear.

Acknowledgment

The authors acknowledge the Research Unit (UID / EMS / 00481/2019-FCT) and the Research Infrastructure (CENTRO-01-0145-FEDER-022083). The author C. Veiga acknowledge ISEC-IPC for all the support granted.

References

[41] Adam D. Lampropoulos, Angelos P. Markopoulos and Dimitrios E. Manolakos, Modeling of Ti6Al4V Alloy Orthogonal Cutting with

Smooth Particle Hydrodynamics: A Parametric Analysis on Formulation and Particle Density, Metals 2019, 9, 388; doi:10.3390/met9040388.

[42] Veiga, C., Davim, J.P., & Loureiro, A.J.R., Review on machinability of titanium alloys: the process perspective, Reviews on Advanced Materials Science, IPME, 34, 2, (2013), 148-164.

[43] A. Modgil, Effects of high speed machining on surface topography of titanium alloy (TI6AL4V) (Thesis (M.S.) - University of Florida, 2003).

[44] N. Churi, Z. Pei and C. Treadwell // International Journal of Precision Technology 1 (2007) 85.

[45] J. Colafemina, R. Jasinevicius and J. Duduch // Proceedings of the Institution of Mechanical Engineers, Part B: Journal of Engineering Manufacture 221 (2007) 999.

[46] M. S. Ahmad Yasir // The Open Industrial and Manufacturing Engineering Journal 2 (2009) 1.

[47] Taylor, C., Hernandez, S., Marshall, M. orcid.org/0000-0003-3038-4626 et al. (1 more author) (2018) Cutting fluid application for titanium alloys Ti-6Al-4V and Ti-10V-2Fe-3Al in a finish turning process. In: Monostori, L., Stepan, G. and Bachrathy, D., (eds.) Procedia CIRP. 8th CIRP Conference on High Performance Cutting (HPC 2018), 25-27 Jun 2018, Budapest, Hungary. Elsevier, pp. 441-444. https://doi.org/10.1016/J.PROCIR.2018.08.279

[48] M. Sadeghi // The International Journal of Advanced Manufacturing Technology 44 (2009) 487.

[49] Pervaiz, S., Anwar, S., Qureshi, I., & Ahmed, N. (2019). Recent advances in the machining of titanium alloys using minimum quantity lubrication (MQL) based techniques. International Journal of Precision Engineering and Manufacturing-Green Technology, 6(1), 133–145.

[50] [76] A. Sharman, J. Hughes and K. Ridgway //Proceedings of the Institution of Mechanical Engineers, Part B: Journal of Engineering Manufacture 222 (2008) 653.

[51] taşcıoğlu, Emre & Gharibi, Armin & Kaynak, Yusuf. (2019). High speed machining of near beta titanium Ti-5553 alloy.

[52] Abu Bakar, Mohd Hadzley & Izamshah, Raja & Siti Sarah, A & Nurul Fatin, M. (2013). Finite Element Model of Machining with High Pressure Coolant for Ti-6Al-4 V Alloy. Procedia Engineering. 53. 624–631. 10.1016/j.proeng.2013.02.080.

[53] M. Bermingham // International Journal of Machine Tools and Manufacture 51 (2011) 500.

[54] Shokrani, A.; Newman, S.T. A New Cutting Tool Design for Cryogenic Machining of Ti–6Al–4V Titanium Alloy. Materials 2019, 12, 477.

[55] Mackerle, J., Finite element analysis and simulation of machining: an addendum: A bibliography (1996-2002). International Journal of Machine Tools and Manufacture. Vol. 43, n.º 1 (2003), p. 103-114.

[56] Kuttolamadom, M., Prediction of the Wear & Evolution of Cutting Tools in a Carbide / Ti-6Al-4V Machining Tribosystem by Volumetric Tool Wear Characterization & Modeling (2012). All Dissertations. Paper 1003.

[57] Hong, SY; Markus, I; Jeong, W - New cooling approach and tool life improvement in cryogenic machining of titanium alloy Ti-6Al-4V. International Journal of Machine Tools and Manufacture. ISSN 0890-6955. Vol. 41, n.º 15 (2001b), p. 2245-2260.

[58] Hong, SY; Ding, Y; Jeong, W - Friction and cutting forces in cryogenic machining of Ti-6Al-4V. International Journal of Machine Tools and Manufacture. ISSN 0890-6955. Vol. 41, n.º 15 (2001a), p. 2271-2285.

[59] Hong, SY; Ding, Y - Cooling approaches and cutting temperatures in cryogenic machining of Ti-6Al-4V. International Journal of Machine Tools and Manufacture. ISSN 0890-6955. Vol. 41, n.º 10 (2001a), p. 1417-1437.

[60] XIE, JQ; BAYOUMI, AE; ZBIB, HM - FEA modeling and simulation of shear localized chip formation in metal cutting. International Journal of Machine Tools and Manufacture. ISSN 0890-6955. Vol. 38, n.º 9 (1998), p. 1067-1087. JOSHI, VA - Titanium alloys: an atlas of structures and fracture features. CRC, 2006.

[61] JOSHI, VA - Titanium alloys: an atlas of structures and fracture features. CRC, 2006.

[62] LEYENS, C; PETERS, M - Titanium and titanium alloys: fundamentals and applications. Vch Verlagsgesellschaft Mbh, 2003.

[63] Donachie, M. J. - Titanium: a technical guide. Metals Park, OH 44073:

Asm Intl, 1988.

Project Ghisallo

A mobile multi-sensor in the city

P. Nunes, J.P. Santos, J. Januário, A. Completotyo
Department of Mechanical Engineering
University of Aveiro
Aveiro, Portugal
pnunes@ua.pt

***Abstract*— Project "Ghisallo" aims the development of an electrically assisted mobility solution conceived to be practical, stylish and safe. In addition to the three-wheel electric vehicle, the solution includes a connectivity platform, an intelligence unit (IU), a smart lock, and an interface based on the user's smartphone, developed to give cyclists more comfort and security during their bicycle trips.**

The IU includes features as an Inertial Measurement Unit (IMU), vandalism detection, GPS and a connectivity module. The engine control unit (ECU) is wired connected to the battery management system (BMS), in order to get battery features as the percentage of charge and number charging cycles. The ECU communicates with IU through UART (universal asynchronous receiver-transmitter) protocol and sends it messages containing the battery and engine data. ECU is also wired connected to a Human Machine Interface (HMI) with buttons, in which the user can choose the engine assistance level and control the illumination system. The IU connectivity module allows the exchange of messages between the bicycle and the connectivity platform using the mobile network. The connectivity platform includes a MQTT [2] (Message Queuing Telemetry Transport) broker which is an intermediary in the process of communication between the connectivity platform and the IU. The communication is of the type publisher/subscriber. The bicycle (IU) can be the publisher when it sends data from sensors, battery and electric motor to the platform and can be subscriber when it requires data from the databases. The connectivity platform allows "Ghisallo" to be integrated into a bike sharing system since it includes services as payment methods and dashboards that facilitate the management and automation of the process of booking / renting a bicycle.

The user interface is based on smartphone use. The communication is made through the connectivity platform, i.e., the IU sends data to the connectivity platform and the user can monitor the bicycle with his smartphone who connects the platform using the mobile network. This allows the user to monitor the vehicle anywhere. He can check if the bicycle was disturbed and in case of theft, he knows where to search it because IU keeps sending GPS information to the platform. In the bike sharing use case, the user can rent a bike in the smartphone interface and pay for it, then the platform will publish the authorization to unlock the bike in the broker and the bikes IU will subscribe that service, in order to activate the smart lock. The user interface also allows him to search for route recommendation, since it has integrated an innovative routing engine algorithm that suggests the optimal route to a cyclist between two points, according to a chosen criterion. The algorithm considers the existence of cycle paths, type of surface, infrastructure characteristics, route singularities, road slope and uses the data sent to the platform in order to detect bad quality road surface or roads with many obstacles to improve the quality of the suggested routes, transforming "Ghisallo" in a mobile multi-sensor in the cities.

Keywords—connectivity platform; intelligence unit; sensors

Introduction

The bicycle use as a means of transport is becoming increasingly popular, especially for commuting trips, as it avoids car congestion in large urban centers [3]. For some journeys, it may be the fastest transport, because it allows for avoiding long stops due to car traffic. The bicycle is a vehicle that promotes higher energy efficiency [4] when compared to the automobile. In addition, it is cheaper, promotes a reduction in pollutant emissions while contributing to improving his user's health.

However, there are some challenges associated with cycling, with safety being a major inherent concern. According to the annual report of the ANSR [5] (National Road Safety Authority), in 2018 there were 17 cyclists who were fatal victims on Portuguese roads, 114 seriously injured, 1984 being the total number of victims that year. There are several reasons for this worrying number. Some relate to the lack of adequate cycling infrastructure, misbehavior of motor vehicle drivers, among others. In addition, for a cyclist with a lack of knowledge of the surrounding cycling network, it is not easy to choose the most suitable route. Often, is done a search to find bike paths. However, due to poor planning when building the infrastructure, this is not always a safe road type for cyclists. Some problems are the non-existence of physical separation from motorized traffic, obstacles as lamp posts in the middle of the track, or closure to a side park [6]. This may endanger the safety of the rider as the track may be obstructed by the open door of a parked vehicle. For the reasons mentioned, more people would consider using this vehicle as a means of locomotion if there were a mechanism that would make it easier to plan bike routes [7].

The creation of a tool for cyclists requires a considerable amount of data. Firstly, it requires the mapping of infrastructures that influence cyclist safety, such as the existence of bike lanes, infrastructure characteristics, slope, route singularities or traffic calm features such as speed bumps [8] [9] [10] [11]. On the other hand, it requires some extra information, such as the state of traffic or the

state of infrastructure such as bicycle lanes. This type of input should be constantly updated as infrastructure and road degradation exist.

Another reason that makes cycling less appealing is related to acts of vandalism and vehicle theft. People are often forced to park their bikes on public roads, and they end up being damaged by attempted thefts, which when unsuccessful end up causing damage to the vehicle and when consummated result in great loss and inconvenience for the owner.

Methods

The project "Ghisallo" aims the creation of a new smooth mobility concept. Therefore, we can say that the project is divided into 3 major parts or blocks designed to ensure maximum comfort, convenience and safety for its user. The blocks are, in particular, the vehicle itself, consisting of a three-wheeled bicycle, with the aim of ensuring the best balance and stability to the rider, allowing the "Ghisallo" to be used by anyone. Two of the three wheels are front, which in conjunction with a tilting steering system that allow this vehicle to be as dynamic as a traditional bike. The other block is constituted by an electrically assisted 8-speed powertrain along with a Li-Ion battery and energy-recovering system for deceleration and braking. This way "Ghisallo" can be used even on longer trips. Finally, we have the so-called connectivity platform and user interface block.

In figure 1 we have a profile image of "Ghisallo" and some of its components. Along with the electric motor we have the engine control unit (ECU) which consists of an electronic board responsible for controlling the engine and the lighting system of the vehicle. The ECU communicates with the battery management system (BMS) to receive battery status data such as percentage of charge and number of charge cycles. In addition, this component sends data received from BMS and motor-related data such as speed, torque, etc. to another component, called the intelligence unit (IU). The IU consists of several modules. There are a sensing and a geolocation module that allows the check of the bike's status (standing or running), some sensors such as IMU (Inertial Measurement Unit) allow the detection of the vehicle disturb, in which case it is possible to sound an alert, which warns people around that someone is trying to steal the bicycle. This type of sensor also gives important contributions to the state of the road surface, particularly in detecting surface irregularities or the existence of holes that undermine the good use of the rider. Also, obstacle detection on the road is possible. The geolocation module allows the user to locate the bike. If it is stolen, this is an added value, since it may allow your recovery. Finally, UI also has a communication module, which uses the mobile network. This specification allows all relevant bicycle information to be sent to an online storage platform (cloud). The other "Ghisallo" constituents that are illustrated are a Human Machine Interface (HMI) with buttons to allow the control of the electric motor and lighting system and a user interface that is based on the user's smartphone.

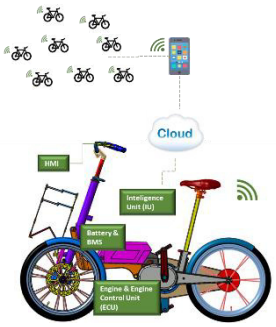

Figure 1: "Ghisallo" main blocks

In Figure 2, we can see how the different components interact with each other. The HMI sends electrical signals to the ECU to control the on / off of the engine and lighting system as well as to control the level of engine assistance. The BMS is wired to the ECU which receives battery status data. The connection and communication between ECU and IU is also made by wires as the UART protocol is used for communication, allowing the IU to receive data about the engine and battery status from the ECU. The communication between each bike and the online cloud is done according to the MQTT protocol which is subscriber/publisher type. For this, there is a broker that is intermediate in the communication, i.e., each bicycle publishes topics in the broker, sending it data related to the battery, the engine, and data resulting from the sensing and geolocation modules. The web platform has a subscriber application that will receive the data on the desired topic. In this way, the broker has the role of intermediary in communicating and distributes the published messages for the subscriber applications.

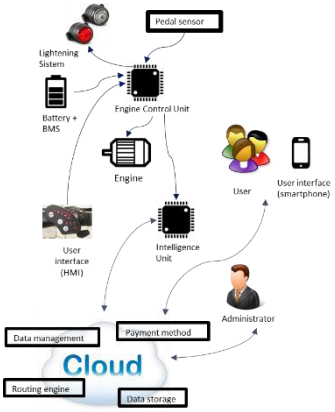

Figure 2: "Ghisallo" interaction scheme

The user can communicate with the bike, with his smartphone, but such communication is not direct, that is, the bike IU communicates with the online cloud. The user's smartphone also communicates with this platform, allowing the exchange of information between the two devices, with the connectivity platform assuming an intermediary paper. In addition to receiving his bike data, the user can also do some remote actions, such as sharing his bike or unlocking it remotely, since it has a smart lock connected to the IU.

Regarding the connectivity platform, it has several services and its architecture has several layers, as shown in figure 3. Thus, we have:

- Sensor and infrastructure layer, which includes all types of sensors and embedded electronics that will generate the data needed for the management platform.
- Integration and management layer, where all the back-office functional modules are concentrated, allowing to configure and structure all the data
- End-user interface layer, which will typically correspond to mobile applications that interact with the management system through APIs.
- Layer of interfaces with operators, which allows the provision of application frontends for the management of various operations.
- External services layer, which, through interconnection with the integration layer, will enable the inclusion of all types of systems and third-party platforms (eg. city mobility application, another bike-sharing system, ,etc.).

Thus, the fact of "Ghisallo" being connected to an online platform, makes it more versatile as its use in a wide range of environments is facilitated. For example, it's integration into a bike-sharing environment becomes more intuitive, as the online connectivity platform allows the inclusion of automatic payment methods, as well as the creation of services and business metrics, defined by the managing entity.

The data collected by the various bicycles are intended to be used to improve the safety and comfort of the rider, since the sensor data, together with the geolocation obtained by the GPS integrated with the IU, allows to measure the conditions of the cycling paths. Among other things, it allows the detection of obstacles, poor pavement condition or even accidents involving "Ghisallo". One of the services offered to the customer is a cyclist-specific routing method which, in addition to static data such as bike lane mapping, road type, route singularities, etc., is intended to encompass data obtained by processing sensor data. The cycling network is modeled by a directed graph, whose edge weights are constantly being updated, taking into account the inputs of the various sensors, as shown in figure 4. This approach gives a more realistic view of the safest routes to take into account by a cyclist.

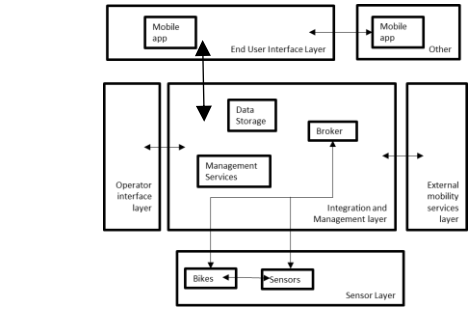

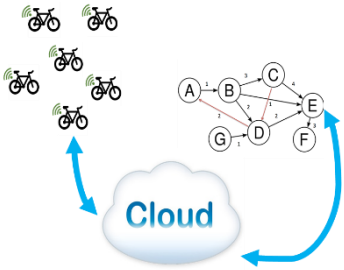

Figure 4: Routing Scheme

Conclusions

This paper presents a methodology for transforming a normal bicycle into a connected bicycle, exposing the inherent advantages of having such a connectivity platform based on the fact that "Ghisallo" can be integrated into a wide range of environments, enhancing the experience of riding a bicycle, with regard to comfort, safety, and convenience, enabling the creation of services such as intelligent routing for cyclists, which makes use of dynamic data from sensing. Moreover, this methodology can be used anywhere if static data for the creation of the directed graph is available.

The project "Ghisallo" has the participation of several entities, the lead promoter, SONAE, University of Aveiro, CEiiA,VRMotors and MSG. The project aims not only to create the connectivity platform but the also the 3-wheel vehicle, including the electrically, assisted engine. For future work, it is intended to integrate and thoroughly test all the blocks of "Ghisallo". Regarding the connectivity platform and the UI, the inclusion of new sensors could be considered, with the objective of having a better understanding of the parameters relevant to cyclist safety.

Acknowledgment *(Heading 5)*

POCI-01-0247-FEDER-033769 - "Ghisallo – Investigação e Desenvolvimento de uma nova solução de comutação urbana, assente num novo conceito de veículo elétrico de próxima geração" – "Ghisallo - Research and Development of a new urban commuting solution, based on a new concept of a next-generation vehicle".

UID / EMS / 00481/2019-FCT

CENTRO-01-0145-FEDER-022083

TOPIC (Heading 5)

2)b. Technologies for the Wellbeing - Innovative technologies for Smart Cities.

References

[1] RS-232 RS-485 RS-422 Communications Specifications [Internet]. [visited 2019 Jun 7]. Available from: http://www.rs-485.com/comspec.html

[2] MQTT Version 5.0. Edited by Andrew Banks, Ed Briggs, Ken Borgendale, and Rahul Gupta. 07 March 2019. OASIS Standard.

[3] Lindsay G, Macmillan A, Woodward A. Moving urban trips from cars to bicycles: impact on health and emissions. Aust NZ J Public Heal. 2011; 35(1):54–60. Available from: https://onlinelibrary.wiley.com/doi/pdf/10.1111/j.1753-6405.2010.00621.x

[4] Hsu Y-T, Kang L, Wu Y-H. User Behavior of Bikesharing Systems Under Demand–Supply Imbalance. Transp Res Rec J Transp Res Board [Internet]. 2016 Jan 1; 2587(1):117–24. Available from: http://journals.sagepub.com/doi/10.3141/2587-14

[5] ANSR Relatório Anual Sinistralidade Rodoviária 2018. 2018;17.

[6] Dondi G, Simone A, Lantieri C, Vignali V. Bike Lane Design: The Context Sensitive Approach. Procedia Eng [Internet]. 2011 Jan 1 [cited 2019 Jul 31]; 21:897–906. Available from: https://www.sciencedirect.com/science/article/pii/S1877705811049265

[7] Akar G, Clifton K. Influence of Individual Perceptions and Bicycle Infrastructure on Decision to Bike. Transp Res Rec J Transp Res Board 2009;2140(2140):165–72. Available from: http://trrjournalonline.trb.org/doi/10.3141/2140-18

[8] Pucher J, Buehler R. Making cycling irresistible: Lessons from the Netherlands, Denmark and Germany. Transp Rev. 2008;28(4):495–528.

[9] Menghini G, Carrasco N, Schüssler N, Axhausen KW. Route choice of cyclists in Zurich. Transp Res Part A Policy 2010;44(9):754–65. Available from: http://dx.doi.org/10.1016/j.tra.2010.07.008

[10] Stinson MA, Bhat CR. Analysis Using a Stated Preference Survey. Burns. 2003;(03):107–15.

[11] Buehler R, Dill J. Bikeway Networks: A Review of Effects on Cycling. Transp Rev. 2016;36(1):9–27. Available from: http://dx.doi.org/10.1080/01441647.2015.1069908

Thermo-Mechanical Analysis of PVC-based Wood Plastic Composite Decking Boards

Sabiq Sulaiman
Research Fellow, Centre for Mechanical Technology and Automation, Dept. of Mechanical Engineering
University of Aveiro,
Aveiro, Portugal
sabiq@ua.pt

Rui Moreira
Assistant Professor, Centre for Mechanical Technology and Automation, Dept. of Mechanical Engineering,
University of Aveiro,
Aveiro, Portugal
rmoreira@ua.pt

***Abstract*— Wood-plastic Composite (WPC) decks are innovative building materials used for outdoor flooring in a wide range of applications. When exposed to hot weather conditions, decking floors are facing thermal deformation by bending. This is a very critical situation, where the bending deck can even break the joints affecting the structural integrity of the deck assembly. Persistence of this situation makes the decking floors less safe and are susceptible to accidents. As an initiative to find a solution for this problem, it is necessary to study the thermo-mechanical behavior of the deck materials. In this work, a comprehensive study on different types of deck specimens, non-reinforced and fiber-reinforced, has been carried out in a specially designed test rig to investigate their thermal responses in terms of deformation and induced stress. From the experimental analysis, it has been observed that the thermal effect provided by temperature variations on decking boards may be important in terms of deformation induced by asymmetric thermal loading. The thermal influence was measured in terms of load measured in the free end of a fixed board, as well as the displacement measured in the same location. In case of the reinforced WPCs, the magnitude of response was almost half as compared to the non-reinforced ones. Results shows that the reinforcement has a noteworthy influence on the thermal stability of WPC decking boards.**

Keywords—WPC; deck; PVC-WPC; thermomechanical

TOPIC

1) a.: Manufacturing processes & Simulation

Introduction

In the area of material research, there has been an increased interest in the development of Natural fiber composites (NFC) with enhanced sustainability, to take over the synthetic fiber composites (Pickering et al, 2016). Biodegradability, lightweight, recyclability, non-toxicity, and renewability are the exceptional qualities of NFCs over synthetic fibers (Oksman et al, 2003). Due to these qualities, NFCs are used in numerous applications such as automotive interiors, building material, biomedical, marine railings etc., (Holbery and Houston, 2006; Cheung et al, 2009; Kalia et al, 2009).

WPCs are a type of NFCs, where the wood fibers/wood flour are embedded into polymer matrices, where the polymer matrix can be of thermosets or thermoplastics (Machado et al, 2016). The practice of compounding wood and polymers dates back to early 20th century, with the thermoset plastics. Since the wood and plastics were completely different industries, they faced many challenges in terms of compatibility due to some undesirable properties of wood such as high moisture content, low bulk density and the enormous difference between the melting point of wood and that of polymers, which causes difficulties in processing (Clemons, 2002). Adhesion between wood and plastic is very weak because wood flour is a hydrophilic substance, whereas the plastics are hydrophobic, and it needs several compounding agents to develop good adhesion (Lu et al, 2000). Later, with the invention of air-formed web technology and melt-blending technology, the possibilities of combining wood and polymers escalated in terms of integrating a wide range of wood fibers and polymers (Youngquist, 1995). Thus, many successful WPC products were launched into the market and it in turn created enormous interest to investigate more about wood and to develop more WPC products and find new markets.

Polyvinyl Chloride (PVC) is one of the most common thermoplastics used in manufacturing WPCs. Sonesson Plast AB, a Swedish company, in 1975 introduced the first commercial product based on PVC/Wood flour called “Sonwood”, as an alternative for veneers. WPCs based on PVC are extensively used in constructions due to their excellent mechanical properties, chemical stability, water resistance, paint-ability and durability. (Jiang and Kamdem, 2004).

According to the conjoint analysis done by Fell et al (2006), in the residential decking market, WPC have been extensively replacing the natural wood and treated wood due to its durability, ease of assembly and lesser maintenance. WPC has good dimensional stability with good resistance against water absorption compared to the natural wood (Defoirdt, 2009). WPC can be treated same as natural wood in terms of cutting and machinability. Moreover, WPC is comparably more stable in machining in such a way that it does not split or generate crack during machining, which is a common problem with natural wood (Carroll et al, 2001).

The thermal stability of the WPCs is an important factor to be considered as the WPC decking floors are mostly used for outdoor purposes where they are susceptible to hot weather conditions. Tamrakar et al (2011) have studied the effect of temperature on the mechanical properties of WPC and concluded that the Modulus of Elasticity (MOE) and Modulus of Rupture (MOR) decreases with increase in temperature. This implicates that WPC decking floors are vulnerable to thermal deformations. These thermal deformations can even affect the structural integrity of the decking system, and it can even break the structural joints. Persistence of this situation make the decking floors less safe and are susceptible to accidents. Thus, the quantification of the thermal responses is necessary for safe construction and structural designs of the deck systems. This experimental work focuses on estimating the thermal responses, in terms of thermal deformation and

forces, developed when WPC decking floors are subjected to elevated temperatures.

Huang et al (2012) developed a finite element model of glass fiber-reinforced WPC to predict the effect of reinforcement on thermal stability of WPCs and concluded that the linear coefficient of thermal expansion (LCTE) was considerably reduced with the presence of reinforcements. In this experimental study, reinforced as well as non-reinforced WPC decking specimens are considered for analyzing the significance of reinforcements in the thermal stability of the component.

Experimental Analysis

Thermo-mechanical analysis (TMA) is performed to study the behavior of a material, in terms of dimensional distortions and developed stress, when it is subjected to change in temperature. The bending deflection of the deck specimen and the associated force are the parameters of concern in this experimental study. A specialized experimental setup was built for analyzing the thermo-mechanical behavior of the deck specimens as shown in Figure 32. The test rig was built with Aluminum blocks and has the provision to mount LVDT and load cell for measuring the thermal force and displacement respectively. Two different deck specimens were used to measure the force and displacement. The specimen allocated for measuring the displacement is free to deform, whereas the other one is constrained with a load cell for measuring the thermal force.

The setup consists of a heating system, Linear Variable Differential Transformer (LVDT), load cell, Data Acquisition System (DAQ), and a thermocouple (K Type). The heating system is provided at the bottom part of the test rig in the form of a heating plate. As the heating plate gets heated, the temperature of the air just above heat plate increases. As a result, conventional currents are formed which transfers the heat to the deck specimen. The deck specimens are mounted upside down, in order to simulate the heat rays from sun falling on the deck surface. K-type thermocouples, which has an operating temperature range of -2700C to 12600C, is used for measuring the temperature of the deck specimen. The LVDT used in this setup is HBM WA100, which has a capacity of 100mm. An S-type load cell with a capacity of 10Kg is used for measuring the force and an HBM Spider 8 is used for data acquisition.

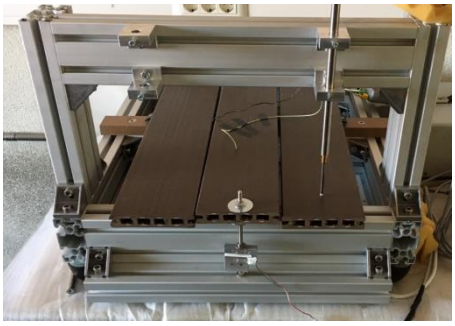

Figure 32: Experimental setup (in Position 1)

Specimen

Reinforced and non-reinforced deck specimens were considered for thermo-mechanical analysis. All the deck specimens have the same cross-sectional dimensions as shown in the Figure 33, with a length of 660mm.

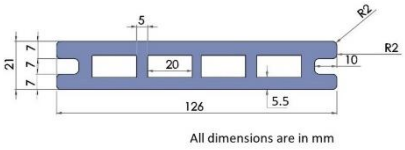

Figure 33: Cross sectional view of the deck

The deck specimens were mounted onto the test rig using 'T' shaped polymer clips. These clips are positioned in between the deck profiles, so as to hold them together against the beam. The arrangement of the decks and the clips are shown in the Figure 34.

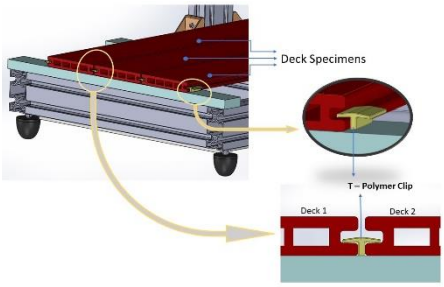

Figure 34: Arrangement of the decks and clips

Three specimens are considered in this study: a reinforced specimen and two non-reinforced specimens. Specimen 1 is non-reinforced decks whereas the specimen 2 is reinforced, as shown in Figure 35, and, Figure 36.

Figure 35: Specimen 1 (Non Reinforced WPC deck)

Figure 36: Specimen 2 (Reinforced WPC deck)

Measuring Thermal deformation and Force

During the heating process, the deck profiles experiences thermal stress. One specimen is allowed free to thermally deform for measuring the deflection, whereas another specimen is arrested by a load cell for measuring the thermal force [See Figure 32]. In this experimental study, the deformation and thermal force are measured in two different positions; position 1 and position 2.

Position 1: In this position, the deck specimens are fixed at one end and in the middle. The objective of this configuration is to measure the thermal responses at the longitudinal end of the decking board. The force measured in this configuration is supposed to be the thermal load carried by the batten at the longitudinal end of the decking floor. The deformation and the thermal force are measured from the free end of the specimen. Since the heater is placed below the deck, the bottom surface of deck undergoes thermal expansion, which makes the deck specimen to bend upward (as shown in Figure 37) and push the LVDT probe upward to obtain the value of thermal deflection. The load cell is also placed at the same free end of a different specimen to measure the thermal force, by constraining the deflection.

Position 2: In this position, the deck specimens are fixed at both the ends and the deflection and the thermal force are measured from middle of the specimen. This configuration refers to the span of decking boards, which are fixed between the beams. When the bottom surface of deck undergoes thermal expansion, the middle portion bends downward (as shown in Figure 38) and push the LVDT probe downward to obtain the value of thermal deflection

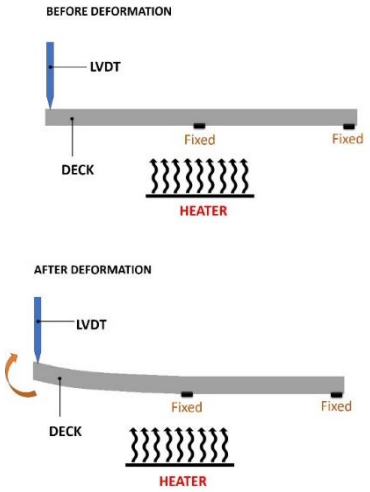

Figure 37: Before and after the thermal deformation in Position 1

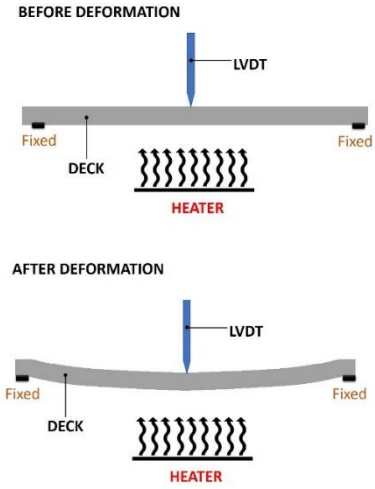

Figure 38: Before and after the thermal deformation in Position 2

5. Experimental Results and Discussion

This section discusses the result of experimental analyses performed on different specimens. The experiments were carried out based on two criteria described as follows:

• Configuration of the experimental setup: This refers to the location of constraints applied on the deck specimens and the position of LVDT/load cell.

• Type of deck specimen: Two types of WPC deck specimens were considered for the analysis; Fiber-reinforced WPC deck specimen and Non-reinforced WPC deck specimen.

For each type of specimen, in each configuration of the experimental setup, at least 10 experiments were performed consecutively, to obtain clarity in terms of the results and inference.

Position 1: Thermal deformation

In position 1, the thermal deformation refers to the vertical displacement made by the free end of the deck due to thermal bending. Figure 39 shows a graph showing thermal deformation induced in the specimen 1 and specimen 2, where the deformation is plotted against ΔT. The graph forms a hysteresis loop starting from zero, reaches a maximum value and then declines towards the initial value. The average deformation of specimen 1, from all experiment, is estimated to be 3.1 mm with a peak value of 3.356 mm. But, for specimen 2, the average deformation is 2.46 mm, with a peak value of 2.562 mm. This difference in values shows the significance of reinforcement in specimen 2. The deformation is decreased by 20.6% with the presence of reinforcement.

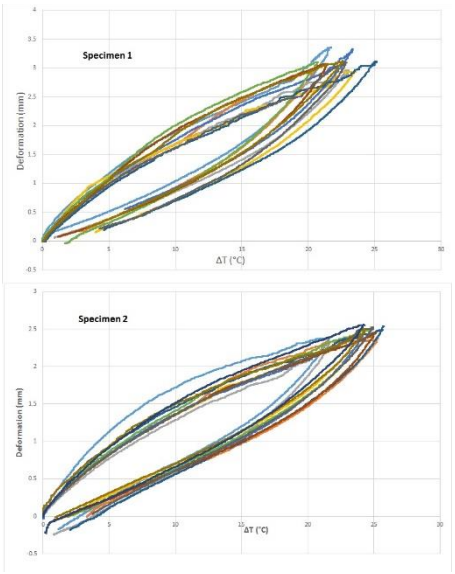

Figure 39: Thermal deformation in Position 1 of specimen 1 (on top) and specimen 2 (bottom)

Thermal force

In position 1, the thermal force refers to the force exerted by the free end of the beam when the thermal deformation is constrained. Figure 40 shows the thermal force developed in specimen 1 and 2, with increase in the temperature, in position 1. It resembles the deformation graph, with a hysteresis loop. Since the force is measured in the tension direction of the load cell, the graph shows negative values. The average of thermal forces developed in specimen 1, from all experiments, is calculated as 42.3 N with highest developed force of 43.05 N, whereas in specimen 2, the average force is 21.93 N with a peak force of 25.33 N. It can be noted that the thermal forces developed in the reinforced specimen (specimen 2) is almost half that of the non-reinforced one, precisely forces are reduced by 48.15%. In other words, the thermal stability is increased by 48.15%. This value shows the significance of the reinforcements in WPC, which makes them more stable in adverse weather conditions.

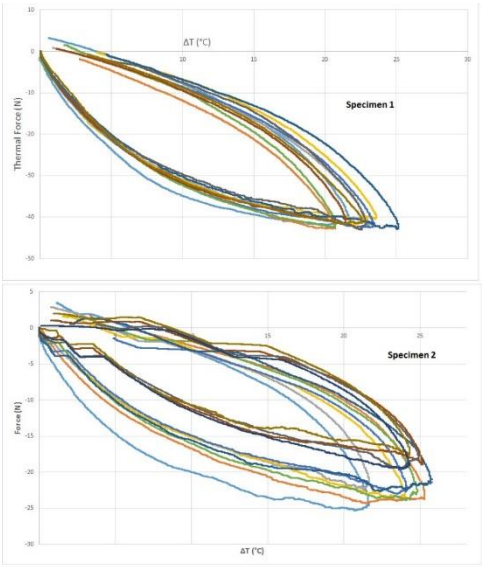

Figure 40: Thermal Force developed in Position 1 for specimen 1 (on top) and specimen 2 (bottom)

Position 2: Thermal deformation

The thermal deformation in position 2 refers to the maximum deflection of the beam developed at the mid-span of the length, when both the ends of the deck are fixed. The deformation developed in this position are comparably less as the ends are fixed, but the thermal forces are extensively high. The average of maximum thermal displacements developed in specimen 1, from all experiments, was found to be 1.286 mm with a highest displacement of 1.368 mm. For specimen 2, the average displacement is calculated as 1 mm with a highest displacement of 1.0375 mm. The deformation of specimen 2 is comparably less as in position1 [See Figure 41].

Thermal Force

The value of thermal forces are high in position 2, as both the ends of the deck are constrained. The average of maximum thermal forces developed in specimen 1, from all experiments, is calculated as 124.35 N with a highest value of 133.07 N. In case of specimen 2, the average force is estimated as 67.43 N with a highest force of 74.093 N.

The thermal stability of the reinforced specimen is confirmed with a figure of 45.8% decrease in thermal forces [See Figure 42].

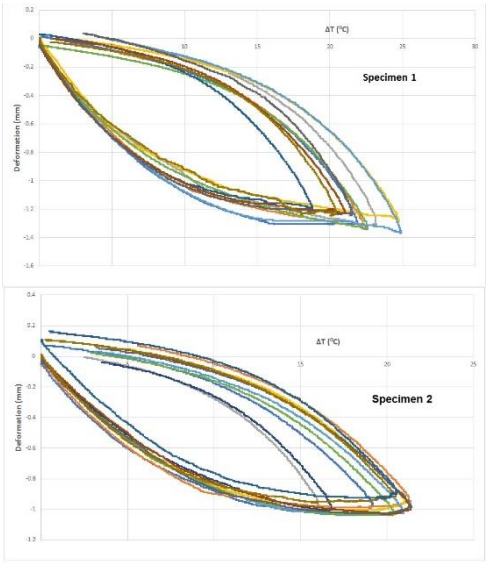

Figure 41: Thermal deformation in Position 2 of specimen 1 (on top) and specimen 2 (bottom)

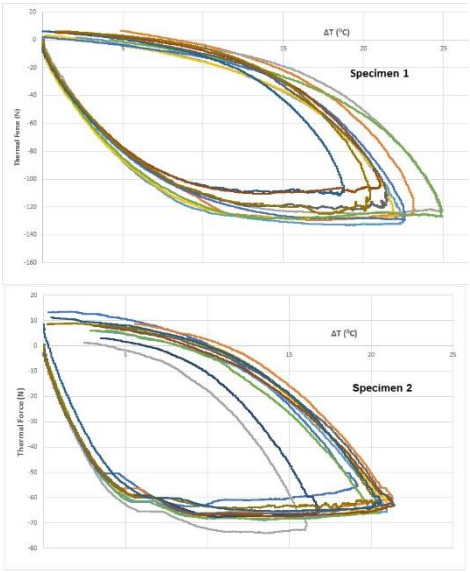

Figure 42: Thermal Force developed in Position 2 for specimen 1 (on top) and specimen 2 (bottom)

Conclusion

The thermal response in terms of thermal force and displacement of the PVC-based WPC deck specimens has been studied through thermo-mechanical analysis. It has been analyzed that the thermal responses were almost half in case of reinforced WPC as compared to the non-reinforced ones. In conclusion, the thermal force developed in the deck specimen must be considered for developing deck-constructional components for safety purpose. It is recommended to consider the forces developed in the non-reinforced deck specimen, as the commercial deck-constructional components are universal for all deck materials.

References

1. Carroll, Douglas R., Robert B. Stone, Anthony M. Sirignano, Rosanna M. Saindon, Stephen C. Gose, and Marc A. Friedman. 2001. "Structural Properties of Recycled Plastic/Sawdust Lumber Decking Planks". Resources, Conservation And Recycling 31 (3): 241-251. doi:10.1016/s0921-3449(00)00081-1.

2. Cheung, Hoi-yan, Mei-po Ho, Kin-tak Lau, Francisco Cardona, and David Hui. 2009. "Natural Fibre-Reinforced Composites for Bioengineering and Environmental Engineering Applications". Composites Part B: Engineering 40 (7): 655-663. doi:10.1016/j.compositesb.2009.04.014.

3. Defoirdt, Nele, Soetkin Gardin, Jan Van den Bulcke, and Joris Van Acker. 2010. "Moisture Dynamics of WPC and the Impact on Fungal Testing". International Biodeterioration & Biodegradation 64 (1): 65-72. doi:10.1016/j.ibiod.2009.07.010.

4. Fell, David R, Jon Thomas, and Eric Hansen. 2006. "Evolving Consumer Preferences for Residential Decking Materials". The Forestry Chronicle 82 (2): 253-258. doi:10.5558/tfc82253-2.

5. Fell, David R, Jon Thomas, and Eric Hansen. 2006. "Evolving Consumer Preferences for Residential Decking Materials". The Forestry Chronicle 82 (2): 253-258. doi:10.5558/tfc82253-2.

6. Ganguly, Indroneil, and Ivan L. Eastin. 2009. "Trends In The US Decking Market: A National Survey Of Deck And Home Builders". The Forestry Chronicle 85 (1): 82-90. doi:10.5558/tfc85082-1.

7. Holbery, James, and Dan Houston. 2006. "Natural-Fiber-Reinforced Polymer Composites in Automotive Applications". JOM 58 (11): 80-86. doi:10.1007/s11837-006-0234-2.

8. Huang, R., Xiong, W., Xu, X. and Wu, Q. (2012). Thermal Expansion Behavior of Co-Extruded Wood-Plastic Composites with Glass-Fiber Reinforced Shells. BioResources, 7(4).

9. Jiang, Haihong, and D. Pascal Kamdem. 2004. "Development of Polyvinyl Chloride/Wood Composites. A Literature Review". Journal of Vinyl and Additive Technology 10 (2): 59-69. doi:10.1002/vnl.20009.

10. Jiang, Haihong, and D. Pascal Kamdem. 2004. "Effects of Copper Amine Treatment on Mechanical Properties of PVC/Wood-Flour Composites". Journal of Vinyl and Additive Technology 10 (2): 70-78. doi:10.1002/vnl.20010.

11. Jiang, Long, Michael P. Wolcott, Jinwen Zhang, and Karl Englund. 2007. "Flexural Properties Of Surface Reinforced

Wood/Plastic Deck Board". Polymer Engineering & Science 47 (3): 281-288. doi:10.1002/pen.20705.

12. Jiang, Long, Michael P. Wolcott, Jinwen Zhang, and Karl Englund. 2007. "Flexural Properties Of Surface Reinforced Wood/Plastic Deck Board". Polymer Engineering & Science 47 (3): 281-288. doi:10.1002/pen.20705.

13. Lopez, J. L., M. Sain, and P. Cooper. 2005. "Performance of Natural-Fiber-Plastic Composites under Stress for Outdoor Applications: Effect Of Moisture, Temperature, And Ultraviolet Light Exposure". Journal Of Applied Polymer Science 99 (5): 2570-2577. doi:10.1002/app.22884.

14. Machado, José S., Sara Santos, Fernando F.S. Pinho, Fábio Luís, Ana Alves, Rita Simões, and José Carlos Rodrigues. 2016. "Impact of High Moisture Conditions on the Serviceability Performance Of Wood Plastic Composite Decks". Materials & Design 103: 122-131. doi:10.1016/j.matdes.2016.04.030.

15. Machado, José S., Sara Santos, Fernando F.S. Pinho, Fábio Luís, Ana Alves, Rita Simões, and José Carlos Rodrigues. 2016. "Impact of High Moisture Conditions on the Serviceability Performance of Wood Plastic Composite Decks". Materials & Design 103: 122-131. doi:10.1016/j.matdes.2016.04.030.

16. Oksman, K., M. Skrifvars, and J.-F. Selin. 2003. "Natural Fibres as Reinforcement in Polylactic Acid (PLA) Composites". Composites Science and Technology 63 (9): 1317-1324. doi:10.1016/s0266-3538(03)00103-9.

17. Pickering, K.L., M.G. Aruan Efendy, and T.M. Le. 2016. "A Review of Recent Developments in Natural Fibre Composites and Their Mechanical Performance". Composites Part A: Applied Science And Manufacturing 83: 98-112. doi:10.1016/j.compositesa.2015.08.038.

18. Tamrakar, Sandeep, Roberto A. Lopez-Anido, Alper Kiziltas, and Douglas J. Gardner. 2011. "Time and Temperature Dependent Response of a Wood–Polypropylene Composite". Composites Part A: Applied Science And Manufacturing 42 (7): 834-842. doi:10.1016/j.compositesa.2011.03.011.

19. Zhou, Aixi, and Thomas Keller. 2005. "Joining Techniques for Fiber Reinforced Polymer Composite Bridge Deck Systems". Composite Structures 69 (3): 336-345. doi:10.1016/j.compstruct.2004.07.016.

20. Lu, J., Wu, Q. and McNabb Jr, H. (2000). Chemical Coupling in Wood Fiber and Polymer Composites: A Review of Coupling Agents and Treatments. Wood and Fiber Science, 32(1).

21. Youngquist, J. (2019). Unlikely partners? The marriage of wood and non-wood materials. Forest products journal (USA), 45(10), pp.25-30.

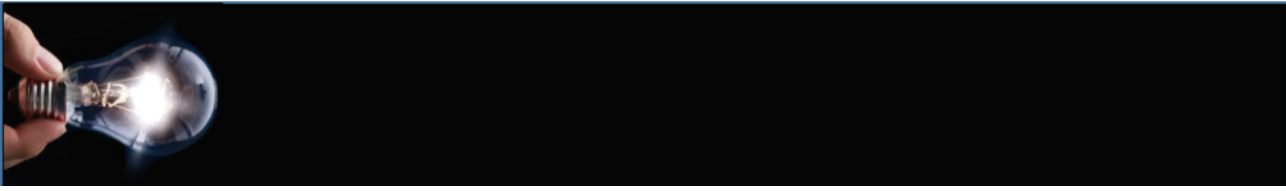

Title:
Book of abstracts of the 2nd International Conference of TEMA: Mobilizing Projects

Editors:
António Pereira, Paula Marques, Margarida Coelho, António Completo, Fernando Neto

Support team:
Ana Quintã, Diana Fidalgo, Kátia Silva, Maria Relvas, Nuno Almeida, Raul Simões

Publisher:
UA Editora
Universidade de Aveiro

1st Edition – July 2019

ISBN: 978-972-789-603-5

TEMA – Centro de Tecnologia Mecânica e Automação
Departamento de Engenharia Mecânica
Universidade de Aveiro
Campus Universitário de Santiago
3810-193 Aveiro

Tel: (+351) 234 370 830
Fax: (+351) 234 370 953
e-mail: tema@ua.pt
Website: http://www.ua.pt/tema/

This book is supported by the projects:
UID/EMS/00481/2019-FCT - FCT - Fundação para a Ciência e a Tecnologia; and
CENTRO-01-0145-FEDER-022083 - Centro Portugal Regional Operational Programme (Centro2020), under the PORTUGAL 2020 Partnership Agreement, through the European Regional Development Fund